University of Strathclyde
Department of Pure and Applied Chemistry

# A Passive and Active Acoustic Study of Bubbles Related to Bioprocess Monitoring

by
Kenneth G. Macpherson B.Sc. (Hons) PGDE AMRSC

A thesis presented in fulfilment of the requirements
for the degree of Master of Philosophy

March 2010

This thesis is the result of the author's original research. It has been composed by the author and has not been previously submitted for examination which has led to the award of a degree.



Signed: K. Macpherson

Date: 01/03/2010

**Acknowledgements**

I would like to thank Dr. Alison Nordon for her continued help and support with the experimental work and in writing this report. I would also like to thank the members of CPACT for their input.

In addition I thank Dr. Anthony Gachagan for his help with the ultrasonic aspects of the project and Dr. Tony Mulholland and his Ph.D. student Mr. Euan Barlow for the mathematical contributions.

I would like to thank the technicians in the analytical laboratory and the administrative and support staff within the Department of Pure and Applied Chemistry.

Lastly, I would like to thank and acknowledge the EPSRC/RSC for studentship funding.

## ABSTRACT

Bioprocesses are operated sub-optimally due to a lack of real-time physical and chemical information and the complexity and variability of biological materials. Currently, optical techniques are favoured for in-line and at-line monitoring of bioprocesses while chromatographic techniques are used as an off-line assay method. In-line probes require contact with the fermentation broth, which raises sterility issues. Therefore, the development of measurement techniques that can be applied non-invasively is attractive.

Acoustic measurements can be invasive or non-invasive and can be used to obtain physical property information, e.g. bubble size. Therefore, the overall aim of this work is to utilise some of the developments made in passive and active acoustics and apply this to the study of bubbles in the area of bioprocess monitoring.

For this work acoustic emission and active acoustic techniques have been investigated. Acoustic emission was used to characterise bubble size by Minnaerts theory. A Design of Experiments approach was used to investigate the effects of the sparger diameter, flow rate and viscosity on bubble production. It was found that using acoustic emission bubbles can be characterised in terms of their resonance frequency, where resonance frequency was inversely proportional to bubble diameter. Also it was shown that increasing viscosity increased repeatability. Repeatability was found to be as low as 0.9 %.

Following this a test cell was developed for the active acoustic characterisation of bubbles in water. By using active acoustics, bubbles can be characterised in terms of the frequency spectra of the received signal and the area under the spectra. Using active acoustics it was found that for bubbles of estimated diameter of 1, 2 and 4 mm the area under the spectra increased linearly with increasing bubble diameter. The lowest repeatability obtained was an RSD of the peak area of 6.8 %.

## CONTENTS

# Chapter 1
# Introduction to Fermentation

Fermentation reactions are of prime importance in modern society.[1] The importance of fermentation reactions can be appreciated by the range of products that they produce. In the food and drink industries fermentation reactions are used in baking and milling, tenderising meat, stabilizing soft drinks and producing bread, cereals, soups and milk concentrates, for example. Fermentation reactions are also used in the textiles and the photographic industries for desizing fabrics and recovering silver from used film, respectively. However, more importantly is the use of fermentation reactions in the pharmaceutical industry for antibiotic production, anti-blood clotting and digestive aids.

## 1.1 Fermentation Reactions

Typically, fermentation reactions are made up of six basic stages:[1]

- formulation of the media to be used for culturing the process organism during development of the inoculum and in the fermenter,
- sterilization of the medium, fermenter and any other equipment which is likely to be used,
- production of the active, pure culture. There has to be enough culture produced to inoculate the production vessel,
- growth of the organism in the fermenter. This is carried out at the optimum conditions for product formation,
- extraction of the desired product and purification of this product,
- finally, safe disposal of any unwanted effluent.

The raw materials which are needed for aerobic fermentation reactions are sources of carbon, energy, nitrogen and oxygen in addition to various other nutrients.[1] Water is the main constituent of fermentation reactions, where it is used for heating and cooling. It is important that the components of the water remain the same; the

dissolved salts, pH and mineral content, for example. Energy is typically generated from the oxidation of carbohydrates, lipids and proteins. Carbon sources are particularly important as this affects the rate of biomass production and inevitably product formation. Common carbon sources include; carbohydrates (the most commonly used is starch) oils and fats, which typically contain 2.4 times the energy of glucose on a weight by weight basis. Also, some micro-organisms can use methanol and hydrocarbons as energy and carbon sources. The main source of nitrogen is ammonia; this usually changes the pH in the alkaline direction, although if ammonium salts are used the pH would shift to the acidic side due to the release of the free acid upon reaction. Oxygen is provided to the microbes via air input. Other raw materials which are important are minerals, buffers, chelators and inducers (enzymes).

Fermentation reactions can be batch, fed-batch or continuous processes, where most product formation occurs in the exponential phase (see later).[2] In batch fermentations all of the substrates are added at the start of the reaction. Batch systems are also closed systems (with the exception for aeration). In fed-batch systems the substrate is added in stages through out the process. Continuous systems operate on the principle of a continual movement of material i.e. continuous feed of raw materials and continuous discharge of product. In a continuous system the amount of material put in must equal the amount of material taken out. Continuous systems are open systems. The principle aim of a fermenter is to give a controllable situation for cellular growth and formation of product. The main difference between laboratory and industrial fermenters is that laboratory fermenters are usually capable of carrying out several different types of fermentation reaction, whereas industrial scale fermenters are purpose built for the specific reaction. For some fermentation reactions to proceed a source of aeration is needed (which can be used to monitor the reaction). Air, which has to be sterile, is introduced into the system from the bottom of the reactor and is spread round the reactor by an agitation system. The agitation system is composed of flat-bedded disc turbines, usually 3, located in the centre of the reactor. Each disc turbine has between 4 and 6 propellers on it. A schematic diagram can be seen in Figure 1.1.

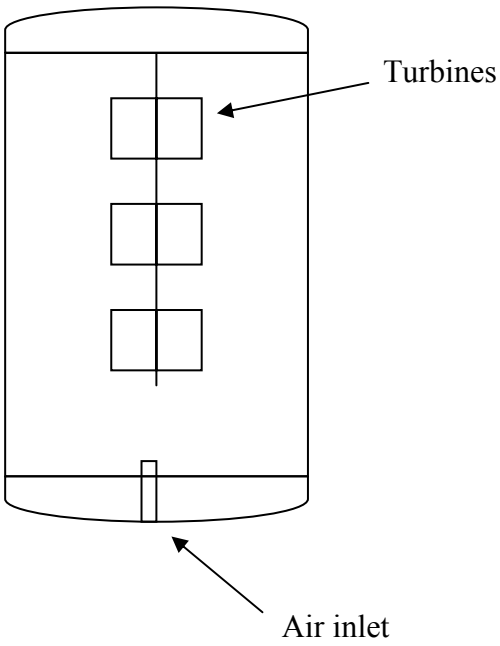


**Figure 1.1 – Schematic diagram of aeration in a typical fermenter[2]**

## 1.2 Growth of Biomass in Fermenters

The growth cycle of a fermentation reaction can be divided into 8 stages (see Figure 1.2):[3]

- lag phase (I),
- acceleration phase (II),
- exponential (logarithmic) phase (III),
- deceleration phase (IV),
- stationary phase (V),
- accelerated death phase (VI),
- exponential death phase (VII),
- survival/death phase (VIII).

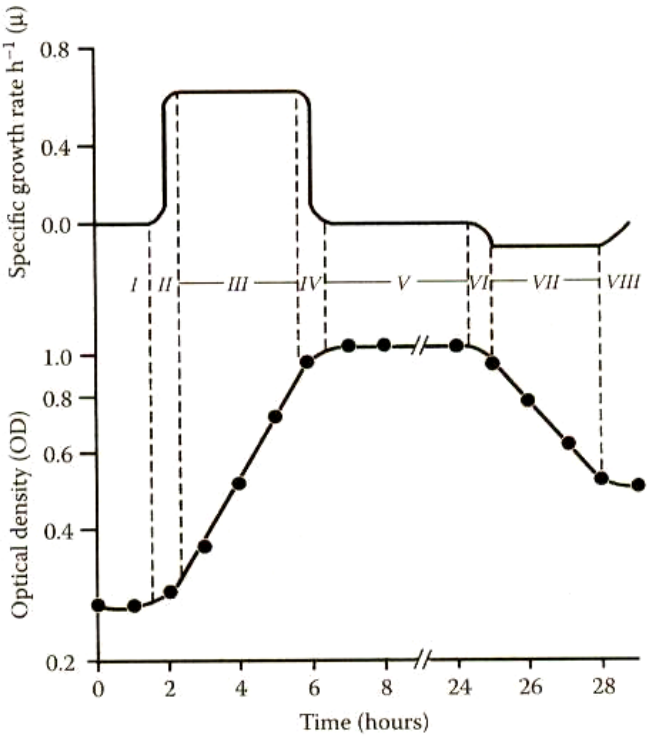


**Figure 1.2 – Growth cycle of a fermentation reaction[3]**

Firstly, the lag phase is where the organism familiarises itself with the environment.[3] When the lag phase is complete the cell is capable of transforming chemicals to biomass i.e. the cell is biochemically alive. In industry the lag phase is costly. To find out if an organism is in the process of going through the lag phase, one simply plots optical density against time, where optical density would be expected to increase slightly over time, as is shown in Figure 1.2. The lag phase is represented by *I* in Figure 1.2. When the lag phase is complete, the organism moves on to the acceleration phase, stage *II*. Following the acceleration phase, the exponential phase, stage *III* takes place. In this, the third phase, the cell increases in size and, if conditions are appropriate, the cell will divide into two. As cell division continues, the time for each cell division is referred to as the generation or doubling time. During the exponential phase, the cell is able to convert the primary carbon source into biochemically useful starting materials, transferring energy into adenosine triphosphate (ATP), for example. These biochemical starting materials are directed via biosynthetic pathways to produce amino acids, fatty acids and sugars that then go

on to give polymers such as proteins, nucleic acids and lipids. The rate of microbial growth during the exponential phase is given by:[4]

$$\frac{dX}{dt} = \mu X \qquad \textbf{Equation 1.1}$$

where $X$ is the cell concentration in grams/litre (or cell number in cells/litre), $t$ is the time and $\mu$ is the specific growth rate in hours$^{-1}$ (or $\mu_n$ specific growth rate in numbers). The (biological) cell number can be measured by different methods; microscopic count, viable plate count or a slide culture. Cell mass can be measured from the dry cell weight or turbidity.[4] Once the cells have reached a maximum growth rate, the rate then slows down. This is the deceleration phase, stage *IV* on Figure 1.2.

As the exponential phase comes to an end, the organism enters the stationary phase, stage *V* and finally the death phase(s), stages *VI – VIII* on Figure 1.2.[3] During the stationary phase the nutrients available to the organism are limited and as a result some organisms die during this phase. However, a great number of organisms continue to survive. The death phase occurs at the point where the death rate is greater than the growth rate.

Sterility is a vitally important factor in fermentation reactions. If any infection does become apparent it can affect production hugely.[5] Infection can be determined by a few methods, for example, direct inspection of the culture, microscopic examinations or culture tests. In industry, infection can come from a variety of sources for example, leaks from pipes, design faults in the infrastructure or when the culture is introduced to the fermenter and problems arise with the inoculation and/or sterilisation procedures.

## 1.3 Monitoring of Fermentation Processes

Fermentation reactions in, for example, the pharmaceutical or food industry require monitoring, in order to monitor how the process is progressing. If the organisms in the fermenter are dying too quickly then the fermentation reaction will not be progressing as it should. No matter what the chemical process, it is desirable to assess if the products being produced are as expected be i.e. that there are no impurities or unwanted by-products present.[6]

**Table 1.1 – Common measurements and their sensors[7]**

| Measurement | Sensor |
|---|---|
| Temperature | Pt – resistance thermometer |
| pH | Glass and reference electrode |
| Dissolved Oxygen | Conductance/capacitance probes |
| Agitation | Tachometer/watt-meter |
| Air Flow | Mass flow meters/rotameters |
| Pressure | Spring/oil-filled diaphragm |

Table 1.1 shows some of the important measurements that are taken during a fermentation reaction to monitor both the progression of the reaction and for infections.[7] No matter what the aim of the bioprocess is, since cells and microorganisms are involved, sterility must be maintained.

In fermentation reactions, the use of microorganisms or mammalian cells is required to yield molecules such as proteins.[8] In this case, pH and temperature need to be monitored to make sure the microorganisms are healthy. Presently, there are a variety of techniques used for process monitoring.. Two beneficial requirements of fermentation monitoring are that the technique should be non-invasive and non-destructive.[9] That is, the measurement technique should not come into direct contact with the process and the sample taken should be able to be returned to the process, and so this minimising waste).[9]

A review by Pons *et al.* discusses the current optical techniques that have been used to monitor bioprocesses *in-situ*, these are; ultraviolet-visible, near infra-red, mid-infra-red and Raman spectroscopies.[9] From this review, and other contemporary literature there is a noticeable lack of applications in which fermentation reactions are monitored on-line, with most applications being restricted to off-line, and at-line monitoring . This is most likely due to the complexity involved in having an on-line or in-line probe inserted into a fermentation process, where sterility is an issue and probe fouling can occur. The use of acoustic techniques has the potential to offer solutions to these problems. The acoustic sensor can be placed on the outside of a fermenter and does not come into contact with the fermentation media, thus eliminating the problems of sterility and probe fouling associated with invasive sampling regimes.[10] The interested reader is directed to reference 10 for a review of state of the art trends in ultrasonic sensors used for process monitoring.

As fermentation broths are complex, multi-phase media, fermentation reaction monitoring is poorly understood. This further complicates the issue of fermentation reaction monitoring because it is difficult to identify the components present in the broth.[9] As the number of components which are being monitored increases, so does the complexity of data processing and identification of compounds. This is where the benefits of multivariate data analysis are advantageous. Therefore, there is a need to improve fermentation reaction monitoring during the development and manufacturing of products. The work carried out in this thesis will make a novel contribution in both passive and active acoustic methodology used to characterise bubbles in a liquid phase.

The next Chapter expands on process analysis and discusses bioprocess monitoring and the spectroscopic and chromatographic techniques which can be used to monitor bioprocesses. Following from this acoustic theory is discussed before a review of passive and active acoustic literature is given in relation to bubbles.

## 1.4 References


1. P. F. Stanbury, A. Whitaker, S. J. Hall, *Principles of Fermentation Technology*, 2nd ed., New York, London, Butterworth Heinemann, 1995, p 9, 93 – 122
2. O. P. Ward, *Fermentation Biotechnology*, 1st ed., Milton Keynes, Open University Press, 1989, p 38 – 58
3. E. M. T. El-Mansi, F. B. Ward, *Fermentation Microbiology and Biotechnology*, Edited by E. M. T. El-Mansi, C. F. A. Bryce, A. L. Demain, A. R. Allman, 2nd ed., New York, London, Taylor and Francis, 2007, p 11 – 46
4. D. I. C. Wang, C. L. Cooney, A. L. Demain, P. Dunnill, A. E. Humphrey, M. D. Lilly, *Fermentation and Enzyme Technology*, 1st ed., New York, Chichester, John Wiley & Sons Ltd., 1979, p 57 – 97
5. C. T. Calan, *Process Development in Antibiotic Fermentations*, 1st ed., Cambridge, New York, Cambridge University Press, 1987, p 181 – 199
6. J. W. Peterson, A. H. Ullman, Process Analysis: Introduction, in *Encyclopedia of Analytical Chemistry*, Edited by. R. A. Meyers, John Wiley & Sons Ltd., Chichester, 2000
7. G. Montague, *Monitoring and Control of Fermenters*, Liverpool, Institute of Chemical Engineers, 1997, p 14 – 35
8. A. Ritzka, P. Sosnitza, R. Ulber, T. Scheper, Fermentation Monitoring and Process Control, *Current Opinion in Biotechnology*, 1997, **8**, 160 – 164
9. M. N. Pons, S. Le Bonté, O. Potier, Spectral Analysis and Fingerprinting for Biomedia Characterisation, *Journal of Biotechnology*, 2004, **113**, 211 – 230
10. P. Hauptmann, R. Lucklum, A. Püttmer and B. Henning, Ultrasonic Sensors for Process Monitoring and Chemical Analysis: State-of-the-art and Trends. *Sensors and Actuators A*, 1998, **67**, 32 – 48

# Chapter 2

# Process Analysis and Bioprocess Monitoring

## 2.1 Process Analysis

The techniques of process analysis used in industry differ, in terms of resolution and sensitivity, to those which are used in the laboratory. Also, the way in which a technique is used, has to be modified to suit the process and/or reactor setting e.g. in the type of analysis that us being carried out.[1] The techniques used in industry should ideally have little or no human intervention. The driving force behind process analytical technologies in industry is economics: to reduce plant down time, reduce sampling time, limit the time for sample transportation, increase safety and improve the yield and quality of product. Of course, reducing these factors has a benefit of reducing labour costs and increasing plant productivity.[1] Process analysis can be carried out in a number of ways:[1]

- Off-line – the sample is taken manually from the process and analysed in a remote laboratory. This method can be time consuming. A problem associated with off-line analysis is obtaining a sample which is representative of the reaction.[1]
- At-line – the sample is taken manually and analysed near the process using simple or complex analytical techniques. However, these techniques can not be time consuming or involve extensive experimental methodologies. The benefits of performing at-line measurements come if the process has a large lag time, e.g. hours.[1]

Both off-line and at-line analyses involve the manual reporting of the results to the control room. There are issues with sampling for both off-line and at-line analyses as the process needs to be disturbed in order to collect the sample.

- On-line analysis is where the probe is part of the process and a sample is withdrawn, through a side stream or a sampling loop, for example, and

analysed directly. The results are sent to the control room in real time. Advantages of on-line sampling are that it can be carried out on a regular (computer-controlled) basis and more than one analysing instrument can be part of the process. Also that there is no time lag between taking measurements and processing data to obtain information about the process being monitored.[1]

- In-line measurements are where a probe is inserted into the process, as opposed to a sample being taken out. Therefore, the sample is analysed *in situ* in the process stream.[1] In-line analysis has the advantage that less valves and pipes are needed, but has the major disadvantage that if the probe needs to be maintained or cleaned then the process must be shut down while the probe is removed.[7] One way of combating this is to use retractable probes.

The main difference between in-line and on-line analysis is that samples are not removed from the process for in-line analysis. Also, on-line analysis is more expensive than in-line analysis due to the complexity in the infrastructure required, for example adding a sampling loop.[1]

In addition to the above terms, process analytical techniques can also be classed as invasive and non-invasive.[1] Invasive techniques involve direct contact with the process stream. These techniques can introduce impurities into the process, which could effect some processes, such as fermentation reactions, where sterility needs to be maintained.[1] The reverse can also be true where the process could damage the probe if, for example, the conditions are too acidic. Non-invasive techniques do not come into contact with the process stream at all.[1] Acoustic monitoring of processes is a prime example of this, where a transducer or sensor can be attached to the outside of a pipe or vessel. Non-invasive measurements using acoustics have the added advantage that ultrasound can travel through optically opaque containers such as pipes, vessels or reactors.[1]

## 2.2 Bioprocess Monitoring

There are various factors which must be taken into account when selecting the most appropriate technique for monitoring of bioprocesses. Some of these are selectivity, sensitivity, response time, robustness, cost of implementation, maintenance and life-time.[1] Techniques reported in the literature for monitoring fermentation reactions include;[2-37] near infra-red (NIR),[2-15,33-35] mid infra-red (MIR),[4,16-26,32,33] Raman[27-35] and ultraviolet/visible (UV/VIS)[4,35-37] spectrometries, gas and liquid chromatography,[5,7,19-21,30,32,33,38-44] oxygen and pH sensors and a variety of other techniques (including on-line mass spectrometry).[35,45-66] All these techniques have applications for off-line, at-line, in-line and on-line analysis, these are discussed in more detail in the sections which follow. From the literature, it is apparent that there are very few applications of on-line monitoring of bioprocesses. Firstly spectroscopic techniques will be discussed, followed by chromatographic techniques and lastly other techniques that are used for bioprocess monitoring will be discussed.

### 2.2.1 Optical Spectroscopic Techniques

Spectroscopic techniques include NIR, MIR, Raman and UV/VIS. For on-line analysis optical techniques (vibrational spectroscopy) are more popular than chromatographic techniques. This is due to their rapid response times and when optical fibre coupled system are used, real time analysis can be carried out.[2] However, chromatographic techniques are used off-line to carry out a reference assay of the fermentation broth.

When comparing NIR with MIR, NIR has the disadvantage that the spectra contain weak, broad and overlapping peaks. Due to the presence of these broad overlapping peaks, there is a need to use chemometrics in data analysis. However, NIR has the advantage over MIR in that NIR allows the use of optical fibres to transmit light over considerable distances.[3] This could be particularly important in processes which contain flammable substances and is also important for on-line measurements.[3] NIR spectrometry can use silica fibres where MIR spectrometry cannot. The NIR region

extends from 780 to 2526 nm (or 12,820 – 3959 $cm^{-1}$).[3] The NIR region is useful when looking for hydrogen atoms bound to a heteroatom (e.g. O-H, N-H, C-H),[4] this means that inorganic compounds that do not contain hydrogen do not give a spectrum.[4] NIR measurements can be made in three different modes; transmission, diffuse reflectance and transflectance.[4] There are few applications of NIR spectrometry to on-line fermentation monitoring. Since fermentation samples are complex multiphase media, scattering and absorption of light can occur, therefore creating difficulties in building robust models to interpret data from the process.[5-15]

Yano *et al.* studied the fermentation of a culture broth of rice vinegar by monitoring the concentrations of ethanol and acetic acid on-line.[5] They concluded that it is possible to measure the concentration of ethanol and acetic acid simultaneously. The time for the measurement was short (5 minutes) and once the culture broth had been analysed on-line, it was possible to return the sample to the fermentor.[5] A further advantage of analysing fermentation reactions by NIR spectrometry, is that more than one chemical species can be analysed (off-line or at-line) at the same time from the same spectrum, therefore reducing the number of samples that need to be taken.[6] Using NIR removes steps such as weighing, dilution etc which improves the precision and accuracy of the results obtained.[6] Forbes *et al.* used X-charts to display results obtained from at-line monitoring of a fermentation reaction over a period of 7 months, which gave an excellent visual representation of the results.[6] X-charts are similar to moving average charts in that they have upper and lower control limits, such that the quality of the product produced can be readily visualised, within acceptable limits. Cozzolino *et al.* investigated the use of NIR spectrometry for in-line monitoring of a wine fermentation.[7] There were changes in absorption in the 2200 – 2300 nm region (corresponding to the alcohol functional group) and this was due to an increase in alcohol concentration and decrease in sugar production as the fermentation reaction progressed.[7] It should be noted that they also observed changes in the visible region (~540 nm) and attributed this to the extraction of the phenolic pigments from the grape skins into the wine as the fermentation reaction continued. They concluded that more work was needed to analyse the spectral changes for a fermentation reaction.[7] However, Zeaiter *et al.* also studied wine

fermentation using NIR spectrometry.[8] Rather then using traditional chemometric methods of data analysis such as correlation plots,[5] analysis of variance, principal component analysis (PCA) and partial least squares (PLS),[6] X-chart analysis,[6] they developed a new method of on-line analysis called dynamic orthogonal projection.[8] This method improves the robustness of the calibration using only a few reference measurements and the calibration database. It consists of the construction of a partial least squares calibration model followed by a dynamic orthogonal projection using a predetermined equation.[8] Dynamic orthogonal projection was used as an on-line diagnosis tool. Advantages of the new method are: the whole calibration data set is used, the correction is embedded into the model and multiple influence factors can be used.[8]

A great deal of work on the NIR monitoring of fermentation reactions has been carried out by the Strathclyde Fermentation Centre.[9-15] Vaidyanathan *et al.* studied the effect of morphology on the NIR spectrum of a fermentation broth.[9] They studied four different morphologies; unbranched, branched, simple clumps and clumps, and concluded that the NIR spectrum is dependent on morphology. They were able to group spectra into low, medium and high biomass concentrations using principal component analysis.[9] Arnold *et al.* cultivated *Streptomyces fradiae* which involved a four phase medium - oil, water, air bubbles and mycelial organism. Measurements were carried out at-line and also in a submerged cultivation. The research highlighted the sampling difficulties which have to be over come when working with a four phase medium.[10] Further at-line analysis with submerged cultivations, which involved more than one phase, was carried out by Vaidyanathan *et al.*. Partial least squares multivariate models were used to obtain good predictions of the analytes.[11] The above work was carried out using laboratory-scale reactors. Work has also been carried out on industrial-scale fermentations using at-line, *in-situ* probes[12] and on-line using a transmission, immersion probe.[13] Work involving mammalian cell cultivation, in which an *in-situ* probe was used in a fed-batch reactor has also been carried out.[14] An earlier publication by the same group involved NIR characterisation of biomass from five microorganisms commonly used in bioprocesses.[15] The five microorganisms were *Escherichia coli, Streptomyces*

*fradiae, Penicillium chrysogenum, Aspergillus niger* and *Aureobasidium pullulans*. They found that drying the cells to minimise free water enhanced the NIR signals of the biomass and that the most important peaks occurred at similar wavelengths for all five microorganisms, this was carried out off-line.[15] It is evident that the use of NIR spectrometry to study fermentation reactions is more commonly applied to off-line and at-line measurements.

An important sub-region of the infrared region is mid-infrared (MIR). The MIR region of the spectrum is 2500 – 40,000 nm (400 – 4000 $cm^{-1}$).[16] Both MIR and NIR spectra arise from transitions between quantised vibrational energy states. Spectra obtained in the MIR region have higher resolution than NIR spectra. MIR itself is not very applicable to on-line process monitoring because of the difficulties in transmitting MIR light down optical fibres, therefore most applications are for off-line or at-line analysis. However, the application and development of optical fibres and probes are allowing some applications to bioprocess monitoring to be established.[16,17,19-26] Unlike NIR, the fibres for MIR have be to shorter (because MIR light cannot travel far along the materials the fibres are made from) and the material from which they are made from can obscure some of the MIR region leaving the important fingerprint region open for interpretation.[18] MIR cannot use standard optical fibres, specially made fibres are required. Typical fibres used for MIR spectroscopy include silver halide and chalcogenide.

The development of Fourier transform-NIR (FT-NIR) and FT-MIR instruments has allowed noise to be reduced thus allowing both techniques to be applied in more cases.[16] Also the development of attenuated total reflectance (ATR) probes has allowed the use of the technique for on-line monitoring, giving rise to FT-MIR-ATR technology. It should be noted that there are different types of systems, for example in MIR there are filter; dispersive; and FT-IR systems. Figure 2.1 shows how MIR can be used *in-situ* and on-line (via a side stream or bypass loop).[16]

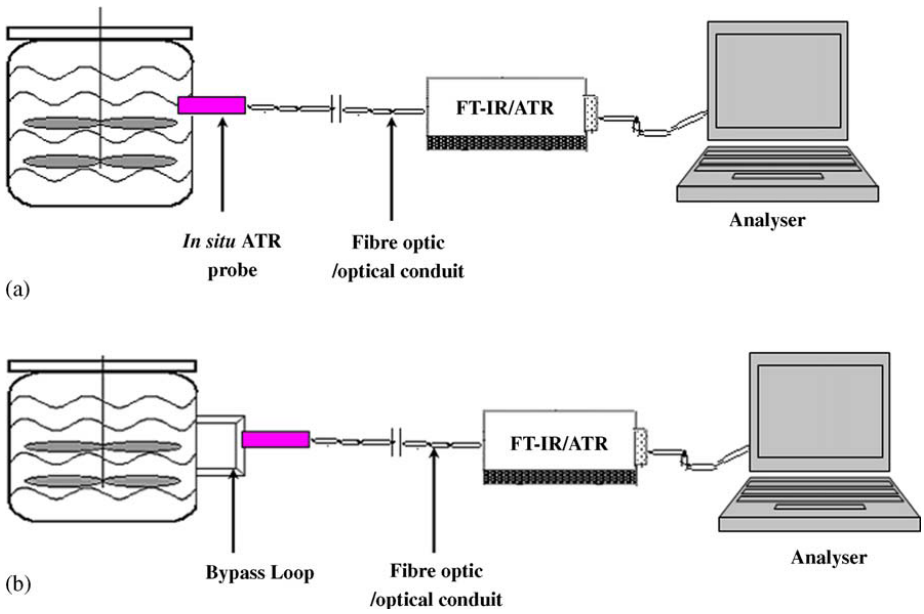


**Figure 2.1 – (a) *In-situ* and (b) on-line process monitoring using FT-MIR-ATR[16]**

The development of the ATR probe has removed the need for sample preparation because the probe is *in-situ* in the fermenter and only requires a small path length. This allows multiple measurements to be taken.[16]

In an application to study wine fermentation, one group investigated a problem where yeast sugar consumption slows down or stops completely.[19] Temperature was found to have an effect on the rate of fermentation and MIR spectrometry was used to monitor the fermentation reaction at-line. The fermentation reaction was monitored over a period of 94 hours. The water peak around 1650 $cm^{-1}$ did not change much. This was expected as the water content in the grape and the finished wine is similar.[19] As the fermentation reaction progressed, the bands at 1036, 1065, 1080, 1104 and 1152 $cm^{-1}$ (corresponding to glucose and fructose) decreased in absorbance, which indicated that the fermentation reaction was progressing. It was concluded that MIR spectroscopy can be used to monitor fermentation reactions. However, it is difficult to predict if problems will occur with the reaction, for example, the reaction not progressing as expected .[19]

Kornmann *et al.* developed an interesting calibration method for data obtained from a reaction monitored on-line and *in-situ* by MIR spectrometry. Sampling was achieved by using an ATR probe. The calibration model used was partial least squares regression.[20] The calibration method involved making synthetic solutions that mimicked the fermentation reaction. Calibration standards were produced for fructose, acetate, ethanol, ammonium, gluconacetan and phosphate, all common chemicals of a fermentation reaction. The advantage of this calibration method is that the standards can be stored and used for more than one fermentation reaction. Fayolle *et al.* monitored lactic acid production at-line during a fermentation reaction using MIR spectrometry.[21] It was possible to monitor the standard fermentation reaction components e.g. lactose, galactose. Again, partial least squares regression was used as the calibration method.

The Strathclyde Fermentation Centre has also investigated fermentation reactions involving the bacterium *Streptomyces (clavuligerus)* which is important for antibiotic production.[22,23] The group managed successful at-line monitoring of glycerol and clavulanic acid with validation using at-line ATR-MIR spectrometry.[22,23] In other work done by the group, again using at-line ATR-MIR spectrometry, they monitored glucose, ammonium, methyl oleate and biomass during the fermentation reaction.[23] In both cases partial least squares was again used as the calibration model.

In addition to the above, on-line monitoring of an acetone-butanol fermentation reaction involving *Clostridium beijerinckii* has also been carried out using MIR spectroscopy.[24] In this work five analytes (acetone, acetate, *n*-butanol, butyrate and glucose) were detected. In addition to fermentation reactions, MIR spectroscopy has also been used to monitor other bioprocesses, such as biotransformations,[25] and it also has a variety of bioanalytical applications such as topical skin analysis, microanalysis of tissues and body fluids.[26]

The next two spectroscopic techniques which will be discussed are that of Raman and UV/VIS spectrometries. From a review of the literature it is evident that these techniques have limited application in the monitoring of fermentation reactions.

Firstly Raman spectroscopy will be considered. This is the measurement of modified scattered laser light, which gives rise to information on the molecular structure of a substance.[27] Fluorescence is a problem associated with Raman spectroscopy and can be significant with lasers of wavelengths of 532 nm and 633 nm, which correspond to a YAG and helium-neon laser, respectively. Lasers of higher wavelengths, for example a 785 nm diode laser, produce less fluorescence. One advantage of using Raman spectroscopy is that the sensitivity is adequate for sampling to be achieved within a matter of seconds or minutes.[27] An advantage of Raman spectrometry over NIR spectrometry is that Raman spectra have more distinct peaks than NIR spectra. Disadvantages associated with Raman include: samples which fluoresce, Raman is less sensitive (application dependent) than NIR and MIR and that lasers do not have a long life-time.[27] If Raman spectrometry is to be used as a process analytical tool then the replacement of the laser must be taken into consideration during the planning stages for reaction monitoring.[27]

One paper describes the use of dispersive Raman spectroscopy for the on-line, non-invasive monitoring of glucose fermentation by following two biotransformations.[28] In this work a 780 nm diode laser was used. The work showed that by monitoring a spectral peak at 877 $cm^{-1}$ it is possible to see the biotransformation taking place, this peak corresponds to C–C–O symmetrical stretching of ethanol.[28] The group reported that the amount of data collected from Raman spectroscopy is larger (compared to MIR and NIR spectrometry) and that it is only necessary to measure known or observed peaks to decrease the amount of data and speed up analysis times.[28] Cannizzaro *et al.* used on-line Raman spectrometry to investigate carotenoid synthesis by microorganisms.[29] Cartenoids are important primarily for their medicinal properties and also their role in photosynthesis, they are often found in food also. Using Raman spectroscopy, the group were able to determine the cartenoid concentration level in the bioprocess without using multivariate techniques.[29]

Lee *et al.* used Raman spectroscopy on-line to monitor two bio-reactions of phenylalanine by *Escherichia coli*, where the main fermentation products are acetate,

formate, lactate and succinate.[30] In more recent work, Kim *et al.* developed a non-invasive Raman method for monitoring pharmaceutical liquids.[31] They were successfully able to monitor the production of the pharmaceutical liquid using a partial least squares technique. This could be a promising technique for at-line reaction monitoring.[31] Modification of the process to incorporate a sampling loop, for example, could yield the technique suitable for on-line monitoring.

As has already been stated MIR spectrometry yields a great deal of spectral information when compared to NIR spectrometry, but the fibre optics for MIR spectrometry are not as good as those for NIR. NIR spectrometry gives little spectral information but the fibre optics are better than MIR. Raman spectrometry offers a solution to both of these problems, as it can generate spectral information relating to structure and it also has a good fibre optic system, which is less expensive, robust and compatible with silica fibres.[27] The performance of Raman spectrometry has been compared to NIR and MIR spectrometries by a few groups.[32-35] Sivakesava *et al.* applied at-line FT-MIR and FT-Raman techniques for monitoring glucose and ethanol combination with multivariate statistical analysis.[32] They were able to assign peaks to the MIR spectrum at various stages throughout the fermentation reaction. In the Raman studies, spectral peaks were observed for glucose, ethanol and proteins, however these were much weaker than the MIR spectral peaks.[32] This highlights the differences in sensitivities between Raman and MIR spectrometries. It was concluded that FT-IR spectrometry could characterise all the components needed, whereas FT-Raman spectrometry is only suitable if they are present in high concentrations.[32] In recent work carried out by the same group they employed NIR spectrometry (in addition to FT-MIR and FT-Raman spectrometries) to study a different bacterium, *Lactobacillus casei*.[33] The same conclusions were drawn that FT-MIR spectrometry was the superior technique and NIR spectrometry was found to be comparable with FT-Raman spectrometry.[33] Other groups have compared process analysis techniques, although not in a fermentation context.[34,35] They concluded that in-line NIR spectrometry gave more precise results than in-line Raman spectrometry. Multivariate calibration models were required for data analysis

using in-line NIR spectrometry whereas univariate calibration models were sufficient for data analysis using in-line Raman spectrometry.

UV spectrophotometers used in fermentation monitoring make use of a charged couple device or photodiode instead of a photomultiplier, which is used in laboratory systems.[36] Benefits of using UV spectrometry to monitor processes are: low cost, high analysis speed and robustness. UV spectrometry, like NIR spectrometry does not share the problem of fibre optic length that MIR spectrometry has. Within pharmaceutical processes, UV/VIS spectrometers can be used in antibiotic manufacturing as antibiotics have strong UV absorptions.[37] One group monitored a fermentation reaction at-line involving the bacterium *Saccharomyces cerevisiae* on a compact UV spectrophotometer.[36] The spectrophotometer was able to collect up to 16 spectra every second. This research demonstrated that the instrument could be attached to any automated control system because of it small size.[36]

### 2.2.2 Chromatographic Techniques

Process gas chromatography (GC) is developing as a very useful technique for the on-line monitoring of processes.[38] The chromatographic read-out from process GC shows any relationship between concentration and time per analyte. Depending on the detector used, some can automatically identify the analyte in question. Some advantages of GC are: that process GC can be included in a closed-loop, less man power is needed, quicker analysis time and it can be used in hazardous environments.[38]

In most current applications chromatographic techniques tend to be used off-line to monitor fermentation reactions. Typically chromatographic techniques are used as an assay reference method where GC[5,35] or high-performance liquid chromatography (HPLC)[7,19-21,30,32,33] are also used to measure concentrations of analytes in the culture broth. The typical detector that is used is the flame ionisation detector,[5] other detectors include the thermal conductivity detector and the flame photometric

detector.[38] Other types of chromatography have been used as reference methods such as ion exchange chromatography.[20]

Liquid chromatography (LC) has been used to monitor fermentation reactions on-line, although an ultrafiltration pre-treatment step was required.[39,40] The ultrafiltration step was carried out before the sample was introduced (in one case the sample was introduced automatically[40]) to the LC and involved passing the sample through a series of membranes (at a pressure of 0.2 – 0.3 bar[39]) between the fermenter and the LC.[40] A peristaltic pump was used to supply the LC with a continual feed of the fermentation medium because the flow rate can be regulated. The bioprocess studied was the production of a recombinant protein using *Escherichia coli*.[39] Anywhere between 5 and 12 samples can be taken per hour using this system.[40] In earlier work the group concluded that up to 15 amino acids could be monitored using this method.[39] Although this method has been tested on-line[40] there was a time delay of 40 – 60 minutes between analysing the sample and getting the concentration information from the chromatogram, which shows it can not deliver real-time measurements. In another study, HPLC has been used to monitor a fermentation process on-line.[41] This group studied the ethanol fermentation of *Zymomonas mobilis*. Samples were taken automatically from the fermenter and introduced to the HPLC. This proved effective for determining ethanol and glucose concentrations.[41]

Chromatographic techniques can also be coupled to mass spectrometers (MS) for fermentation monitoring.[42-44] The sample is transferred automatically from the fermenter to the GC by a probe and then from the GC to the MS *via* a capillary column. The probe, which is inserted into the fermentation medium, allows gases and volatile components to be absorbed through the membrane and semi-volatile components are dissolved in the membrane; particles and ions do not interfere with the probe membrane at all.[42] Other research commented on the use of a thermal membrane desorption application,[43] where analytes absorb according to their affinity for the membrane. It appears from reading the literature, that most sampling from the liquid phase of a fermentation reaction, has been done by a peristaltic pump for

GC-MS systems.[43] The sampling time, injection time, flow rate and temperature were all varied to asses the way the analytes were adsorbed onto the membrane. It was shown that the thermal membrane desorption application is suited to non-polar and aprotic analytes.[43] The above applications employed a quadrapole MS system.[42,43] There has been an application of LC–electrospray ionisation (EIS)–MS–MS to monitoring 20 amino acids during fermentation.[44] The aim of this work was to develop a rapid LC–EIS–MS–MS laboratory method (by rapid, the authors indicated less than 5 minutes).[44]

### 2.2.3 Other Techniques

A variety of other techniques have been used in bioprocess monitoring. An important feature of (bio-)sensors, and indeed the techniques mentioned so far, is that they must be capable of functioning over the duration of the fermentation reaction, even in extreme conditions, without encountering problems, such as fouling.[45] There are a large number of sensors that have been developed in the laboratory but only a handful of these actually may see the light of day in an industrial application.[45] The 'classical' sensors used for monitoring a fermentation reaction are those for monitoring pH, dissolved oxygen and dissolved carbon dioxide.[46] In a fermentation reaction it is known that one of the contributing factors to biomass growth is pH. To monitor these properties a glass electrode is employed.[46] Another factor which contributes to cell growth is that of dissolved oxygen. This can be monitored in the off-gas or in the liquid to make a measure of how much oxygen is being taken up by the culture. The typical instrument used to measure oxygen in the exhaust gas is the Clark-type electrode.[46] Another method for measuring dissolved oxygen is by fluorescence (see later), these techniques can complement each other as Clark electrodes are better for measuring high concentrations and fluorescence is better for low concentrations.[46] It is also possible to measure carbon dioxide, the resultant product of respiration. One such sensor is the Severinghaus-type electrode used in the exhaust gas.[46] Furthermore, if the membrane in a carbon dioxide sensor was to fail and break, it would contaminate the reaction broth.[46] An example of the use of a pH sensor is in the fermentation of yeast under aerobic conditions.[47] It was

concluded that the specific rate of proton production should be proportional to biomass concentration; where the ratio of protons concentration to biomass concentration should remain constant with a mean value of 0.15 .[47]

A series of sensors for the monitoring of key fermentation compounds has been developed.[48] One of these was a chemiluminescence sensor, which incorporated the use of a photodiode, for the determination of serum uric acid. A second sensor for monitoring hydrogen peroxide was used to monitor a glutamate fermentation reaction. Here both glucose and glutamate were monitored as these key compounds show if the reaction is progressing.[48] An enzyme field effect transistor sensor was used to monitor penicillin-G contamination in a penicillin fermentation process.[48] However, it was not possible to determine the concentration of penicillin-G using the sensor alone, due to the specificity of the enzyme in the reaction, therefore off-line HPLC was used in addition to the sensor. For all three sensors it was found that the precision of repeat measurements was within 8 %, and so further refining of the sensors will be needed before they can be used in an industrial application.[48] In addition to the above sensors, there have also been successful attempts at making sensors for glucose and other key fermentation analytes.[49] A sensor has been developed that utilises the glucose oxidase catalysed reaction of glucose. A product of this reaction is hydrogen peroxide, which can be detected using the sensor.[49] This sensor was automated to give results in real-time. The authors say that the sensor developed for glucose could be modified to monitor for lactate and sucrose.[49] Other sensors developed for fermentation monitoring include the enzyme thermistor[50] and capacitance probes.[51] In 2008, Fan *et al.* produced a comprehensive review of biosensors, which are used for detecting various biomolecules, the interested reader is directed to this reference.[52]

Mass spectrometry as a tool for process analysis has already been described when coupled to gas chromatography. The largest use of mass spectrometry, in this context, is for the analysis of the volatile off-gases and bulk gases ($CO_2$ and $O_2$) from a fermentation reaction. However mass spectrometry can also be used on its own with a membrane inlet system.[53,54] In addition to the spectroscopic, chromatographic

and sensor methods for fermentation monitoring, the following are other methods which have been described in the literature for bioprocess monitoring: flow injection analysis,[55-59] process NMR,[60,61] fluorescence,[62-64] electrophoresis,[65] biocalorimetry,[66] non-linear dielectric spectroscopy[67] and electronic tongue.[68] More recently, for the use of fluorescence, a new method of multivariate fluorescence spectroscopy has been developed to monitor bioprocesses on-line without the need for reference concentrations of analytes, such as biomass and ethanol.[64]

It has been shown that a variety of spectroscopic, chromatographic and other techniques have been used for off-line or at-line bioprocess monitoring, where active sampling of material from the process stream is required i.e. directly taking a sample out. Disadvantages of using some spectroscopic techniques are, for example, MIR spectrometry due to the fibre optics, NIR spectrometry due to the spectral resolution and information it yields. Generally, Raman spectrometry is very much application dependent, less sensitive and has problems with fluorescence. Optical techniques tend to give rise to chemical information, in the case of NIR spectrometry physical information can also be obtained, although currently there is a need to develop techniques which give rise to more physical information. Currently, chromatographic techniques tend to be limited to off-line analysis and the assaying of references. Sampling is major issue associated with monitoring fermentation reactions because sterility has to be maintained. Therefore a non-invasive method would be most advantageous. Another problem associated with fermentation reactions are that they are multiphase media, this gives rise to problems in identifying components of the media. Hence, this is why robust multivariate models of data analysis are required. The use of acoustics to address these problems is developed further in the next chapter.

## 2.3 References


1. J. W. Peterson, A. H. Ullman, Process Analysis: Introduction, in *Encyclopedia of Analytical Chemistry*, Edited by R. A. Meyers, John Wiley & Sons Ltd., Chichester, 2000
2. C. Coffey, B. E. Cooley Jr., D. S. Walker, Real Time Quantitation of a Chemical Reaction by Fiber Optic Near-infrared Spectroscopy, *Analytica Chimica Acta*, 1999, **395**, 335 – 341
3. D. S. Goldman, Near-infrared Spectroscopy in Process Analysis, in *Encyclopedia of Analytical Chemistry*, Edited by. R. A. Meyers, John Wiley & Sons Ltd., Chichester, 2000
4. M. –N. Pons, S. Le Bonté, O. Potier, Spectral Analysis and Fingerprinting for Biomedia Characterisation, *Journal of Biotechnology*, 2004, **113**, 211 – 230
5. T. Yano, T. Aimi, Y. Nakano, M. Tamai, Prediction of the Concentrations of Ethanol and Acetic Acid in the Culture Broth of a Rice Vinegar Fermentation Using Near-Infrared Spectroscopy, *Journal of Fermentation and Bioengineering*, 1997, **84 (5)**, 461 – 465
6. R. A. Forbes, M. Z. Luo, D. R. Smith, Measurement of Potency and Lipids in Monensin Fermentation Broth by Near-Infrared Spectroscopy, *Journal of Pharmaceutical and Biomedical Analysis*, 2001, **25**, 239 – 256
7. D. Cozzolino, M. J. Kwiatowski, M. Parker, W. U. Cynkar, R. G. Dambergs, M. Gishen, M. J. Herderich, Prediction of Phenolic Compounds in Red Wine Fermentations by Visible and Near Infrared Spectroscopy, *Analytica Chimica Acta*, 2004, **513**, 73 – 80
8. M. Zeaiter, J. M. Roger, V. Bellon-Maurel, Dynamic Orthogonal Projection. A New Method to Maintain the On-line Robustness of Multivariate Calibrations. Application to NIR-based Monitoring of Wine Fermentations, *Chemometrics and Intelligent Laboratory Systems*, 2006, **80**, 227 – 235
9. S. Vaidyanathan, S. White, L. M. Havey, B. McNeil, Influence of Morphology on the Near-Infrared Spectra of Mycelial Biomass and its Implications in Bioprocess Monitoring, *Biotechnology and Bioengineering*, 2003, **82 (6)**, 715 – 724

10. S. A. Arnold, J. Crawley, S. Vaidyanathan, L. Matheson, P. Mohan, J. W. Hall, L. M. Harvey, B. McNeil, At-line Monitoring of a Submerged Filamentous Bacterial Cultivation using Near-Infrared Spectroscopy, *Enzyme and Microbial Technology*, 2000, **27**, 691 – 697

11. S. Vaidyanathan, L. M. Harvey, B. NcNeil, Deconvolution of Near-Infrared Spectral Information for Monitoring Mycelial Biomass and other Key Analytes in a Submerged Fungal Bioprocess, *Analytica Chimica Acta*, 2001, **428**, 41 – 59

12. J. W. Hall, B. NcNeil, M. J. Rollins, I. Draper, B. G. Thompson, G. Macaloney, Near-Infrared Spectroscopic Determination of Acetate, Ammonium, Biomass and Glycerol in an Industrial *Escherichia coli* Fermentation, *Applied Spectroscopy*, 1996, **50 (1)**, 102 – 108

13. S. A. Arnold, R. Gaensakoo, L. M. Harvey, B. McNeil, Use of At-line and In-Situ Near-Infrared Spectroscopy to Monitor Biomass in an Industrial Fed-batch *Escherichia coli* Process, *Biotechnology and Bioengineering*, 2002, **80 (4)**, 405 – 413

14. S. A. Arnold, J. Crowley, N. Woods, L. M. Harvey, B. McNeil, In-Situ Near Infrared Spectroscopy to Monitor Key Analytes in Mammilian Cell Cultivation, *Biotechnology and Bioengineering*, 2003, **84 (1)**, 13 – 19

15. S. Vaidyanathan, G. Macaloney, B. McNeil, Fundamental Investigation on the Near-Infrared Spectra of Microbial Biomass as Applicable to Bioprocess Monitoring, *The Analyst*, 1999, **124**, 157 – 162

16. P. Roychoudhury, L. M. Harvey, B. McNeil, The Potential of Mid-Infrared Spectroscopy (MIRS) for Real Time Bioprocess Monitoring, *Analytica Chimica, Acta*, 2006, **571**, 159 – 166

17. B. Lendi, B. Mizaikoff, in *Handbook of Vibrational Spectroscopy*, Edited by J. M. Chalmers, P. R. Griffiths, vol. 2, John Wiley & Sons Ltd., Chichester, 2002, p. 1541

18. P. J. Melling, M. Thomson, in *Handbook of Vibrational Spectroscopy*, Edited by J. M. Chalmers, P. R. Griffiths, Vol. 2, John Wiley & Sons, Chichester, 2002, p. 1551

19. A. Urtubia, J. R. Pérez-correa, F. Pizarro, E. Agosin, Exploring the Applicability of MIR Spectroscopy to Detect Early Indications of Wine Fermentation Problems, *Food Control*, 2008, **14 (4)**, 382 – 388

20. H. Kornmann, S. Valentinotti, P. Duboc, I. Marison, U. von Stockar, Monitoring and Control of *Gluconacetobacter xylinus*, Fed-Batch Cultures using In Situ Mid-IR Spectroscopy*, Journal of Biotechnology*, 2004, **113**, 231 – 245

21. P. Fayolle, D. Picque, G. Corrieu, Monitoring of Fermentation Processes Producing Lactic Acid Bacteria by Mid-Infrared Spectroscopy, *Vibrational Spectroscopy*, 1997, **14**, 247 – 252

22. P. Roychoudhury, B. McNeil, L. M. Harvey, Simultaneous Determination of Glycerol and Clavulanic Acid in an Antibiotic Bioprocess using Attenuated Total Reflectance Min Infrared Spectroscopy, *Analytica Chimica Acta*, 2007, **585**, 246 – 252

23. P. Roychoudhury, L. M. Harvey, B. McNeil, At-line Monitoring of Ammonium, Glucose, Methyl Oleate and Biomass in a Complex Antibiotic Fermentation Process using Attenuated Total Reflectance-Mid-Infrared (ATR-MIR) Spectroscopy, *Analytica Chimica, Acta*, 2006, **561**, 218 – 224

24. M. Kansiz, J. R. Gapes, D. McNaughton, B. Lendl, K. C. Schuster, Mid-Infrared Spectroscopy Coupled to Sequential Injection Analysis for the On-line Monitoring of the Acetone-Butanol Fermentation Process, *Analytica Chimica Acta*, 2001, **438**, 175 – 186

25. M. R. Dadd, D. C. A. Sharp, A. J. Pettman, C. J. Knowles, Real-time Monitoring of Nitrile Biotransformation by Mid-Infrared Spectroscopy, *Journal of Microbiological Methods*, 2001, **41**, 69 – 75

26. H. M. Heise, L. Küpper, L. N. Butvina, Bio-analytical Applications of Mid-Infrared Spectroscopy using Silver Halide Fibre-Optic Probes, *Spectrochimica Acta Part B*, 2002, **57**, 1649 – 1663

27. M. A. Leugers, E. D. Lipp, Raman Spectroscopy in Process Analysis, in *Encyclopedia of Analytical Chemistry*, Edited by R. A. Meyers, John Wiley & Sons Ltd, Chichester, 2000

28. A. D. Shaw, N. Kaderbhal, A. Jones, A. M. Woodward, R. Goodacare, J. J. Rowland, D. B. Kell, Non-invasive, On-Line Monitoring of the Biotransformation by Yeast of Glucose to Ethanol Using Dispersive Raman Spectroscopy and Chemometrics, *Applied Spectroscopy*, 1999, **53 (11)**, 1419 – 1428

29. C. Cannizzaro, M. Rhiel, I. Marison, U. von Stockar, On-Line Monitoring of *Phaffia rhodozyma* Fed-Batch Process with In Situ Dispersive Raman Spectroscopy, *Biotechnology and Bioengineering*, 2003, **83 (6)**, 668 – 680

30. H. L. T. Lee, P. Boccazzi, N. Gorret, R. J. Ram, A. J. Sinskey, In Situ Monitoring of *Escherichia coli*, Bioreactions using Raman Spectroscopy, *Vibrational Spectroscopy*, 2004, **35**, 131 – 137

31. M. Kim, H. Chung, Y. Woo, M. S. Kemper, A new Non-Invasive, Quantitative Raman Technique for the Determination of an Active Ingredient in Pharmaceutical Liquids by Direct Measurement through a Plastic Bottle, *Analytica Chimica Acta*, 2007, **587**, 200 – 207

32. S. Sivakesava, J. Irudayaraj, A. Demirci, Monitoring a Bioprocess for Ethanol Production using FT-MIR and FT-Raman Spectroscopy, *Journal of Industrial Microbiology & Biotechnology*, 2001, **26**, 185 – 190

33. S. Sivakesava, J. Irudayaraj, A. Demirci, Simultaneous Determination of Multiple Components in Lactic Acid Fermentation using FT-MIR, NIR and FT-Raman Spectroscopic Technique, *Process Biochemistry*, 2001, **37**, 371 – 379

34. A. Nordon, A. Mills, R. T. Burn, F. M. Cusick, D. Littlejohn, Comparison of Non-Invasive NIR and Raman Spectrometries for Determination of Alcohol Content in Spirits, *Analytica Chimica Acta*, 2005, **548**, 148 – 158

35. C. A. McGill, A. Nordon, D. Littlejohn, Comparison of in-line NIR, Raman, UV-Visible Spectrometries, and at-line NMR Spectrometry for the Monitoring of an Esterification Reaction, *The Analyst*, 2002, **127**, 287 – 292

36. L. Noui, J. Hill, P. J. Keay, R. Y. Wang, T. Smith, K. Yeung, G. Habib, M. Hoare, Development of a High Resolution UV Spectrophotometer for At-line Monitoring of Bioprocesses, *Chemical Engineering and Processing*, 2002, **41**, 107 – 114

37. R. S. Saltzman, Ultraviolet/Visible Spectroscopy in Process Analysis, in *Encyclopedia of Analytical Chemistry*, Edited by R. A. Meyers, John Wiley & Sons Ltd, Chichester, 2000

38. J. M. Clemons, Chromatography in Process Analysis, in *Encyclopedia of Analytical Chemistry*, Edited by R. A. Meyers, John Wiley & Sons Ltd, Chichester, 2000

39. N. C. van de Merbel, P. Zuur, M. Frijlink, J. J. M. Holthuis, H. Lingeman, U. A. Th. Brinkman, Automated Monitoring of Amino Acids during Fermentation Process using On-Line Ultrafiltration and Column Liquid Chromatography: Application to Fermentation Medium Improvement, *Analytica Chimica Acta*, 1995, **303**, 175 – 185

40. N. C. van de Merbel, The use of Ultrafiltration and Column Liquid Chromatography for On-Line Fermentation Monitoring, *Trends in Analytical Chemistry*, 1997, **16 (3)**, 162 – 172

41. Y. –C. Liu, F. –S. Wang, W. –C. Lee, On-Line Monitoring and Controlling System for Fermentation Processes, *Biochemical Engineering Journal*, 2001, **7**, 17 – 25

42. G. Matz, F. Lennemann, On-Line Monitoring of Biotechnological Processes by Gas Chromatographic – Mass Spectrometric Analysis of Fermentation Suspensions, *Journal of Chromatography A*, 1996, **750**, 141 – 149

43. G. Matz, M. Loogk, F. Lennemann, On-Line Gas Chromatography – Mass Spectrometry for Process Monitoring using Solvent-Free Sample Preparation, *Journal of Chromatography A*, 1998, **819**, 51 – 60

44. J. J. Dalluge, S. Smith, F. Sanchez-Riera, C. McGuire, R. Hobson, Potential of Fermentation Profiling via Rapid Measurement of Amino Acid Metabolism by Liquid Chromatography – Tandem Mass Spectrometry, *Journal of Chromatography A*, 2004, **1043**, 3 – 7

45. V. Vojinović, J. M. S. Cabral, L. P. Fonseca, Real-Time Bioprocess Monitoring Part 1: In Situ Sensors, *Sensors and Actuators B*, 2006, **114**, 1083 – 1091

46. P. Harms, Y. Kostov, G. Rao, Bioprocess Monitoring, *Current Opinion in Biotechnology*, 2002, **13**, 124 – 127

47. A. Vicente, J. I. Castillo, J. A. Texeira, U. Ugalde, On-Line Estimation of Biomass Through pH Control Analysis in Aerobic Yeast Fermentation Systems, *Biotechnology and Bioengineering*, 1998, **58 (4)**, 445 – 450

48. J. Liu, G. Li, Application of Biosensors for Diagnostic Analysis and Bioprocess Monitoring, *Sensors and Actuators B*, 2000, **65**, 26 – 31

49. L. Lidgren, O. Lilja, M. Krook, D. Kriz, Automatic Fermentation Control Based on a Real-Time In Situ SIRE® Biosensor regulated Glucose Feed, *Biosensors and Bioelectronics*, 2006, **21**, 2010 – 2013

50. K. Ramanathan, M. Rank, J. Svitel, A. Dzgoev, B. Danielsson, The Development and Application of Thermal Biosensors for Bioprocess Monitoring, *Tibtech*, 1999, **17**, 499 – 505

51. A. A. Neves, D. A. Pereira, L. M. Vieira, J. C. Menezes, Real Time Monitoring Biomass Concentration in *Streptomyces clavuligerus* Cultivations with Industrial Media using a Capacitance Probe, *Journal of Biotechnology*, 2000, **84**, 45 – 52

52. X. Fan, I. M. White, S. I. Shopova, H. Zhu, J. D. Suter, Y. Sun, Sensitive Optical Biosensors for Unlabeled Targets: A Review, *Analytica Chimica, Acta*, 2008, 8 – 26

53. S. Chauvatcharin, K. B. Konstantinov, K. Fujiyama, T. Seki, T. Yoshida, A Mass Spectrometry Membrane Probe and Practical Problems Associated with Its Application in Fermentation Processes, *Journal of Fermentation and Bioengineering*, 1995, **79 (5)**, 465 – 472

54. V. Tarkianinen, T. Kotiaho, I. Mattila, I. Virkajärvi, A. Aristidou, R. A. Ketola, On-line Monitoring of Continuous Beer Fermentation Process using Automatic Membrane Inlet Mass Spectrometric System, *Talanta*, 2005, **65**, 1254 – 1263

55. R. W. Min, V. Rajendran, N Larsson, L. Gorton, J. Planas, B, Hahn-Hägerdal, Simultaneous Monitoring of Glucose and *L*-Lactic Acid during a Fermentation Process in an Aqueous Two-Phase System by On-Line FIA with Microdialysis Sampling and Duel Biosensor Detector, *Analytica Chimica Acta*, 1998, **366**, 127 – 135

56. I. Rocha, E. C. Ferreira, On-Line Simultaneous Monitoring of Glucose and Acetate with FIA during High Cell Density Fermentation of Recombinant *E. coli*, *Analytica Chimica Acta*, 2002, **462**, 293 – 304

57. O. –J. Sohn, K. –A Han, J. I. Rhee, Flow Injection Analysis for Monitoring of Succinic Acid in Biotechnological Processes, *Talanta*, 2005, **65**, 185 – 191

58. S. S. M. Hassan, M. S. A. Hamza, A. H. K. Mohamed, A Novel Spectrophotometric Method for Bath and Flow Injection Determination of Sulfate in Beverages, *Analytica Chimica Acta*, 2006, **570**, 232 – 239

59. L .H. Christensen, J. Marcher, U. Schuize, M. Carisen, R. W. Min, J. Nielsen, J. Villadsen, Semi-On-Line Analysis for Fast and Precise Monitoring of Bioreaction Processes, *Biotechnology and Bioengineering*, 1996, **52**, 237 – 246

60. A. Nordon, C. A. McGill, D. Littlejohn, Process NMR Spectrometry, *The Analyst*, 2001, **126**, 260 – 272

61. S. Clark, N. W. Barnett, M. Adams, I. B. Cook, G. A. Dyson, G. Johnston, Monitoring a Commercial Fermentation with Proton Nuclear Magnetic Resonance Spectroscopy with the Aid of Chemometrics, *Analytica Chimica Acta*, 2006, **563**, 338 – 345

62. J. I. Rhee, T. –H. Kang, On-Line Process Monitoring and Chemometric Modelling with 2D Fluorescence Spectra obtained from Recombinant *E. coli* Fermentations, *Process Biochemistry*, 2007, **42**, 1124 – 1134

63. E. Skibsted, C. Lindemann, C. Roca, L. Olsson, On-Line Bioprocess Monitoring with Multi-Wavelength Fluorescence Sensor using Multivariate Calibration, *Journal of Biotechnology*, 2001, **88**, 47 – 57

64. J. M. Amigo, A. Surribas, J. Coello, J. L. Montesinos, S. Maspoch, F. Valero, On-line Parallel Factor Analysis. A step forward in the Monitoring of Bioprocesses in Real Time, *Chemometrics and Intelligent Laboratory Systems*, 2008, **92,** 44 - 52

65. H. Tahkoniemi, K. Helmja, A. Menert, M. Kaljurand, Fermentation Reactor Coupled with Capillary Electrophoresis for On-Line Bioprocess Monitoring, *Journal of Pharmaceutical and Biomedical Analysis*, 2006, **41**, 1585 – 1591

66. M. Türker, Development of Biocalorimitry as a Technique for Process Monitoring and Control in Technical Scale Fermentations, *Thermochimica Acta*, 2004, **419**, 73 – 81

67. A. M. Woodward, A. Jones, X. –Z Zhang, J. Rowland, D. B. Kell, Rapid and Non-Invasive Quantification of Metabolic Substrate in Biological Cell Suspensions using Non-Linear Dielectric Spectroscopy with Multivariate Calibration and Artificial Neural Networks. Principles and Applications, *Bioelectrochemistry and Bioenergetics*, 1996, **40**, 99 – 132

68. A. Legin, D. Kirsanov, A. Rudnitskaya, J. J. L. Iversen, B. Seleznev, K. H. Esbensen, J. Mortensen, L. P. Houmøller, Y. Vlasov, Multicomponent Analysis of Fermentation Growth Media using the Electric Tongue (ET), *Talanta*, 2004, **64**, 766 – 772

# Chapter 3

# Acoustic Techniques for Bubble Characterisation

## 3.1 Theory of Acoustic (Ultrasonic) Waves

### 3.1.1 Ultrasonic Waves

In 1982, Kinsler defined acoustics "as the generation, transmission and reception of energy in the form of vibrational waves in matter".[1] Acoustic waves can be propagated through a material in different ways, depending on the nature of the material. Two main examples of this are as follows;

*Compression (Longitudinal) Plane Wave*

In compression waves the particles which a material are made from are shifted from their position in a direction parallel to the direction of the propagating wave.[2] Solids, liquids and gases support longitudinal wave modes. This generates high density, high pressure regions, called compressions, and low density, low pressure regions called rarefractions[3] as shown in Figure 3.1.

*Transverse (Shear) Displacement Wave*

Conversely, here the propagating wave is directed parallel to the surface of the material and the particles move in a perpendicular direction i.e. they move up and down.[2] A transverse wave can be visualised by shaking a rope. The rope moves up and down but the wave travels from one end of the rope to the other end. Solids can support transverse waves, where particles move in a perpendicular direction to that of the propagated wave. Liquids and gases do not support transverse waves due to their low viscosity.[3] Longitudinal and transverse waves are shown diagrammatically in Figure 3.1.

It has to be stressed that when acoustic waves are passed through a material, it is the wave which is travelling and not the particles. The particles themselves do have slight movement in their local environment.[2]

There are other types, or modes, of ultrasonic waves that can be produced in a solid medium. These are Rayleigh, Lamb, Love, Stoneley and Faraday waves.[2] This work is primarily concerned with compression waves, although shear waves are supported in the solid vessel walls.

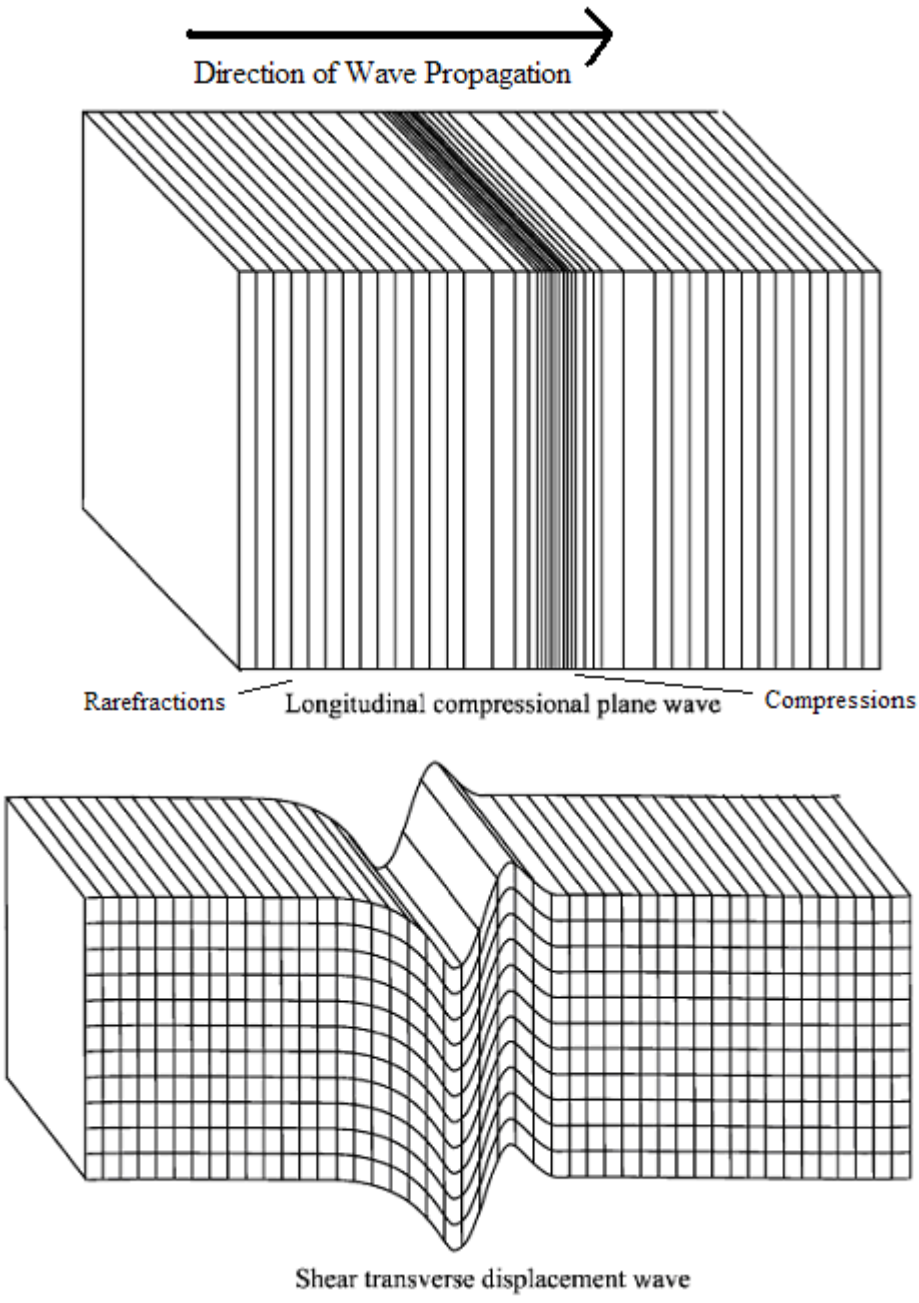


**Figure 3.1 – Compression and transverse waves[2]**

There are two main types of acoustic measurement. The first method is passive acoustics (or acoustic emission), where acoustic waves are produced by the sample itself and the sensor only acts in reception. The second method is active acoustics, where an acoustic wave is transmitted through a sample and the interaction between the sample and the propagating wave is monitored.[3]

### 3.1.2 Properties of Ultrasonic Waves

Ultrasonic waves can be characterised by a number of important physical properties including attenuation, amplitude, wavelength, velocity[3] and frequency[4]. The wavelength and attenuation are frequency dependent and are characteristic of a particular material.[4] Some of these will now be discussed. There is a mathematical equation (Equation 3.1) which relates the physical properties of a material to the ultrasonic properties of the material.[3]

$$\left(\frac{q}{\omega}\right)^2 = \frac{\rho}{E} \qquad \textbf{Equation 3.1}$$

Where:

- $\rho$ is the density,
- $E$ is the elastic modulus,
- $q$ is the complex wave number . This is material dependent given by $\omega/c + i\alpha$, $c$ is the speed of sound (group), $\alpha$ is the attenuation coefficient and $i$ is the mathematical complex number, which comprises of its real and imaginary parts,
- $\omega$ is the angular frequency (note that $\omega = 2\pi f$, where f is the frequency in Hz).[4] The physical properties of density and elastic modulus are simply related to the ultrasonic properties of the attenuation coefficient and angular frequency.

*Ultrasonic Velocity*

When the wavelength and frequency of an ultrasonic wave are known then its velocity can be found from the simple relationship $c = f\lambda$, where $c$ is the speed of sound in the medium, $f$ is the frequency and $\lambda$ is the wavelength.[4] The ultrasonic velocity can also be determined using $c = d/t$ , (where $c$ is again the speed of sound in the medium, $t$ is the time taken for the ultrasonic wave to be received and $d$ is the distance travelled by the wave) if the time taken for a wave to travel a pre-determined distance is known.[4]

For a material with low attenuation properties the velocity of the ultrasonic wave is related to the physical properties of density, $\rho$ and elastic modulus, $E$ by Equation 3.2.[4]

$$E = \rho c^2 \qquad \textbf{Equation 3.2}$$

From Equation 3.2 it may be surmised that an ultrasonic wave will travel faster for materials that have lower densities. Therefore one would expect that the ultrasonic velocity in fluids to be greater than that in solids.[4] However this is not the case as differences in the elastic moduli of materials affects the ultrasonic velocity more than density, consequently the ultrasonic velocity in solids is greater than that in liquids.[4]

*Acoustic Impedance*

Acoustic impedance can be used to measure the fraction of an ultrasonic wave that is reflected from a surface.[4] The specific acoustic impedance ($Z$) is measured as the product of the density of the material the ultrasonic wave is passing through ($\rho$) to the ultrasonic velocity ($c$), described by the equation below.

$$Z = \rho c \qquad \textbf{Equation 3.3}$$

Mathematically, $Z$ is a complex number and can be split into a real and an imaginary component, which are the resistive and reactive components respectively.[4] In materials where ultrasonic attenuation is small the imaginary part can be ignored.

The result of this is that $Z$ equals the resistive component and the acoustic impedance is now known as the characteristic impedance.

*Attenuation (Coefficient)*

Attenuation is the property of an ultrasonic wave that describes the energy that is lost from an ultrasonic wave to the medium it is travelling through. This results in a decrease in the amplitude of the ultrasonic wave.[4-5] The attenuation of an ultrasonic wave is given by the following equation.

$$A = A_0 e^{-\alpha x} \qquad \textbf{Equation 3.4}$$

where $A_0$ is the initial amplitude of the wave, $x$ is the distance travelled by the wave through the material and $\alpha$ is the attenuation coefficient. The unit of attenuation is defined in terms of length and typically is Nepers per centimetre (Np $cm^{-1}$).[6] The above relationship shows that one can measure the attenuation coefficient as a function of distance travelled.

There are two main processes responsible for attenuation of ultrasound; these are absorption and scattering. Ultrasonic wave behaviour is analogous to the behaviour of light waves. Molecular processes in homogeneous and heterogeneous materials are responsible for absorption, which results in the conversion of some ultrasound energy into heat and other forms of energy.[7] In liquids and gases adsorption usually occurs through thermal conduction, viscosity and molecular processes.[3] Scattering, on the other hand is only relevant when considering heterogeneous materials, and occurs when the ultrasonic wave encounters a irregularity in the material, which will not allow ultrasonic wave to pass through it. This results in the ultrasonic wave being scattered in a different direction to that of the incident pathway.[8] Scattering is dependent on the relationship between the wavelength of the ultrasound and the size of the particle. Scattering differs from adsorption in that the energy is still able to propagate through the medium.[8] The degree to which absorption or scattering occurs depends of the differences in the acoustic impedances of the materials.[3] The larger difference in the acoustic impedance of the materials the ultrasonic wave has to

travel through, the larger proportion of the wave which is scattered. For example, air and water will show a larger degree of scattering than oil and water.[3]

Also, since this thesis deals with the interaction of ultrasound with bubbles of air, the curved surface of the bubble must be taken into account. Here the angle of incidence must also be taken into consideration. A process called resonant scattering occurs in bubbles. This is because when an ultrasonic wave is near a bubble is pulsates at an extremely fast rate at a certain frequency (the resonance frequency of the bubble). Since there are large differences between the compressibility of a bubble and the compressibility of the surrounding liquid then most of the incident ultrasound is scattered in all directions.[3]

## 3.2 Bubble Oscillations and Bubble Sizing

### 3.2.1 Damped and Undamped Simple Harmonic Oscillators

The oscillation of a bubble can be compared to the famous mass on a spring analogy favoured by physists (otherwise called the undamped simple harmonic oscillator).[6] The radial frequency (which represents a bubble's resonance frequency) is given by Equation 3.5.[6]

$$\omega_0{}^2 = \frac{k}{m} \qquad \textbf{Equation 3.5}$$

where $k$ is the spring constant, $m$ is the mass of the bob attached to the spring and $\omega_0$ is the radial frequency.

Alternatively, if one thinks of a viscous solution, then the damped simple harmonic oscillator can be applied in this case, where the damping occurs due to the viscosity of the medium.[6] The extent to which the damping occurs is proportional and in an opposite direction to the velocity of the bubble. By application of Newton's Second Law of motion a general quadratic equation can be produced.[6]

$$S = \frac{-b \pm \sqrt{b^2 - 4km}}{2m}$$ **Equation 3.6**

There can be three solutions to Equation 3.6 (where S is the angular frequency). These are dependent on the spring constant, *k*, the mass of the bob (bubble), *m*, the degree to which dampening of the wave has occurred, *b*, and the resonance frequency (described by Equation 3.5).[6] Namely, these are;

1. Overdamped Oscillation – where $b^2 > 4km$, for example a light bob in a very viscous fluid.
2. Critical Dampening – *where* $b^2 = 4km$, when an oscillation is rapidly lost.
3. Lightly Damped Oscillation – where $b^2 < 4km$, for example a heavy bob in a liquid of low viscosity, where damping is weak.[6]

### 3.2.2 Minnaerts Resonance Frequency and Bubble Sizing

Bubbles can be produced under a number of different static or agitated conditions.[9,10] This is particularly true in the biotechnology and mineral processing industries where the use of passive acoustics is the favoured method for the monitoring of gas-liquid mass transfer rate.[9] The size of a bubble can be altered using spargers of differing diameters. The size of a bubble is related to its resonance frequency by Equation 3.7, proposed by Minnaert in 1933 (this equations is true under adiabatic conditions).[11]

$$f = \sqrt{\left(\frac{3\gamma P_\infty}{(2\pi)^2 \rho}\right)} \frac{1}{R_o}$$ **Equation 3.7**

where $P_\infty$ is the absolute liquid pressure, $f$ is the frequency (Hz), $\gamma$ is the ratio of the specific heats for the gas at a constant pressure to that at a constant volume, $\rho$ is the liquid density and $R_0$ represents the radius of the bubble.[9]

Minnaert, who used the relationships described in section 3.2.1, was the first to show a relationship between the size of a bubble and its resonant frequency.[11] Due to the

fact that the linear resonance frequency of a bubble is given as $\omega_o / (2\pi)$, then the Minnaert resonance frequency, $\omega$, is usually given as.[11]

$$\omega = \frac{1}{R_o}\sqrt{\frac{3\gamma p_o}{\rho}} \qquad \textbf{Equation 3.8}$$

Specifically for water (at 1 atmosphere pressure), Equation 3.8 can be reduced because heat conduction and surface tension do not need to be taken into account.[11]

$$\omega \,.\, R_o = 3\ ms^{-1} \qquad \textbf{Equation 3.9}$$

In addition to ultrasound other methods have been used to investigate bubble sizes. There are summarised in Table 3.1, the interested reader is directed to these references.[12-15]

**Table 3.1 – Methods used to investigate bubble size**

| *Method* | *Reference* |
|---|---|
| Capacitance Probes | 12 |
| Electrical Impedance Tomography | 13 |
| High-speed Photography | 12, 14 |
| Endoscopic Optical Probes | 15 |

## 3.3 Transducers and Ultrasonic Sensors

### 3.3.1 Transducers

An ultrasonic transducer is the primary component in the transmission and detection of acoustic signals.[16] Transducers typically incorporate a matching layer, backing material and an active piezoelectric layer. Matching layers are used to improve the acoustic impedance matching between the piezoelectric material and the radiation medium. This ultimately results in better transducer performance. The purpose of

the backing layer is to absorb ultrasonic waves at the back face of the piezoelectric layer. The active piezoelectric layer is one of the most important layers in transducers as it converts electrical energy into mechanical (vibrational) energy and vice versa through the piezoelectric effect. Figure 3.2 shows a simplified schematic of the layers involved in a piezoelectric transducer and the acoustic impedance terminology associated with each layer. Note the relative thickness of each layer in Figure 3.2 is not to scale.

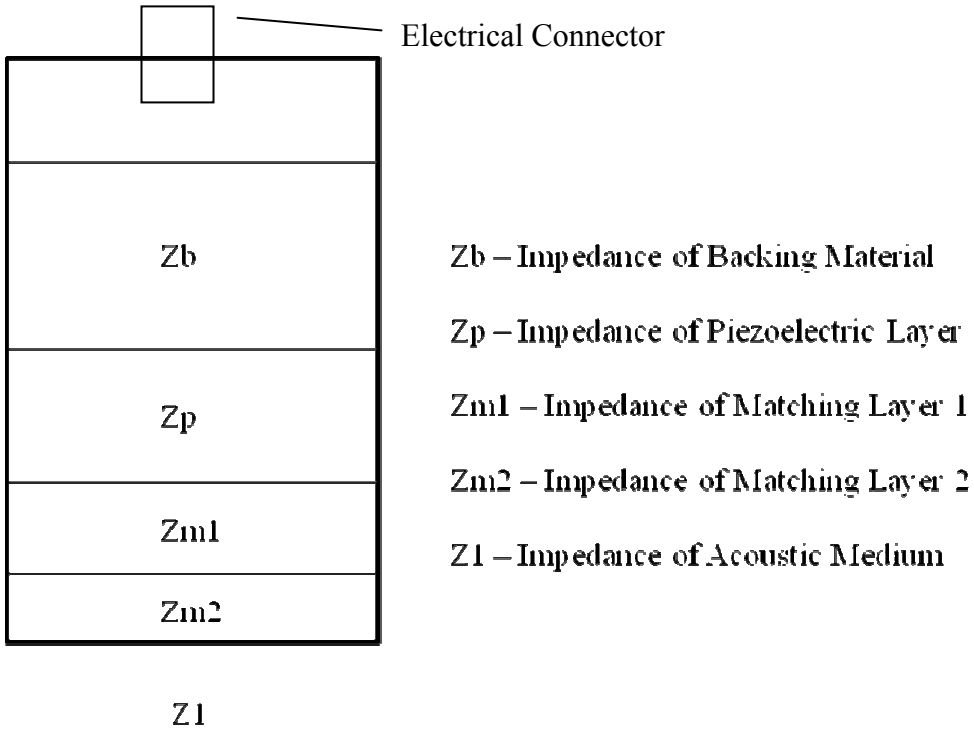


**Figure 3.2 – Schematic of typical transducer showing impedance of each layer**[16]

Key to a transducers performance is optimising the matching layers. For a single matching layer system, the impedance of the matching layer is determined as the geometric mean of the transducer and the load impedances. For the example of a lead zirconate titanate transducer operating into a water load the ideal matching layer impedance will be 6.9 MRayls.[17] Such layers are manufactured using metal loaded organic polymers i.e. suspensions of a metal powder in a suitable thermosetting

polymer base.[16,17] Tungsten is frequently chosen as the metal due to its high acoustic impedance and its unreactivity. The metal suspension is used to improve the acoustic impedance of the whole transducer.[16] The purpose of the backing layer is to stop the ultrasonic wave from being reflected back to the front of the piezoelectric layer.[16] Ultimately the design of a transducer is application dependent and this is particularly true for the matching layers in the transducer.[18] Applications of ultrasonic transducers can be split into two main fields, these are for high resolution purposes and high power purposes.[19]

The piezoelectric layer can be made from lead magnesium niobate, lead zinc niobate or lead zirconium titanate (PMN, PZN and PZT respectively), these can also be doped with lead titanate.[20,21] PZT is the most common piezoelectric component. There are a larger number of configurations of the piezoelectric material. The piezoelectric component of a transducer can be composed of a piezoelectric composite, which is a combination of an active ceramic phase and a passive polymer phase. In addition to the ceramic polymer composites described above there are also composites made from ceramic-metal[21] and single piezoelectric elements.[22]

The bandwidth of transducers can be either resonant or broadband and this is typically dependent on the constituent materials from which the transducer has been constructed.[22] Broadband transducers have a wide transmitting frequency range and resonant transducers have a narrow transmitting frequency range. In this thesis both commercial piezoelectric ceramic transducers (www.olympusndt.com\) and proprietary piezoelectric ceramic composite devices[23] have been used to match the bandwidth of the selected devices to the desired application.

### 3.3.2 Ultrasonic Sensors

Currently the use of ultrasonic sensors to monitor flow, particle distribution and concentration has seen application within the automation of a process.[24] Ultrasonic sensors involve the use of transducers.[25] It is typical to find ultrasonic sensors

attached to control systems which also employ the use of additional sensor technology.

The use of ultrasonic sensors has the following advantages:[25]

- Non-invasive and non-intrusive (ultrasonic wave can penetrate the walls of reaction vessels or pipes),
- Rapid response,
- Long-term stability (robust),
- High resolution and accuracy,
- Can be used in explosive atmospheres.[28]

However there are drawbacks, these being that there is an increase in sound attenuation with increasing frequency[25] and that the acoustic properties of a substance are concentration dependent.[28] The second draw back here can also be an advantage if one wanted to measure the concentration of a particular entity. Advantages and drawbacks are very much application dependent.

Hauptmann *et al.* classified ultrasonic sensors for process monitoring applications into four main types. These are distance sensors, propagation path sensors, impedance sensors and mass sensitive sensors. Table 3.2 illustrates the particular properties which each type of sensor can measure and subsequently monitor.[25]

**Table 3.2 – Sensor types and usage[25]**

| Type of Sensor | Measurable Properties |
|---|---|
| Ultrasonic Distance Sensors | Distance, process monitoring |
| Propagation Path Sensors | Volume and mass flow velocity |
| Impedance Sensors | Density, acoustic impedance |
| Mass Sensitive Sensors | Mass, viscosity, multi-component areas |

Ultrasonic flow sensors (propagation path sensors) are developed from three acoustic effects: the drift effect, the Doppler effect (motion, speed and path) and the

attenuation effect.[25] An example of an ultrasonic sensor for density measurements was proposed by Püttmer *et al.* where they state that the accuracy of a (density) sensor is determined by the signal-to-noise ratio.[26] This was carried out using a pulse-echo technique where an acoustic reference is compared to the experimentally measured echo.[26] This sensor was tested for different combinations of longitudinal and shear waves and it was the time-of-flight of these waves which was measured instead of the received amplitude.[26] It can be imagined that if a sensor is placed into a process which contained solid media (or fermentation media) there is a large possibility that the sensor could be 'fouled' or have deposits on its surface which would affect the validity of the results. It was shown that the velocity of an ultrasonic wave was affected to a lesser extent than the amplitude of an ultrasonic wave when measured using a fouled sensor i.e. one that has deposits on it.[27]

Acoustic sensors are used as a means of determining density, viscosity, concentration (both particulate and solution) and are typically used in the chemical and pharmaceutical industries (e.g. polymerisation, waste water treatment), the food industry (margarine production[29] and starch production) and the biotechnology industry (fermentation reactions).[28] Acoustic sensors can be applied actively[29] or passively.[30] Figure 3.3 shows where ultrasonic pressure sensors can be placed in a process and the method by which they give rise to information.[30] Once a problem has been detected by the acoustic sensor in the process pump the signal passes though an amplifier and is processed by the ultrasonic system to determine if a problem has occurred. An alarm is then activated and Plant Assess Management can intervene to rectify the problem.

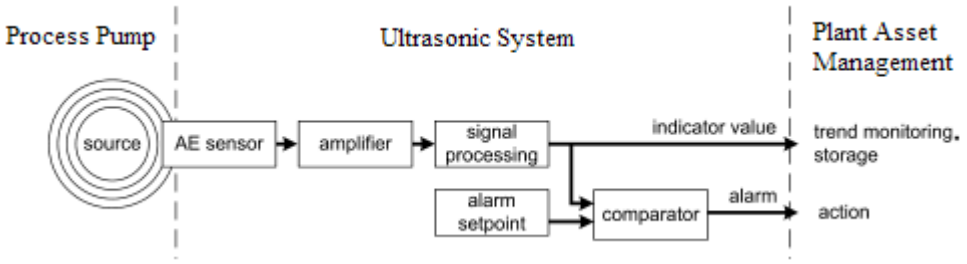


**Figure 3.3 – Typical set-up of AE monitoring system[30]**

On page 42 the advantages of using acoustic (or ultrasonic) sensors were discussed in relation to process monitoring. However in addition to the monitoring of the actual process, for example a fermentation reaction, acoustic (ultrasonic) sensors can also be used to monitor the equipment in a plant, e.g. the pump, valves, pipes etc.[30] For example bearing failures can be detected by temperature measurements, or leaks in pipes and valves can be detected by pressure measurements, but there is a slow response.[30] Acoustic emission can be used here to monitor the vibrations within the pipe line, which can be done on-line and in real time to give the engineer a warning that there may be a leak in the pipe.[30]

## 3.4 Acoustics Applied to Bubble Characterisation

### 3.4.1 Acoustic Emission

There have been many reports of acoustic emission (or passive acoustics) being using within the laboratory for a variety of applications, with bubbles being the primary entity under investigation.[31-39] Two methods which have been reported and are extremely applicable to investigating the properties of bubbles, were carried out by Boyd and Varley when they investigated plunge jets[31] and bubble columns.[32] The key differences between both of these methods is that plunge jets are commonly used within a process as a means of introducing air into the liquid of a process by recycling liquid through a pump. The liquid is then ejected through a nozzle to create bubbles.[31] Whereas bubble columns introduce air into a process from the bottom of the vessel,[32] in a similar fashion to fermentation reactions. The latter method is similar to the methodology adapted for this research. The experimental set-up for both these methods can be seen in Figures 3.4 and 3.5.[31,32]

In the set-up shown in Figure 3.4, the hydrophone that was used was a Bruel and Kjaer 8103[31] and in the set-up shown in Figure 3.5, it was a Bruel and Kjaer 8301 hydrophone that was used.[32] Different hydrophones were used due to their different bandwidths.

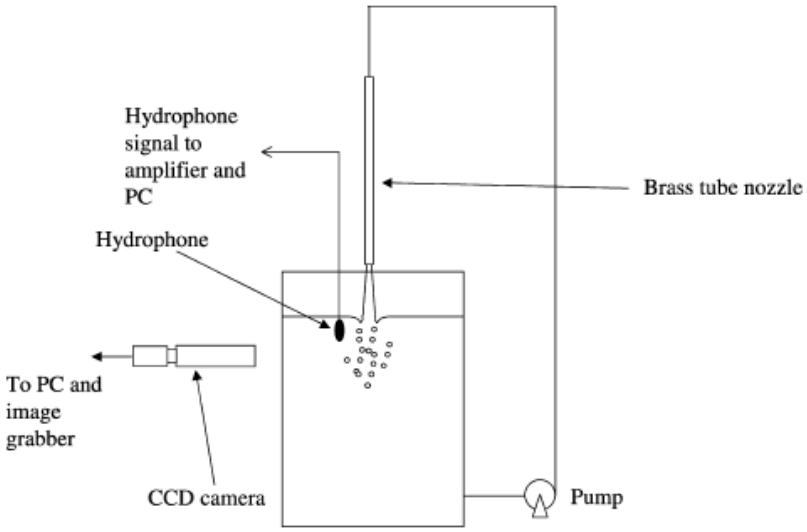


**Figure 3.4 – Plunging jet experimental set-up[31]**

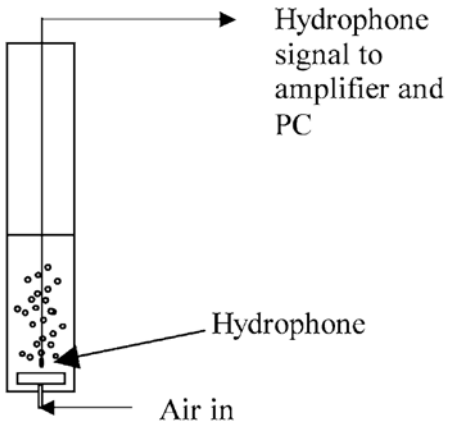


**Figure 3.5 – Bubble column experimental set-up[32]**

In Boyd and Varley's plunging jet experiments they compared acoustic and photographic measurements.[31] Their acoustic measurements showed an increase in the amplitude and disorder of the signals as the flow rate of the plunging jet was increased. The signals acquired at lower flow rates, 2 L $min^{-1}$, showed less disorder than those acquired with a flow rate of 4 L $min^{-1}$.[31] This was assumed to be because the rate of bubble formation was increasing and, therefore, the rate of bubble break-up and rate of bubble coalescence would be increasing to give a more chaotic and disturbed environment.[31] A similar effect was observed after the signals had been fast Fourier transformed into the frequency domain. The peak frequency also

changed with flow rate.[31] Acoustic spectra contained frequencies between 4 and 80 kHz for bubble diameters between 0.08 mm and1.60 mm.. The nozzle was placed 5 mm above the surface of the water.[31] Figure 3.5 illustrates the bubble production method favoured by Boyd and Varley; introducing air, through a sparger, into the bottom of a chamber containing liquid (chamber dimensions were 0.075 m diameter by 0.8 m column height).[32] This is similar to the system employed in an aerated fermentation reaction.[34] The column was filled to 0.2, 0.3, 0.45 and 0.6 m above the sparger. It was found that increasing the flow rate, decreases the frequency value of the peak maximum, as shown in Figure 3.6.[31]

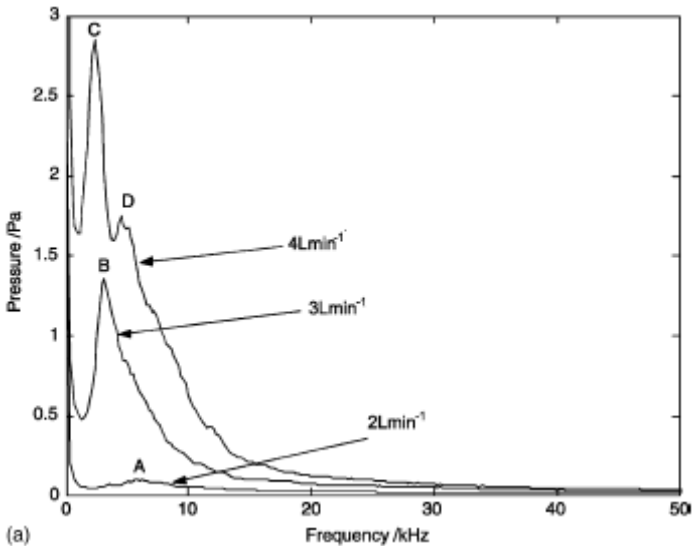


**Figure 3.6 – Effect of air flow rate on frequency[31]**

It is possible to determine the bubble size from the frequency of acoustic emission using Minnaert's equation. It was found that only one peak formed for bubbles less than 1 mm diameter and that above 1 mm diameter two peaks were visible and attributed the formation of this second peak to bubble coalescence and break-up.[31] A similar pattern was observed for photographic methods. It should be noted that all these experiments were carried out in deionised water. Following on from this two further experiments were carried out, these were adding salt (NaC*l*), which reduces coalescence, and adding xanthan gum to increase viscosity.[31] It was found that by increasing the salt concentration, the flow rate at which a bubble reaches constant

diameter is reduced i.e. adding salt appeared to stabilise they system. An increase in viscosity gave rise to an increase in bubble diameter.[31]

One other method set out by Boyd and Varley for investigating bubble sizes was an adaptation of Figure 3.5, where a turbine was added above the air in-let to give a mixing effect of the bubbles.[32] The hydrophone was placed 10 mm from the propeller and the vessel diameter was 96 mm.[32]

It has been established that for plunging jets the diameter of the bubble produced changes as it progresses up the column.[33] Bin defined two regions about the plunging jet. The first is the primary area near the conical region of the plunging jet where bubbles of a diameter of less than 1 mm were produced. The second area, which surrounds the conical region, is where bubbles coalesce and here bubbles of a diameter of 3 – 4 mm can be found.[33]

Currently methods which are used to monitor gas dispersion are photographic and those used to monitor bubble size need direct contact with the air bubble,[34] which is impractical for fermentation reactions (where sterility needs to be maintained). The use of a non-invasive ultrasonic transducer can solve both these problems as ultrasound can pass through opaque materials and does not need to come into direct contact with the fermentation medium.[34] The added advantage is that on-line, real-time measurements can be made. The experimental set-up of Figure 3.5 is very similar to the set-up of a bioreactor, where important parameters such as gas hold-up, type of flow, gas bubble size need to be measured to understand and monitor the process.[34]

Another approach to bubble production by Manasseh *et al.* was to introduce bubbles into a vessel of water through a pressure controlled method.[35] This involved a pressure regulator and flow meter attached to an air cylinder as shown in Figure 3.7.[35] In this method, bubbles of internal diameter 0.3, 0.5, 1.0, 2.0 and 4.0 mm were generated and were monitored using a Bruel and Kjaer type 8103 hydrophone. The bubbling rate was 12 Hz.

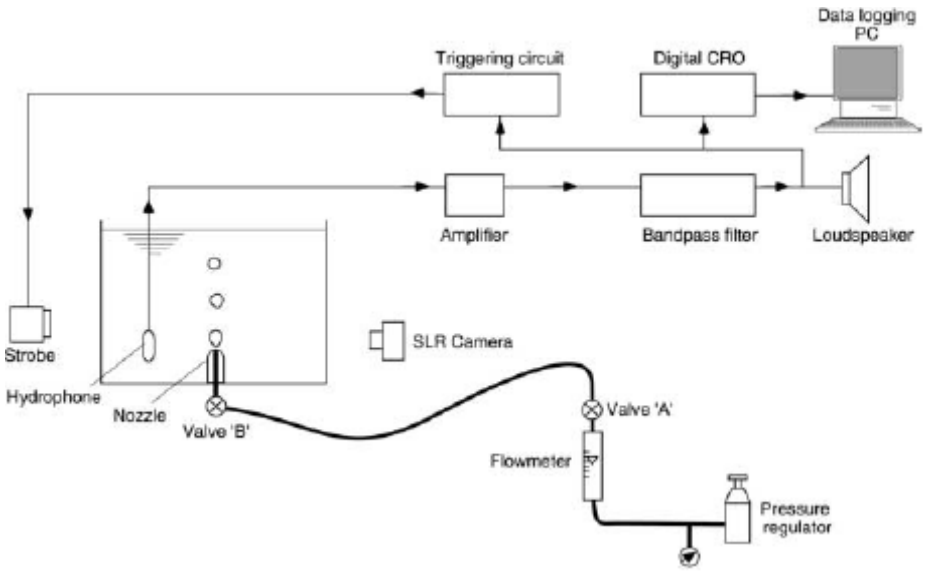


**Figure 3.7 – Method of bubble production employed by Manasseh *et al.*[35]**

Other work done by this group found that as bubbles are produced and oscillate, their acoustic pulse has a modulated appearance and that this modulated appearance is greater at higher flow rates (similar to what Boyd and Varley discovered) and also changes with bubble shape.[36] Within the acoustic pulse of a bubble, the frequency of the signal decreases with time. This group found that bubbles with a smaller diameter are more likely to resonate at Minnaert's theoretical frequency due to the smaller influence of non-linear effects. Again, Manasseh *et al.* compared photographic techniques with acoustic techniques and found a good correlation.[35] To develop the results obtained, the group repeated , the above experiment with a stirred tank, where the propeller speed was kept constant, and found that data taken when the hydrophone was closer to the bubble production site were more reliable than when it was positioned further away. They reported a difference in the time taken to collect 100 signals when the hydrophone was placed close to bubble production site (minimum of 1.97 s), compared to when it was positioned further away (over 30 minutes).[35]

Wu and Gharib produced bubbles through an L-shaped capillary controlled by a syringe pump which was connected to two syringes, see Figure 3.8.[37]

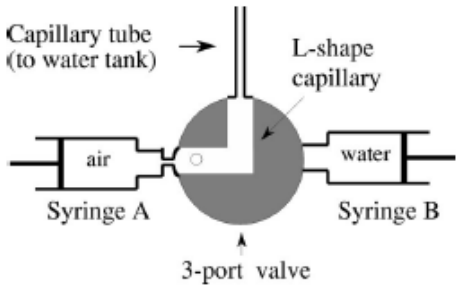


**Figure 3.8 – Syringe pump set-up[37]**

A water tank (150 mm x 150 mm x 610 mm) and syringe B were initially filled with water. The L-shape capillary is rotated at 90° clockwise from the position shown in Figure 3.8, this allows the air bubble to be pushed out and enter the capillary. Syringe B is used to introduce the air bubble into the L-shape capillary.[37] Both syringes were controlled by syringe pumps. The group reported that this experimental procedure had to be carried out at flow rate of 2 μl $min^{-1}$ or less in order to achieve repeatable results.[37] Note that this is considerably lower than the flow rates used by Manasseh *et al.* and Boyd and Varley. This group found that as a bubble rises, the path or trajectory which it follows is dependent on diameter.[37] Ellipsoidal bubbles with a diameter of 1.31 mm had an approximately straight trajectory. As the bubble sizes increased to a diameter of 2.08 mm the trajectory became more spiral. For spherical bubbles the trajectory changed from straight to zig-zag as the bubble diameter increases.

The change in a bubble's geometry and size from the bubble being produced at the sparger orifice and as it travels up the water column has also been reported by other groups.[38,39] One group reported that there are two distinct mechanisms by which a bubble grows.[38] These are when a bubble is immobile at its growth site, where it has a first rapid of growth for 2 seconds, then has a linear increase and when it is detached from the nozzle, where the size grows exponentially as it rises up the water column. Kazakis *et al.* concluded that a bubble's development was influenced by gas flow rate, the properties of the liquid, forces acting on the bubble during formation (e.g. surface tension, buoyancy and gas pressure).[39]

In a paper by Vazquez *et al.* they discussed the importance of gas-liquid bubble flow for fermentation reactions in bio-reactors and compared three methods for determining bubble sizes.[40] These were acoustic emission, video imaging and using an inverted funnel. The inverted funnel method was first detailed by Leighton and Walton, where a bubble was trapped in the cone of the funnel. The bubble was then transferred to a capillary tube where it was possible to measure the length of air in the column.[41] A diagram showing the experimental set-up is shown in Figure 3.9.[40]

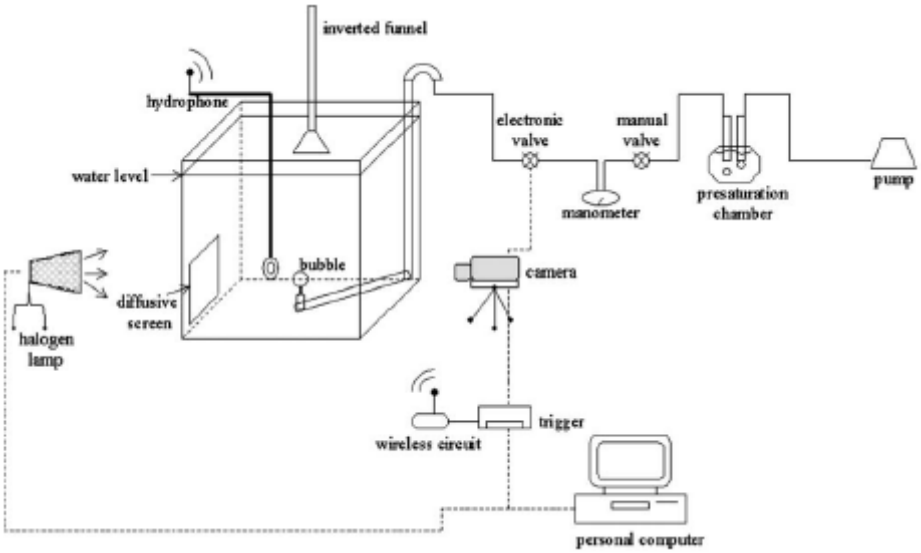


**Figure 3.9 – Experimental set-up showing acoustic emission, video imagine and inverted funnel methods[40]**

During their experiments they found that the inverted funnel method had the greatest repeatability and therefore used this method as a reference with which to compare the acoustic and video methods.[40] They found that both the acoustic and the video method have good repeatability to within 5 %. However, they noted that the acoustic method was improved when a hydrophone was used rather than a non-invasive transducer, which has obvious implications for using such acoustic techniques in a fermentation process. Improvements in the video method were observed when an image superposition method was employed.

Other methods for bubble production and bubble characterisation have been reported in the literature. These include bubble generation using foamed-aluminium stirrers[42] and optical tomography for characterisation of aeration parameters.[43]

Acoustic emission has been used in both the laboratory and in an industrial setting to monitor heterogeneous reactions.[44,45] Previous work done by Nordon *et al.* with heterogeneous (particulate) reactions involved the esterification reaction of itaconic acid and 1-butanol in a glass batch reactor[44] and the modelling of a heterogeneous system; itaconic acid with toluene.[45] The effects of particle concentration and particle size were investigated using a transducer which resonated at 90 kHz.[44] Differences in the rate of reaction could be identified from the acoustic emission spectra.[44] In further work by Nordon *et al.*, the 90 kHz transducer was replaced with a broadband transducer, which was sensitive up to 750 kHz. Experiments were carried out to investigate the effects of particle size, concentration, temperature, and transducer position and attachment on the AE signals obtained from a heterogeneous system.[45] It was concluded that the position and the attachment of the transducer were important factors to consider. In addition, temperature and stir rate should be recorded because the acoustic emission signal is sensitive to changes in these parameters. Furthermore, they concluded that the use of a broadband transducer yielded better data than a resonant transducer.[45]

Particulate slurries can come in a variety of forms, from simple water to cement slurries and even dangerous chemical solutions that might be toxic.[46] Therefore, the type of slurry dictates the method used for process monitoring.[46] As acoustic emission can be non-invasive and so does not require direct contact-sampling of the slurry, it may be possible to characterise each different form of slurry. Acoustic emission has also been used to monitor granulation processes[47] and powder breakage.[48]

### 3.4.2 Active Acoustics

When ultrasound interacts with bubble oscillations, at low amplitudes the interaction is linear i.e. if the propagating frequency is *f*, then the frequency *f* will be detected.[49] Bubble pulsations are linear at low amplitudes (as demonstrated by the Rayleigh-Plasset equation[6]), this means that non-linearity will occur at higher pressure amplitudes.[49] If the interaction of the ultrasound with bubble oscillations is at high pressure amplitudes (i.e. non-linear behaviour) then harmonics can be detected i.e. the detected frequency is that of *nf* where $n$ = 2,3 etc. When dealing with these frequencies care has to be taken over the received (scattered) signal. This is because a phenomenon known as 'false-triggering' can occur. False triggering occurs when turbulence in the vessel, for example, produces a signal which is close to that of the desired harmonic frequency, implying the presence of a bubble when there isn't one. False triggering can also occur at the fundamental frequency. Types of non-linear interactions involving the propagation of a signal, *f*, and measuring the returned signal of *f/n*, ($n$ = 2,4,6 etc) are known as sub-harmonic frequencies, brought about by the sub-harmonic oscillations of the bubble. At subharmonic frequencies false triggering does not occur. The choice of whether one chooses to monitor harmonics or sub-harmonics depends on the accuracy required. For example measuring the second harmonic, *2f*, will give a maximum value at bubble resonance but on the other hand the second harmonic can include distortions from other sources (false triggering). Measuring the third harmonic does not give any information that can relate bubble resonance frequency to bubble diameter. The sub-harmonic frequencies are the best for measuring the non-linearity of bubble oscillations because the signal is unambiguous and is present due to lower attenuation and with low noise i.e. that less energy is lost from the ultrasonic wave.[49]

Significant input to knowledge in the area of active acoustics of bubbles have been made by Leighton *et al.*,[49-59] Ferrara *et al.*[78-80,82,84-90] and de Jong *et al*.[91-95] Leighton *et al.* stated that since gas bubbles are low amplitude pulsation oscillators they are abundant in nature.[50] Bubbles can oscillate to produce high and low order harmonic and subharmonic frequencies that can result in physical, chemical and biological

changes. Information about bubbles or bubble content can be used to monitor processes to achieve a better final product, which could be a product on the market, a laboratory or a clinical product.

In one paper Leighton *et al.* studied the non-linear response of a bubble to an acoustic field to estimate the polytropic index of air, helium and propane and to use this technique to resolve bubble arrays acoustically.[51] The experiment was carried out in a poly methylmethacrylate tank with dimensions 250 mm x 250 mm x 500 mm. The tank had an acoustic absorber placed in it and filled with water, see Figure 3.10. A continuous wave of 3.35 MHz was generated from a signal generator and used to excite a transducer. The air bubble had a radius of 0.645 mm. A loudspeaker was present to provide the pump signal which varied in frequency between 3 kHz and 6 kHz.

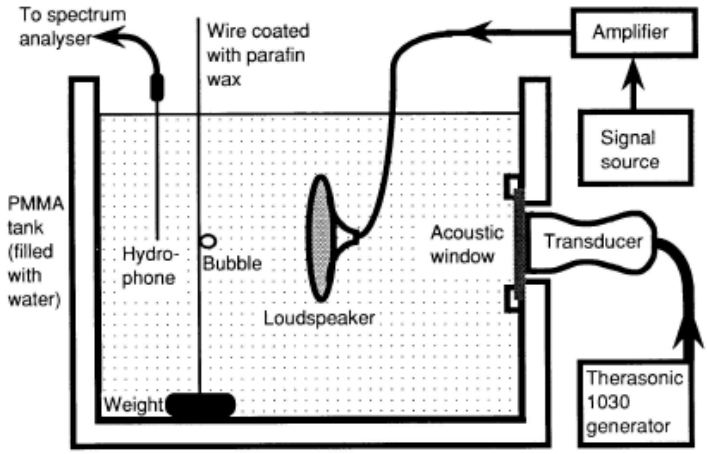


**Figure 3.10 – Acoustic set-up to determine polytropic index of air, helium and propane[51]**

In order that coupling did not occur between the speaker and the transducer they were placed at an angle of 135° in the same horizontal plane. The bubble was produced by blowing underwater from a drawn glass pipette.[51] The bubble was held on a 0.5 mm diameter wire, where the transducer axes intersect. To assist the bubble to stay on the wire a thin film of paraffin wax was coated on the wire. It was concluded that decay time of the subharmonic signal was longer than that of the

harmonic i.e. the subharmonic signal lasted longer than the harmonic signal (the wavelength will be much larger for subharmonic signals).

More recent work by Leighton *et al.* used the same experimental set up, Figure 3.10, to investigate the sizing of bubbles.[52] One particularly interesting addition to the experimental set-up described in Figure 3.10 was that after the studies on a particular bubble were finished, the bubble was transferred to a glass flask, where its size could be determined by a rotating microscope. Again it was concluded that the subharmonic components were sharper than the higher harmonic components. The subharmonic components gave an error between 0.5 % and 2 % for the bubble resonance frequency. The group did not report an error value for the higher harmonics. It was also found that when increasing the pump frequency the spectra showed the presence of one peak and when decreasing the pump frequency the spectra showed the presence of a double peak. Sometimes the double peak had one portion at the original frequency and the other portion at a smaller frequency, this was attributed to bubbles coalescing with neighbouring bubbles.

In work carried out by Leighton and Phelps they investigated the sum and difference signals of single bubbles at resonance.[53,54] The test was carried out in a 1.8 m x 1.2 m x 1.2 m deep plastic tank made from reinforced plastic. The tank was filled to a depth of 1 m.[53,54] A moving underwater coil was employed as the low frequency projector, which provided a continuous tone of around 1 MHz[53] or 1.1 MHz.[54] The imaging signal (high frequency) was produced from an ultrasonic generator. The receiving transducer was an unfocused immersion transducer with a resonance frequency of 1 MHz. In order for the alignment of the transducers to stay constant the transducers were fixed to a stainless steel bar, which had the same width of the tank.[67] Leighton and Phelp found that the signal from the subharmonic sum and difference gave a sharper response and hence more a more accurate estimate of the bubble resonance frequency.[53,54] In these studies bubbles with radii between 0.65 mm to 1.035 mm were studied.

Other studies by Leighton *et al.* include the active acoustic study of bubbles in a 6' x 4' x 4' tank, which contained 1400 mm x 300 mm Tico pads to isolate vibration.[55] The tests were split into three categories. The first and second investigated a bubble trapped on a wire within the focus of the transducers using different hardware whereas the third investigated moving bubbles generated from compressed air. They concluded that a bubbles' resonance frequency can be found using the sub-harmonic component and that is component is easier to spot because it lies higher above the noise component than the harmonic.

Leighton *et al*. have carried out a great deal of research into the active acoustic sizing of bubbles, many of which use similar experimental set-ups to those described above.[56,57] The research outcomes suggests that the sub-harmonic component is better for bubble sizing.[56,57]

In addition to studying the sizing of bubbles in laboratory tanks, described above, Leighton *et al.* have studied bubbles in pipes.[58,59] These tests use the same principles as previously described i.e. harmonic versus sub-harmonic frequencies. It was found that the percentage error between a free-field measurement and a pipe measurement increased as the resonance frequency of a bubble increased from 3 to 10 kHz.[58]

Didenkulov *et al.* looked into a new method, called the difference frequency Doppler technique.[60] This technique is non-linear and was experimentally confirmed with bubbly water. Experiments were carried out in a tank of dimensions of 910 x 300 x 450 mm. An ultrasonic beam was focused though two focused transducers with resonance frequencies of 2.25 MHz, a diameter of 2.54 cm and a focal length of 10 cm. The group studied the responses of bubbles with resonance frequencies between 70 kHz and 200 kHz, which equates to bubbles of radii between 0.045 mm and 0.015 mm. The experimental set-up is shown in Figure 3.11. They found that it was possible to measure both bubble diameter and bubble flow rate.

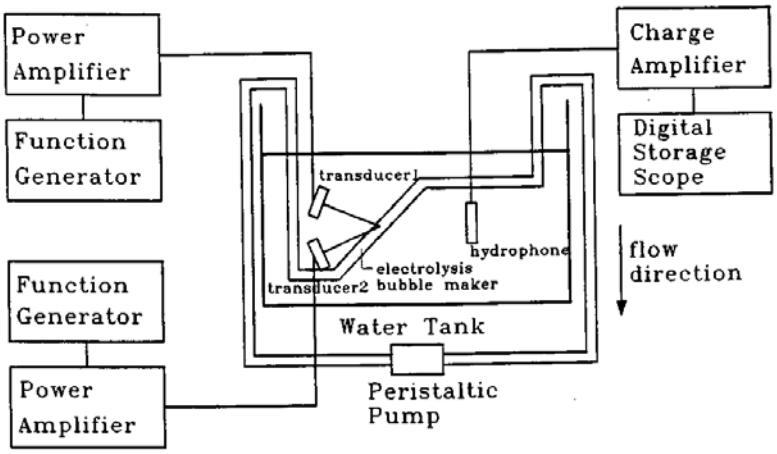


**Figure 3.11 – Experimental set-up to investigate bubbles between 15 µm and 45 µm[60]**

Since this method uses non-linear scattering, it was concluded that it could have future applications in monitoring the flow inside pipes or blood flow, since the non-linear component is very sensitive to bubble sizes.[60]

Active acoustics has already been used in the non-invasive on-line monitoring of fermentation reactions.[61,62] However most applications of active acoustics are concerned with non-destructive testing in the food industry.[63-65]

Resa *et al.*, have carried out the on-line monitoring of lactic acid fermentation using ultrasonic velocity, on a laboratory scale.[61] The growth of lactic acid media is very complex and efficient of monitoring the process is required. Current methods employed are the monitoring of pH and $pO_2$. The group set up a test cell (shown in Figure 3.12) with two transducers, one for transmitting and one for receiving. The transmitting transducer was at a resonant frequency of 2 MHz. The ultrasonic velocity was determined using a Fast Fourier Transform (FFT) of the signal and time of flight measurements. The group concluded that the monitoring of lactic acid fermentation media using ultrasonic velocity is feasible. It was shown that an increase in the bacterial concentration gave rise to an increase in the ultrasonic velocity.

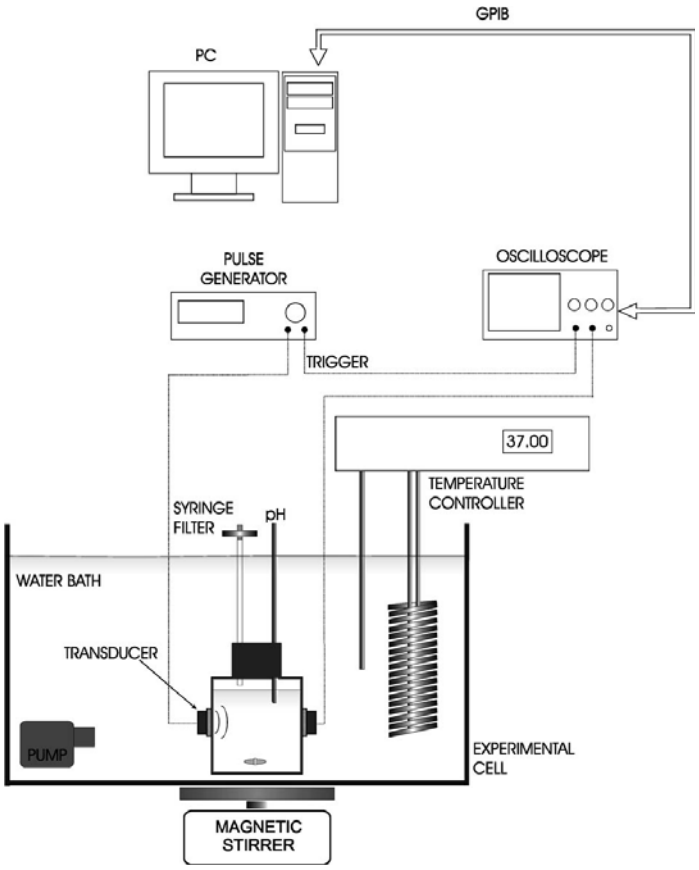


**Figure 3.12 – Fermentation Test-cell[61]**

Another fermentation reaction where active acoustic methods were employed on-line was in the monitoring of a yogurt fermentation reaction.[62] Again as with the above case it was a lactic acid fermentation reaction that was monitored using the ultrasonic velocity. The experimental set-up was similar in that two 3.7 MHz transducers were employed and each connected to an oscilloscope and computer. Factors which affect the ultrasonic velocity were identified e.g. temperature, pressure and density.

Active acoustics have been used in the food industry to characterise air bubbles within food products.[63,64] A variety of food types contain bubbles or air pockets, for example ice cream and desserts. Active acoustics can also be used to determine if there is leakage of air into foods stored in vacuum packaging.[63] It is possible to monitor changes in bubbles in foods over time, which can be used to monitor the condition of food. As some foods are opaque the use of acoustics is particularly

attractive. Acoustics could be used in many areas of food processing e.g. manufacture, storage and handling.[64]

Active acoustics have also been used in on-line process monitoring of batters, to determine if a batter had a high air content or not.[65] Ultrasound was used to measure the acoustic impedance of the batter. This was achieved by placing a transducer in direct contact with the batter. The measurement of acoustic impedance was chosen over density derived measurements because as batters are highly viscous have a high acoustic attenuation. Active acoustics has also been used in the food industry for the in-line determination of the concentration of substances in beer and fruit juice, and to measure the fat and (solid) non-fat concentration.[66] The sensor system measured sound velocity, impedance coefficient, attenuation coefficient and temperature.[67]

In separate applications, active acoustics has been used in particle sizing.[67,68] Two methods which have been used for particle sizing are ultrasonic diffraction grating spectroscopy[67] and ultrasonic attenuation spectroscopy.[68] Active acoustics has seen further applications in fluids and slurries using density measurements,[69,70] ultrasonic velocity measurements[71-73] and attenuation.[74] In these applications most measurements were taken using a transducer attached to the outside of a pipe.

### 3.5 Use of Active Acoustics in Medical Ultrasound and Microbubbles

The use of active acoustics in the biomedical field with contrast agents have been investigated extensively and used since the 1960s. In contrast agents, microbubbles resonate with a specific frequency which is determined by the diameter of the microbubble.[75] Detection of microbubbles in the blood stream, for example, results through the non-linear interaction of ultrasound with such bubbles. It is this principle that this research aims to take advantage of, by exciting a non-linear interaction of ultrasound with bubbles in a fermentation process.

Microbubbles, used in the medical imaging of parts of the body, operate as echo-enhancers, where the backscattered ultrasound intensity is proportional to the

acoustic impedance change between the gas bubble and blood.[76] Microbubbles are typically 1 – 7 μm and resonate between 2 and 15 MHz. What is measured when active acoustics is applied to microbubbles is not the frequency of the propagated ultrasound but that of a higher frequency, typically that of twice the propagated frequency. Frequencies which are sum multiple of the propagated wave, i.e. *2f, 3f* etc show a decrease in intensity with time, but the second harmonic conveniently lasts longer than other harmonics. The advantage of using harmonic frequencies over the propagated frequency is that it is only microbubbles which resonate with harmonic frequencies, and no interferences from reflected ultrasonic waves, will be detected. Therefore any results obtained can be attributed solely to the microbubbles. It is considered that the advantages for using the second harmonic for medical imaging can be adapted to be used in active acoustic monitoring of fermentation reactions.

Ultrasound imaging has seen vast improvements over the past decade with the development of better bandwidths in transducers and the use of contrast agents, incorporated in microbubbles.[77] The use of contrast agents in harmonic imaging for image enhancement has produced clarity close to that of images produced by magnetic resonance imaging. The clinical applications fall into two areas. The first area is the non-linear interaction of bubbles; this is the use of contrast agents in harmonic imaging, where higher frequencies are generated by the reflection and scattering of the ultrasound by microbubbles. The second area is the non-linear propagation; here the use of grey-scale or tissue harmonic imaging is used where the harmonic frequency is produced as a gradual process as the ultrasonic wave passes though the tissue. Harmonic imaging is generally performed at low MHz frequencies.

One possible future application for contrast agents is drug delivery.[77] This would incorporate the treatment drug into the microbubble. Firstly the microbubble would be used to enhance the image and ensure that the contrast agent is at the correct location in the body. Once it has succeeded in doing this, the microbubble can be

pulsed with a signal of higher amplitude, than that which was used in the imaging process, causing it to burst and hence deliver the drug to a specific site.

Current imaging schemes have difficulty in telling the difference between echoes from contrast agents and non-linear propagation of ultrasound in tissue.[78] Similar problems are found in fermentation reactions, where there is difficulty in telling the difference between the signals obtained from bubbles and those obtained from other interactions (e.g. biomass). Ferrara,[78-80,82,84-90] have researched the non-linear interaction of ultrasound with bubbles, microbubbles and contrast agents. By applying the fundamentals of active acoustics techniques used with contrast agents, this method can be adapted to be used to monitor fermentation reactions. Typical contrast agents have bubble diameters between 1 and 10 μm,[78] which is significantly less than the bubble diameter common in fermentation reactions. In addition, the shell of the microbubble affects the oscillations of the bubble within the ultrasonic field and increases the dampening of the radial oscillations. Nevertheless, the work by Ferrara was selected as the starting point for the active acoustic investigation in a fermentation reaction.

In order to validate the software and experimental set-up used in the research for this thesis, the experimental set-up in Figure 3.13 was recreated. In Ferrara's experiment pulses were generated by an arbitrary waveform generator and amplified before being transmitted from a broadband transducer with a centre frequency of 2.25 MHz, a diameter of 0.75 inches and a bandwidth of 2.7 MHz. Echoes were received by a second broadband transducer with a centre frequency of 5 MHz, a diameter of 0.5 inches and a bandwidth of 6.2 MHz. Both transducers had a focal length of 2 inches. The received signal was amplified and digitized at a sampling rate of 50 MHz. In order to minimise multiple reflections a 2-inch block of acoustically absorbent rubber is placed in the corner of the box between the two transducers. One hundred echoes were taken between tests and the data were processed using Matlab. Transmitted signals were calibrated using a needle hydrophone and a pre-amp linked to a digital oscilloscope.

The ultrasound contrast agent studied by Ferrera *et al.* was a nitrogen filled microbubble with a bi-layered shell (M1091, POINT Biomedical ,San Carlos, CA). The shell was made from biodegradable polymer and had human serum albumin outer coating. A diagram of the experimental set-up can be seen in Figure 3.13.

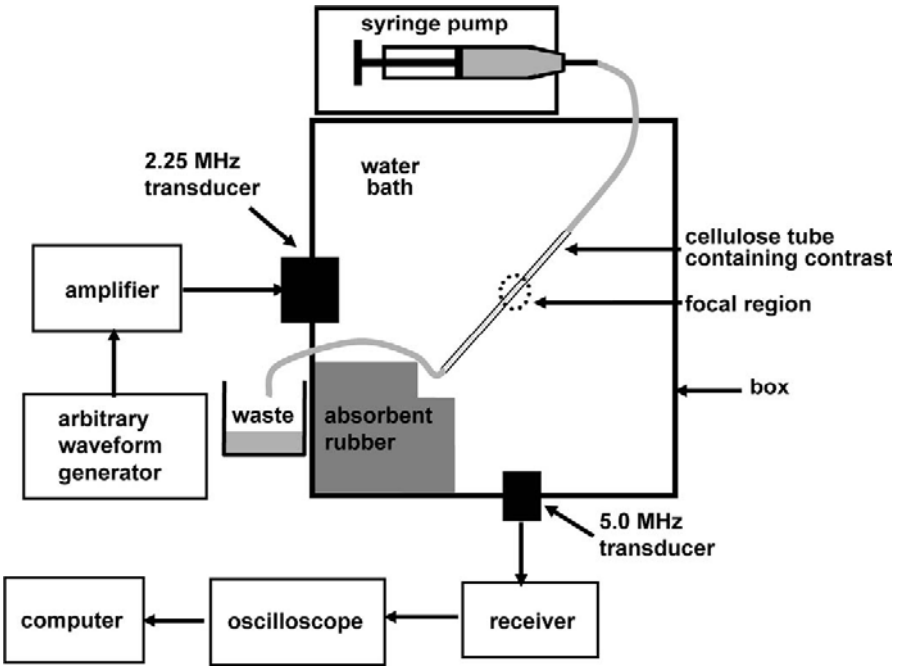


**Figure 3.13 – Experimental Set-up for the Study of Single Contrast Agent Microbubbles[78]**

To compare echoes from those of living tissue, a homogeneous 2 inch cube of phantom material was placed in the water tank and centred at the acoustic focus. Again 100 echoes were taken and processed in Matlab.[78] The 2.25 MHz transducer was used for both transmission and reception. Five pulse sequences at centre frequencies of 1.5, 2.25 and 3 MHz were studied from a range of transmitted pressures. It was shown that both wideband and narrowband strategies can be used to differentiate hard-shell submicron sized contrast agents from those by a tissue-mimicking phantom. It should be noted that second and fourth harmonics were observed. It was concluded that soft-shell contrast agents can be imaged, successfully.

Ferrara *et al.* have carried out work studying acoustics of contrast agents including; different frequency combinations of transducers together with differing focal lengths and having the transducers placed in different positions relative to the contrast agent, for example having transducers that can be rotated through different angles[79] and where the transducers were arranged confocally and coaxially.[85] In these works the contrast agent has been passed through cellulose tubing.[79-80] The main findings are as follows. As the equilibrium radius of the bubble is increased, damping decreases and the relative magnitude of the expansions decreases.[79] Microbubbles with a 1.3 μm radius produced stronger echoes with a slower ring down whereas microbubbles with a 0.7 μm radius produced weaker echoes with rapid ring down. It has been found that the theoretical oscillation is highly correlated with the experimental observation when cellulose or acrylic tubes were used for microbubbles greater than 200 μm. Submicron sized hard-shelled contrast agents have also been used.[80,82] In further work it was shown that transmission of a chirp compared to that of a tone bust increased the sensitivity of detection.[82] It has also been seen that microbubbles can be detected using subharmonic components.[83] A technique for generating subharmonics is that of transmission at twice resonance, when the transmitted pulse is twice the resonance frequency of the bubble.[84] Microbubbles that are near to each other couple acoustically and give rise to a harmonic response that is different from that produced by single microbubbles.[85] Ferrara *et al.* have frequently used optical studies in combination with acoustical studies to record the oscillations and destruction of contrast agents.[86,87] The results of the combined optic-acoustic studies gave rise to a working simultaneous optical and acoustical method for the characterisation of microbubbles.[87] Ferrara *et al.* have recently, in addition to characterising microbubbles acoustically (and optically), studied microbubbles in deep vessels in the body[88,89] and vessels networks.[90]

De Jong *et al.* of Thoraxcentre, The Netherlands, have made great contributions to research into ultrasound contrast agents.[91-95] This work, like Ferrara's, involved using different frequency combinations of transducers in different positions. In earlier work carried out by de Jong *et al*. involved investigations into Albunex contrast agent.[91,92] The transmitted signal was a 2.2 MHz signal and the

backscattered signal contained 2.2 MHz and 4.4 MHz, which correspond to the fundamental and the second harmonic.[93] They found that Albunex response at the second harmonic was high, illustrating the non-linear behaviour of Albunex. The group have also studied the non-linear response of the contrast agent Quantison.[94] They found that encapsulated gas bubbles last longer than free-gas microspheres. In other work carried out by de Jong *et al.* it was shown that bubbles behave differently in water than in blood, since blood is thicker than water it acts to dampen a bubbles oscillations.[95] In this paper it is concluded that a microbubbles' behaviour will tend towards linearity for the more flexible shell options. This means a microbubble will tend towards free bubble behaviour.

The active acoustic monitoring of microbubbles and bubbles offers advantages to process analytical technology in that it is non-invasive and information can be generated in real-time.[96] Hence, this shows that the principles of the non-linear behaviour of microbubbles with ultrasound can be applied to the monitoring of bubbles in fermentation reactions. Also that if both ultrasound and other techniques (e.g. radio-imaging in medicine and IR in process analysis) are used in connection with the information provided may complement each other and lead to a greater understanding of diagnosis or industrial processes. It should be noted that in medical applications a microbubble is used, where as in fermentation monitoring applications it is anticipated that the theory will extend to bubbles of diameters of around 4 mm, which are typical of a fermentation reaction.

## 3.6 Project Aims

The aim of the first part of this project is to use acoustic emission to characterise bubbles i.e. to investigate various factors and find the optimum conditions which give rise to analytically repeatable measurements. The next stage will be to study the active acoustics of contrast agents focussing on the second harmonic components with the aim of validating the methodology and the data capturing software.

Once this software and methodology are validated the project will move on to using sub-harmonic frequencies to size bubbles. The sub-harmonic component has been reported to be better for monitoring than the harmonic component because it lies further above the noise level.[66] It is expected the information obtained from the experiments carried out in this thesis can be developed for real-time monitoring of bioprocesses using *in situ* active acoustic methods.

This project is in collaboration with the Centre for Ultrasonic Engineering (Dr. Anthony Gachagan) and the Department of Mathematics, where Dr. Tony Mulholland and his Ph.D. student, Mr. Euan Barlow, are working on theoretical aspects of bubble sizing parameters using mathematical modelling.

## 3.7 References


1. L. E. Kinsler, *Fundamentals of Acoustics*, 3rd ed., New York, Chichester, Wiley, 1982
2. T. G. Leighton, What is Ultrasound?, *Prog. Biophys. & Mol. Biol.*, 2007, **93**, 3 – 83
3. J. W. R Boyd, J. Varley, The Use of Passive Measurement of Acoustic Emissions from Chemical Engineering Processes, *Chem. Eng. Sci.,* 2001, **56**, 1749 – 1767
4. D. J. McClements, Ultrasonic Characterisation of Food and Drinks: Principles, Methods and Applications, *Crit. Rev. Food Science & Nutrition*, 1997, **37(1)**, 1 – 46
5. Ellis Horwood, *Physical Principles of Medical Ultrasonics*, Edited by C. R. Hill, Chichester, Wiley, 1983
6. T. G. Leighton, *The Acoustic Bubble*, 1st ed., London, Academic Press, 1997
7. A. B. Bhatia, *Ultrasonic Absorption*, Dover, New York, 1967
8. D. J. McClements, Ultrasonic Characterisation of Emulsions and Suspensions, *Adv. Colloid Int. Sci.,* **37**, 1991, 33 – 72
9. R. Manasseh R. F. LaFontaine, J. Davey, I. Shepherd, Y. –G. Zhu, Passive Acoustic Sizing in Sparged Systems, *Exp. in Fluids,* 2001, **30**, 672 – 682
10. A. Vazquez, R. M. Sanchez, E. Salinas-Rodríguez, A. Soria, R. Manasseh, A look at Three Measurement Techniques for Bubble Size Determination, *Exp. Thermal and Fluid Science,* 2005, **30**, 49 – 57
11. M. Minnaert, On Musical Air-bubbles and Sounds of Running Water*, Phil. Mag*, 1933, **16**, 235 – 248
12. I. Leifer, G. De Leeuw, L H. Cohen, Optical Measurement of Bubbles: System, Design and Application, *J. Atmos. Oceanic Technol. 17*, 2000, **17 (10)**, 1392 – 1402
13. M. C. Kim S. Kim, H. J. Lee, Y. J. Lee, K. Y. Kin, Int. Commun., An Experimental Study of Electrical Impedance Tomography for the Two-phase Flow Visualization, *Heat Mass Transfer*, 2002, **29**, 193 – 202

14. M. Wu, M. Gharib, Experimental Studies on the Shape and Path of Small Air Bubbles Rising in Clean Water, *Phys. Fluids 14*, 2002, L49 – L52
15. M. R. Rząsa, A. Pląskowski, Application of Optical Tomography for Measurement of Aeration Parameters, *Meas. Sci. Technol.*, 2003, **14**, 199 – 204
16. Y. B. Kim., Y. Roh, New Design of Matching Layers for High Power and Wide Band Ultrasonic Transducers, *Sensors and Actuators A*, 1998, **71**, 116 – 122
17. C. S. Desilets, J. D. Fraser and G. S. Kino, The Design of Efficient Broadband Piezoelectric Transducers, *IEEE Transactions on Sonics and Ultrasonics*, **SU-25 (3)**, 1978.
18. J. Krautkramer, H. Krautkramer, *Ultrasonic Testing of Materials*, Springer-Verlag, New York, USA, 1990
19. F.S. Foster, J. W. Hunt., The Design and Characterisation of Short Pulse Ultrasound Transducers, *Ultrasonics*, 1978, **23**, 116 - 122
20. F. Levassort, M. P. Tai, H. Hemery, P. Marechal, L. –P. Tran-Huu-Hue, M. Lethiecq, Piezoelectric Textured Ceramics: Effective Properties and Application to Ultrasonic Transducers, *Ultrasonics*, 2006, **44**, e621 – e626
21. K. D. Rolt, History of the Flextensional Electroacoustic Transducer, *Journal of Acoustic Society of America*, 1990, **87**, 1340
22. S. Alkoy, A. Dogan, A. –C. Hladky, P. Langlet, J. K. Cochran, R. E. Newnham, Miniature Piezoelectric Hollow Sphere Transducers (BB's), *IEEE Trans UFFC*, 1997, **44**, 1067
23. M. Tramontana, A. Gachagan, G. Hayward, A. Nordon and D. Littlejohn, Ultrasonic Monitoring of Heterogeneous Chemical Reactions, *IEEE International Ultrasonics Symposium*, 2006, 910
24. P. Hauptmann, N. Hoppe, A. Püttmer, Application of Ultrasonic Sensors in the Process Industry, *Measurement Science and Technology*, 2002, **13**, R73 – R83
25. P. Hauptmann, R. Lucklum, A. Püttmer, B. Henning, Ultrasonic Sensors for Process Monitoring and Chemical Analysis: State-of-the-art and Trends, *Sensors and Actuators A*, 1998, **67**, 32 – 48

26. A. Püttmer, R. Lucklum, B. Henning, P. Hauptmann, Improved Ultrasonic Density Senor with Reduced Diffraction Influence, *Sensors and Actuators A*, 1998, **67**, 8 – 12
27. A. Püttmer, N. Hoppe, B. Henning, P. Hauptmann, Ultrasonic Density Sensor – Analysis of Errors due to Thin Layers of Deposits in the Sensor Surface, *Sensors and Actuators*, 1999, **76**, 122 – 126
28. B. Henning, J. Rautenberg, Process Monitoring using Ultrasonic Sensor Systems, *Ultrasonics*, 2006, **44**, e1395 – e1399
29. M. J. W. Povey, *Ultrasonic Techniques for Fluids Characterisation*, San Diego, Academic Press, 1997
30. A. Püttmer, New Applications for Ultrasonic Sensors in Process Industries, *Ultrasonics*, 2006, **44**, e1379 – e1383
31. J. W. R. Boyd, J. Varley, Acoustic Emission Measurements of Low Velocity Plunging Jets to Monitor Bubble Size, *Chemical Engineering Journal*, 2004, **97**, 11 – 25
32. J. W. R. Boyd, J. Varley, Measurement of Gas Hold-up in Bubble Columns from Low Frequency Acoustic Emissions. *Chemical Engineering Journal*, 2002, **88**, 111 – 118
33. A. K. Bin, Gas Entertainment by Plunging Liquid Jets, *Chemical Engineering Science*, 1993, **48 (21)**, 3585 – 3630
34. J. W. R. Boyd, J. Varley, The Uses of Passive Measurements of Acoustic Emission from Chemical Engineering Processes, *Chemical Engineering Science*, 2001, **56**, 1749 – 1767
35. R. Manasseh, R. F. LaFontaine, J. Davey, I. Shepherd, Y. –G. Zhu, Passive Acoustic Bubble Sizing in Sparged Systems, *Experiments in Fluids*, 2001, **30**, 672 – 682
36. R. Manasseh, Bubble-pairing Phenomena in Sparging from Vertical-axis Nozzles, Proceedings of Chemeca 96: 24$^{th}$ Australian and New Zealand Chemical Engineering Conference, Sydney, **5**, 27 – 32
37. M. Wu, M. Gharib, Experimental Studies on the Shape and Path of Small Air Bubbles Rising in Clean Water, *Physics of Fluids*, 2002, **14 (7)**, L49 – L52

38. X. Frank, N. Dietrich, J. Wu, R. Barraud, H. Z. Li, Bubble Nucleation and Growth in Fluids, *Chemical Engineering Science,* 2007, **62**, 7090 – 7097

39. N. A. Kazakis, A. A. Mouza, S. V. Paras, Experimental Study of Bubble Formation at Metal Porous Spargers: Effect of Liquid Properties and Sparger Characteristics on the Initial Bubble Size Distribution, *Chemical Engineering Journal,* 2008, **137**, 265 - 281

40. A. Vazquez, R. M Sanchez, E. Salinas-Rodríguez, A. Soria, R. Manasseh, A Look at Three Measurement Techniques for Bubble Size Determination, *Experimental Thermal and Fluid Science*, 2005, **30**, 49 – 57

41. T. G. Leighton, A. J. Walton, An Experimental Study of the Sound Emitted from Gas Bubbles in a Liquid, *European Journal of Physics*, 1987, **8**, 98 – 104

42. S. M. Oak, B. J. Kim, W. T. Kim, M. S. Chun, Y. H. Moon, Physical Modelling of Bubble Generation in Foamed-aluminium, *Journal of Materials Processing Technology*, 2002, **130-131**, 304 – 309

43. M. R. Rząsa, A. Pląskowski, Application of Optical Tomography for Measurement of Aeration Parameters in Larger Water Tanks, *Measurement Science and Technology*, 2003, **14**, 199 – 204

44. A. Nordon, R. J. H. Waddell, L. J. Bellamy, A. Gachagan, D. McNab, D. Littlejohn, G. Hayward, Monitoring of a Heterogeneous Reaction by Acoustic Emission, *The Analyst*, 2004, **129**, 463 – 467

45. A. Nordon, Y. Carella, A. Gachagan, D. Littlejohn, G. Hayward, Factors Affecting Broadband Acoustic Emission Measurements of a Heterogeneous Reaction, *The Analyst*, 2006, **131**, 323 – 330

46. R. Hou, A. Hunt, R. A. Williams, Acoustic Monitoring of Pipeline Flows: Particulate Slurries, *Powder Technology*, 1999, **106**, 30 – 36

47. M. Whitaker, G. R. Baker, J. Westrup, P. A. Goulding, D. R. Rudd, R. M. Belchamber, M. P. Collins, Application of Acoustic Emission to the Monitoring and End Point Determination of a High Shear Granulation Process, *International Journal of Pharmaceutics*, 2000, **205**, 79 – 91

48. J. Huang, S. Ose, S. de Silva, K. H. Esbensen, Non-invasive Monitoring of Powder Breakage during Pneumatic Transportation using Acoustic Emission, *Powder Technology*, 2003, **129**, 130 – 138

49. T. G. Leighton, A. D. Phelps, D. G. Ramble, D. A. Sharpe, Comparison of the Abilities of Eight Techniques to Detect and Size a Single Bubble, *Ultrasonics*, 1996, **34**, 661 – 667

50. T. G. Leighton, From Seas to Surgeries, From Babbling Brooks to Baby Scans: The Acoustics of Gas Bubbles in Liquids, *International Journal of Modern Physics B*, 2004, **18(25)**, 3267 – 3314

51. T. G. Leighton, R. J. Lingard, A. J. Walton, J. E. Field, Acoustic Bubble Sizing by Combination of Subharmonic Emissions with Imaging Frequency, *Ultrasonics*, 1991, **29**, 319 – 323

52. T. G. Leighton, R. J. Lingard, A. J. Walton, J. E. Field, Bubble Sizing by the Nonlinear Scattering of Two Acoustic Frequencies, Natural Physical Sources of Underwater Sound, ed. B. R. Kerman, 1993, 453 – 466

53. A. D. Phelps, T. G. Leighton, Investigations into the Use of Two Frequency Excitation to Accurately Determine Bubble Sizes, Proceedings of the IUTAM Conference on Bubble Dynamics and Interface Phenomena, 1994, 475 – 484

54. A. D. Phelps, T. G. Leighton, High-Resolution Bubble Sizing Through Detection of the Subharmonic Response with a Two-Frequency Excitation Technique, *Journal of the Acoustical Society of America*, 1996, **99 (4)**, 1985 – 1992

55. A. D. Phelps, T. G. Leighton, M. F. Schneider, P. R. White, Active and Passive Acoustic Bubble Sizing, ISVR Technical Report 237, Southampton, University of Southampton, 1994

56. T. G. Leighton, D. G. Ramble, A. D. Phelps, The Detection of Tethered and Rising Bubbles using Multiple Acoustic Techniques, *Journal of the Acoustical Society of America*, 1997, **101 (5)**, 2626 – 2635

57. A. D. Phelps, T. G. Leighton, M. F. Schneider, P. R. White, Acoustic Bubble Sizing, Using Active and Passive Techniques to Compare Ambient and Entrained Populations, ISVR Technical Report 229, Southampton, University of Southampton, 1994

58. T. G. Leighton, D. G. Ramble, A. D. Phelps, Measurement of Bubbles in a Pipe using Multiple Acoustic Techniques, ISVR Technical Report 258, Southampton, University of Southampton, 1996

59. T. G. Leighton, D. G. Ramble, A. D. Phelps, C. L. Morfey, P. P. Harris, Acoustic Detection of Gas Bubbles in a Pipe, *Acoustica*, 1998, **84**, 801 – 814

60. I. N. Didenkulov, S. W. Yoon, A. M. Sutin, E. J. Kim, Nonlinear Doppler Effect and its use for Bubble Flow Velocity Measurements, *The Journal of the Acoustical Society of America*, 1999, **106 (5)**, 2431 – 2435

61. P. Resa, T. Bolumar, L. Elvira, G. Pérez, F. M. de Espinosa, Monitoring of Lactic Acid Fermentation in Culture Broth using Ultrasonic Velocity, *Journal of Food Engineering*, 2007, **78**, 1083 – 1091

62. H. Ogasawara, K. Mizutani, T. Ohbuchi, T. Nakamura, Acoustical Experiment of Yogurt Fermentation Process, *Ultrasonics*, 2006, **44**, e727 – e730

63. A. Kulmyrzaev, C. Cancelliere, D. J. McClements, Characterisation of Aerated Foods using Ultrasonic Reflectance Spectroscopy, *Journal of Food Engineering*, 2000, **46**, 235 – 241

64. J. A. Bamberger, M. S. Greenwood, Non-invasive Characterisation of Fluid Foodstuffs based on Ultrasonic Measurements, *Food Research International*, 2004, **37**, 621 – 625

65. J. Salazar, A. Turó, J. A. Chávez, M. J. García, Ultrasonic Inspection of Batters for On-line Process Monitoring, *Ultrasonics*, 2004, **42**, 155 – 159

66. B. Henning, P. –C. Daur, S. Prange, K. Dierks, P. Hauptmann, In-line Concentration Measurement in Complex Liquids using Ultrasonic Sensors, *Ultrasonics*, 2000, **38**, 799 – 803

67. M. S. Greenwood, S. Ahmed, Ultrasonic Diffraction Grating Spectroscopy and the Measurements of Particle Size, *Ultrasonics*, 2006, **44**, e1385 – e1393

68. P. Mougin, D. Wilkinson, K. J. Roberts, R. Jack, P. Kippax, Sensitivity of Particle Sizing by Ultrasonic Attenuation Spectroscopy to Material Properties, *Powder Technology*, 2003, **134**, 243 – 248

69. M. S. Greenwood, J. A. Bamberger, Ultrasonic Sensor to Measure the Density of a Liquid or Slurry During Pipeline Transport, *Ultrasonics*, 2002, **40**, 413 – 417

70. J. A. Bamberger, M. S. Greenwood, Measuring Fluid and Slurry Density and Solids Concentration Non-invasively, *Ultrasonics*, 2004, **42**, 563 – 567

71. M. S. Greenwood, J. A. Bamberger, Measurement of Viscosity and Shear Wave Velocity of a Liquid or Slurry for On-line Process Control, *Ultrasonics*, 2002, **39**, 623 – 630

72. M. S. Greenwood, J. D. Adamson, J. A. Bamberger, Long-path Measurements of Ultrasonic Attenuation and Velocity for Very Dilute Slurries and Liquids and Detection of Contaminates, *Ultrasonics*, 2006, **44**, e461 – e466

73. M. S. Greenwood, A. Brodsky, L. Burgess, L. J. Bond, M. Hamad, Ultrasonic Diffraction Grating Spectroscopy and Characterisation of Fluids and Slurries, *Ultrasonics*, 2004, **42**, 531 – 536

74. J. A. Bamberger, M. S. Greenwood, Using Ultrasonic Attenuation to Monitor Slurry Mixing in Real Time, *Ultrasonics*, 2004, **42**, 145 - 148

75. F. A. Duck, Nonlinear Acoustics in Diagnostic Ultrasound, *Ultrasound in Medicine and Biology*, 2002, **28 (1)**, 1 – 18

76. F. Calliada, R. Campani, O. Bottinelli, A. Bozzini, M. G. Sommaruga, Ultrasound Contrast Agents Basic Principles, *European Journal of Radiology*, 1998, **27**, S157 – S160

77. P. A. Lewin, Quo Vadis Medical Ultrasound?, *Ultrasonics*, 2004, **42**, 1 – 7

78. D. N. Patel, S. H. Bloch, P. A. Dayton, K. W. Ferrara, Acoustic Signatures of Submicron Contrast Agents, *IEEE Transactions on Ultrasound, Ferroelectrics and Frequency Control*, 2004, **51 (3)**, 293 – 301

79. K. E. Morgan, J. S. Allen, P. A. Dayton, J. E. Chomas, A. L. Kilanov, K. W. Ferrara, Experimental and Theoretical Evaluation of Microbubble Behaviour: Effect of Transmitted Phase and Bubble Size, *IEEE Transactions on Ultrasound, Ferroelectrics, and Frequency Control*, 2000, **47(6)**, 1494 – 1509.

80. E. R. Wisner, K. Ferrara, J. D. Gabe, D. Patel, T. G. Nyland, R. E. Short, T. B. Ottoboni, Contrast Enhanced Intermittent Power Doppler Ultrasound with Sub-Micron Bubbles for Sensitive Node Detection, *Academic Radiology*, 2002, **9 (2)**, S389 – S391

81. B. B. Goldberg, J. S. Raichlen, F. Forsberg, *Ultrasound Contrast Agents, Basic Principles and Clinical Applications*, London, Martin Dunitz, 2001

82. Y. Sun, D. E. Kruse, P. A. Dayton, K. W. Ferrara, High-Frequency Dynamics of Ultrasound Contrast Agents, *IEEE Transactions on Ultrasound, Ferroelectrics, and Frequency Control*, 2005, **52 (11)**, 1981 – 1991

83. G. Bhagavatheeshwaran, W. T. Shi, F. Forsberg, P. M. Shanker, Subharmonic Signal Generation from Contrast Agents in Simulated Neovessels, *Ultrasound in Medicine and Biology*, 2004, **30**, 199 – 203

84. J. Chomas, P. Dayton, D. May, K. Ferrara, Non-destructive Sub-harmonic Imaging, *IEEE Transactions on Ultrasound, Ferroelectrics, and Frequency Control*, 2002, **49**, 883 – 892

85. S. Zhao, D. E. Kruse, K. W. Ferrara, P. A. Dayton, Acoustic Response from Adherent Targeted Contrast Agents, *Journal of the Acoustical Society of America*, 2006, **120 (6)**, EL63 – EL69

86. A. F. H. Lum, M. A. Borden, P. A. Dayton, D. E. Kruse, S. I. Simon, K. W. Ferrara, Ultrasound Radiation Force Enables Targeted Deposition of Model Drug Carriers Loaded on Microbubbles, *Journal of Controlled Release*, 2006, **111**, 128 – 134

87. Y. Sun, S. Zhao, P. A. Dayton, K. W. Ferrara, Observation of Contrast Agent Response to Chirp Insonation with a Simultaneous Optical-Acoustical System, *IEEE Transactions on Ultrasound, Ferroelectrics and Frequency Control*, 2006, **53 (6)**, 1130 – 1137

88. Y. Sun, D. E. Kruse, K. W. Ferrara, Contrast Imaging with Chirped Excitation, *IEEE Transactions on Ultrasound, Ferroelectrics and Frequency Control*, 2007, **54 (3)**, 520 – 529

89. M. A. Borden, H. Zhang, R. J. Gillies, P. A. Dayton, K. W. Ferrara, A Stimulus-Responsive Contrast Agent for Ultrasound Molecular Imaging, *Biomaterial*, 2007, doi: 10.1016.j.biomaterials.2007.10.011

90. C. F. Caskey, S. M. Stieger, S. Qin, P. A. Dayton, K. W. Ferrara, Direct Observation of Ultrasound Microbubble Contrast Agents Interaction with the Microvessel Wall, *Journal of the Acoustical Society of America*, 2007, **122(2)**, 1191 – 1200

91. N. de Jong, R. Cornet, C. T. Lancée, Higher Harmonics for Vibrating Gas-Filled Microspheres. Part One: Measurements, *Ultrasonics*, 1994, **32(6)**, 447 – 453

92. N. de Jong, R. Cornet, C. T. Lancée, Higher Harmonics for Vibrating Gas-Filled Microspheres. Part Two: Measurements, *Ultrasonics*, 1994, **32(6)**, 455 – 459

93. N. de Jong, F. J. Ten Cate, New Ultrasound Contrast Agents and Technological Innovations, *Ultrasonics*, 1996, **34**, 587 – 590

94. P. J. A. Frinking, N. de Jong, E. I Céspedes, Scattering Properties of Encapsulated Gas Bubbles at High Ultrasound Pressures, *Journal of the Acoustical Society of America*, 1999, **105 (3)**, 1989 – 1996

95. N. de Jong, A. Bouakaz, F. J. Ten Cate, Contrast Harmonic Imaging, *Ultrasonics*, 2002, **40**, 567 – 573

96. Y. Matsumoto, J. S. Allen, S. Yoshizawa, T. Ikeda, Y. Kaneko, Medical Ultrasound with Microbubbles, *Experimental Thermal and Fluid Science*, 2005, **29**, 255 – 265

# Chapter 4
# Experimental Arrangements

The passive acoustic experiments included an evaluation of three methods of bubble production (syringe pump, peristaltic pump and air cylinder) using two ultrasonic devices; a low frequency transducer[1] (non-invasive) and a hydrophone (invasive). Different experimental conditions were used for evaluating the three methods of bubble production due to experimental restrictions, for example tubing length, special tubing and attachment. The active acoustic experiments involved validating the software used in this research (see Chapter 3 pages 59 and 60) prior to applying this to the active acoustic sizing of bubbles in terms of frequency and diameter.

The aim of both the passive and active acoustic experiments was to characterise bubbles of various sizes, in particular 4 mm diameter bubbles, which are typical of fermentation reactions. The Matlab® programmes used in the data analysis were written by Dr. Alison Nordon, Centre for Process Analytics and Control Technology, University of Strathclyde.[1] The raw data were combined to give power spectra and then Fourier transformed, using Matlab®. It is the Fourier transformed data that is plotted in all spectra throughout Chapters 5 and 6. The y-axis in all the spectra is labelled 'Intensity (arbitrary units)', as per chemistry convention.

## 4.1 Acoustic Emission Set-Up and Signal Capture

The bubble detection device was connected to a 2/4/6C pre-amplifier with a BP-SYS filter - 60 dB gain (Physical Acoustics, Cambridge, UK) which was connected to an Agilent oscilloscope 54624A. The data were transferred from the oscilloscope to a PC via a USB/General purpose interface board. The signals were collected with a sampling rate of 200 kHz and transferred to the data capturing software. Each signal consisted of 100,000 points. Fifty repeat measurements were taken and downloaded to the PC. The data was processed on a PC by carrying out a Fourier transform and calculating the power spectrum. The power spectra were then generated from summation of 10 spectra into 5 blocks to give 5 repeat measurements and the areas

under the spectra calculated using Matlab® (version 7.3.0.267, R2006b) and Partial Least Squares toolbox. Statistical analysis was then carried out using Microsoft Excel®. The Relative Standard Deviation (RSD) of the peak areas was calculated using the area under the spectra between 1 and 4 kHz.

Figure 4.1 illustrates the set-up which was used to conduct measurements of bubbles produced using an air cylinder.

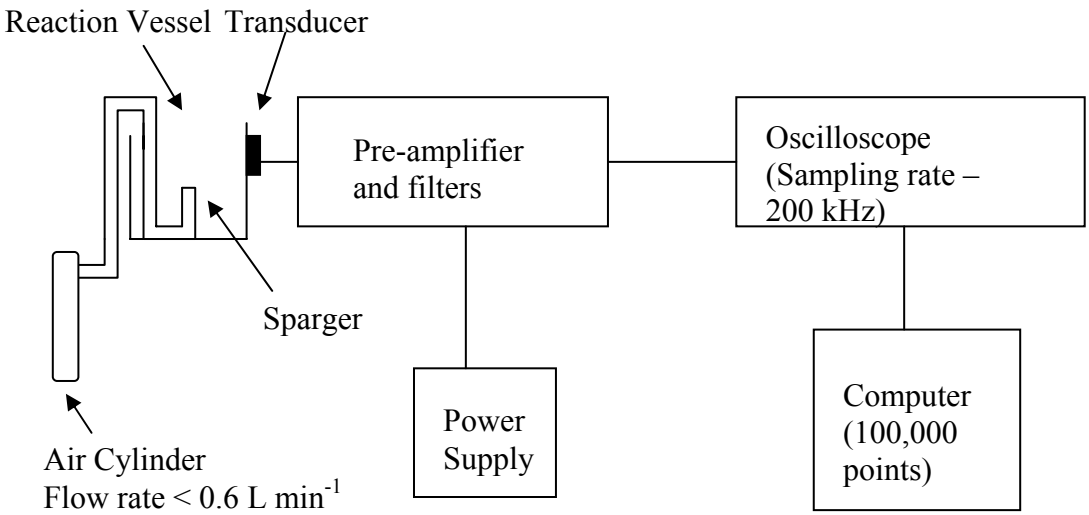


**Figure 4.1 – Acoustic emission set-up for bubbles produced using an air cylinder**

To determine the most favourable conditions for the production and characterisation of bubbles, the following devices were investigated: a low frequency transducer (10 – 180 kHz), developed by Manuel Tramontana[1] and a hydrophone (model 8103, 0.1 Hz – 180 kHz), purchased from Brüel & Kjær UK Limited. The low frequency transducer was made from five layers of PZT4D ceramic with a fundamental resonance at 40 kHz and 50% - 3 dB bandwidth. The hydrophone had an operational bandwidth between 0.1 Hz and 20 kHz.[2] High density vacuum grease (Dow Corning, USA) was used to acoustically couple the transducer to the reaction vessel and the transducer was held in place with a clamp stand. The hydrophone was placed in water and held in place by a clamp stand.

## 4.2 Evaluation of Bubble Production Methods and Bubble Production Conditions

Preliminary tests were carried out using the hydrophone and transducer. Details of how bubbles were produced are given under the relevant section.

### 4.2.1 Syringe Pump

Bubbles produced using the syringe pump were carried out using the set-up outlined in section 4.1 with the following modifications. A 600 mL beaker was filled to a height of 9.1 cm (500 mL mark) with water. Fifty repeat measurements were taken without bubble production to collect a background spectrum. The tubing was connected to the syringe pump (Gilson Dilutor 401) and attached to the side of the beaker using electrical tape. The syringe pump was employed in dispense mode with a volume of 5 mL per injection.

The hydrophone was used for detecting bubbles being produced and was placed at two different locations (see Figure 4.2);

(i) 4.8 cm from the base of the beaker, in the centre of the beaker,

(ii) 4.8 cm from the base of the beaker, at the side of the beaker next to the tubing outlet.

Tubing with a diameter of 2 mm was used, which was submerged to just below the water line. Note 4.8 cm from the base of the beaker corresponds to the 250 mL mark on a 600 mL beaker.

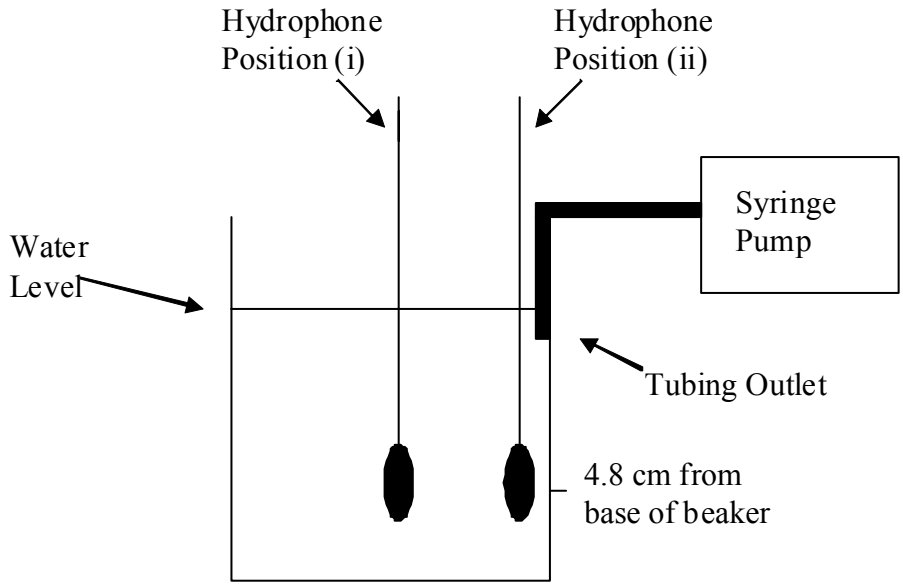


**Figure 4.2 – Position of hydrophone relative to tubing for syringe pump tests**

### 4.2.2 Peristaltic Pump

The peristaltic pump used was a Watson Marlow. All tubing was attached so that the tubing outlet was at a height of 6.5 cm (350 mL mark on a 600 mL beaker) with electrical tape. Tubing with a diameter of 2.5 mm was attached to the inner wall of the beaker. Again, the hydrophone was tested at two positions; at the centre of the beaker and at the edge of the beaker close to the bubble source, see Figure 4.3.

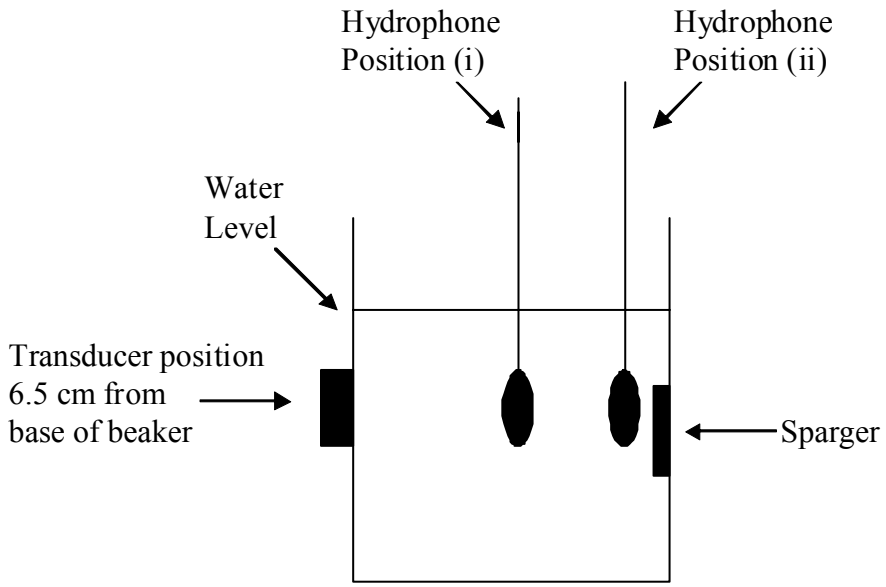


**Figure 4.3 – Position of hydrophone and transducer relative to sparger for peristaltic pump tests**

To evaluate the acoustic emission spectra and various bubble diameters and flow rates the hydrophone was kept at position (ii) in Figure 4.3 and acoustic emission spectra were obtained for bubbles produced from 3 diameters of tubing; 1.1, 1.9 and 2.5 mm at three different flow rates; 2.7, 3.1 and 5.6 mL $min^{-1}$. Following this, three other sparger diameters were tested; 0.38, 0.76 and 1.4 mm with a flow rate of 2.7 mL $min^{-1}$.

To investigate if the bubbles produced were interacting with the beaker wall the position of the tubing was moved 1 cm from the beaker wall and the hydrophone was placed to within 1 cm of the tubing outlet, still in the same horizontal plane as the tubing outlet, see Figure 4.4. The acoustic emission spectra of bubbles produced from three tubing diameters (1.1, 1.9 and 2.5 mm) at a flow rate of 2.7 mL $min^{-1}$ were obtained.

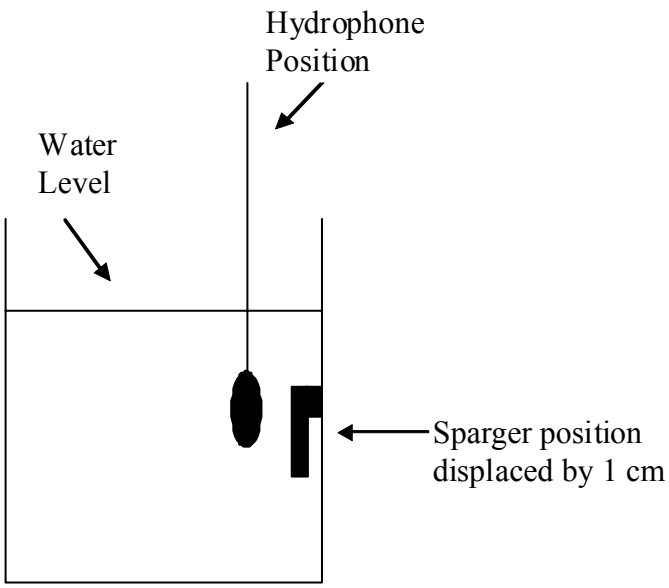


**Figure 4.4 – Position of hydrophone and sparger displaced by 1 cm to investigate interaction with the beaker wall**

The hydrophone was replaced by a 3-1 connectivity transducer, placed directly opposite the bubble production site, see Figure 4.3. A repeat of the following hydrophone experiments was carried out; AE spectra were obtained for bubbles produced from tubing diameters of 0.38, 0.76, 1.1, 1.4 and 2.5 mm at a flow rate of 3.1 mL $min^{-1}$.

### 4.2.3 Air Cylinder

A 5 L beaker was filled to a height of 19.2 cm (4 L mark) with ordinary tap water. The sparger was fixed to the centre of the beaker and rose to a height of 9.7 cm from the base of the beaker. The transducer was attached 9.7 cm from the base of the beaker (250 mL mark), the hydrophone was placed 1 – 2 cm from the sparger in a horizontal direction. The transducer and hydrophone were in the same horizontal plane as the sparger. The air flow rate was kept reasonably stable with a single bubble being produced every second. It should be noted that it was extremely difficult to keep a constant (low) flow rate over a period of time; this was because at such low pressures and low flow rates the pressure tended to drop off over time. To

help regulate the pressure Hoffmann clips were used to clamp the tubing between the sparger and the flow meter.

The sparger diameters which were investigated were 1, 1.5, and 2 mm. All 3 spargers were made at the glassblowing workshop within the Chemistry Department at the University. The pressure regulator was 0 – 2 bar and the flow meter ranged from 0 – 800 mL $min^{-1}$.

## 4.3 Factors to Investigate

To assess the influence of different factors on bubble size and repeatability of bubble production, the following factors were considered and tested:

- Attachment of transducer and hydrophone,
- Measurement repeatability,
- Sparger diameter,
- Sparger position in relation to bubble production site,
- Air flow rate,
- Liquid viscosity.

Details of the individual parameters that were used to investigate the above factors are given in the appropriate section of the results in Chapter 5.

In the study of flow rate and viscosity a different resolution of spectra was used. Since higher flow rates were used in these experiments a train of bubbles were detected by the hydrophone as opposed to a single bubble. Therefore the oscilloscope displayed a series of signals, corresponding to the train of bubbles which were detected. An example of the oscilloscope trace can be seen in Figure 4.5.

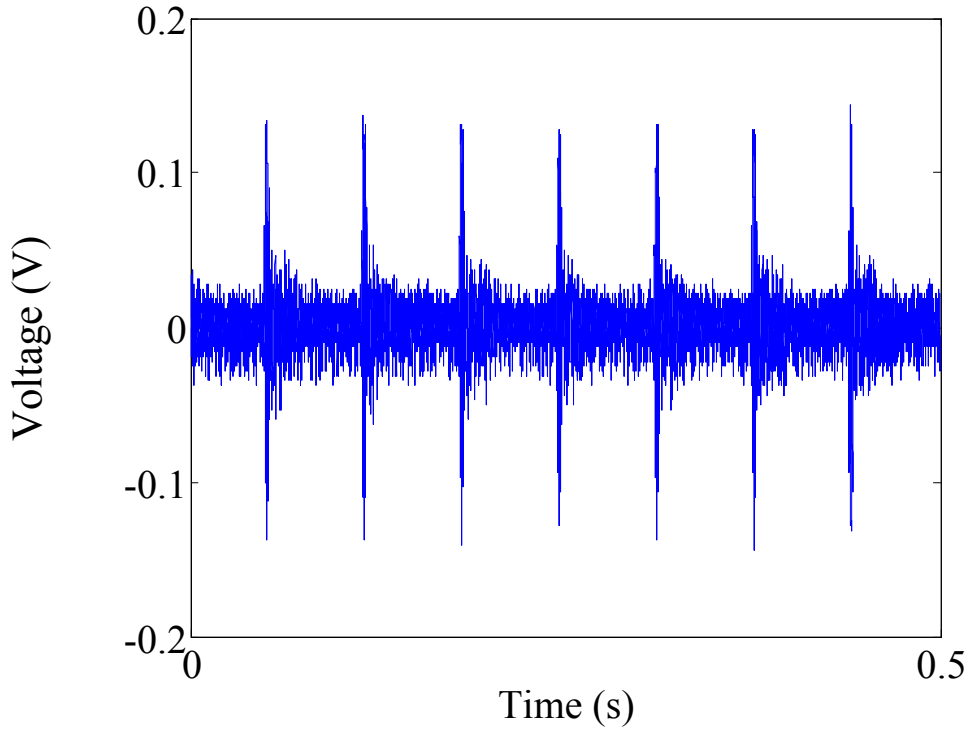


**Figure 4.5 – Example of typical oscilloscope trace obtained for flow rate experiments. Time trace shows 7 signals which were divided in Matlab® to give 7 repeat signals**

In Figure 4.5 each signal arises from the detection of a single bubble, therefore 7 bubbles were detected in Figure 4.5. Matlab® was used to divide the signal into 7 separate signals. As a consequence of this the number of data points was reduced, hence giving a different resolution.

## 4.4 Active Acoustic Set-Up and Signal Capture

This section describes the general set-up for active acoustic experiments. Details of any deviations from this experimental set-up are given under the relevant section in the results (Chapter 6).

Experiments were carried out in a 40 x 28 x 28 cm tank filled to a depth of 15 cm with water. The transducers used were immersion transducers, purchased from OlympusNDT (Rotherham, UK) with properties summarised in Table 4.1.

**Table 4.1 – Properties of Transducers purchased from OlympusNDT® used for active acoustic experiments**

| | Transducer 1 | Transducer 2 | Transducer 3 |
|---|---|---|---|
| Centre Frequency (MHz) | 0.5 | 2.25 | 5.0 |
| Nominal Element Size (mm) | 29 | 19 | 19 |
| Focal Length (mm) | 50.8 | 50.8 | 50.8 |

Figure 4.6 shows a schematic diagram of the experimental set-up. The transducers were mounted at 90° to each other on a plastic tile (17 x 17 cm), which was raised 5 cm from the base of the tank. Signal input was controlled from a computer using code written in the software package Matlab®. In this work the transducer excitation signal was a linear chirp function: which is defined by a start and end frequency and a specified time duration; through which a linear frequency sweep is generated. Signal chirps were downloaded from the computer and stored in a function generator (Agilent 332050A), a Hamming window was applied to the signal. The signal generator was connected to a power amplifier (KALMUS 155LCR) which in turn was connected to the oscilloscope (Agilent 54624A). The oscilloscope was connected to the transmitting transducers through channel one of the oscilloscope. The receiving transducer was connected to channel two of the oscilloscope. The received signal was amplified with a 41 dB gain (UTEX UT340 Pulser Receiver System) visualised using the oscilloscope and acquired by the computer. The sampling rate was 500 Ms $s^{-1}$ and the capture window length was 120 μs. Ten repeat measurements were taken and summed together in the frequency domain. Figure 4.7 shows a picture of the experimental set-up as it was on the laboratory bench.

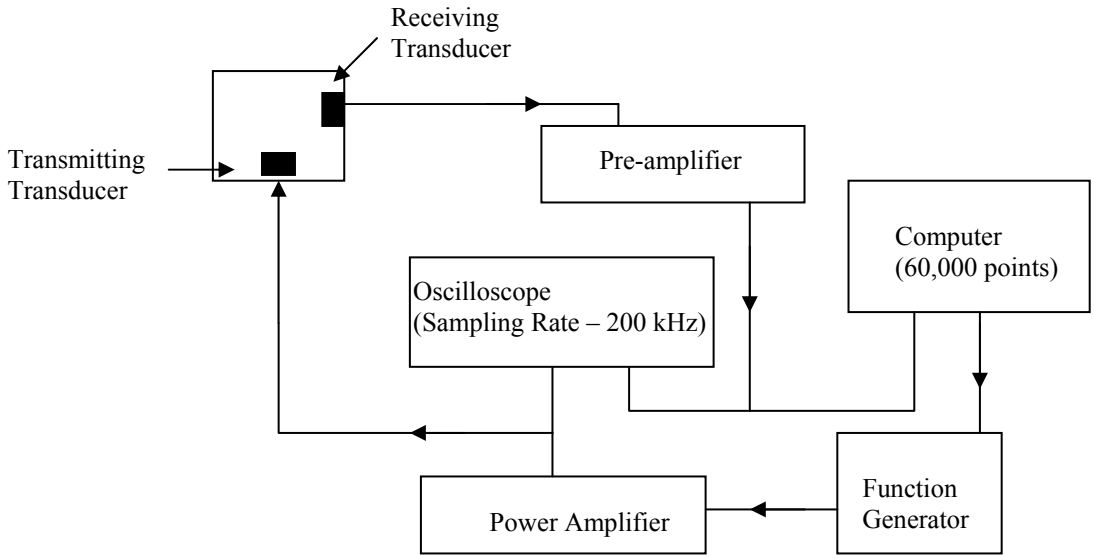


**Figure 4.6 – Schematic Diagram of the experimental set-up employed for the active acoustic experiments**

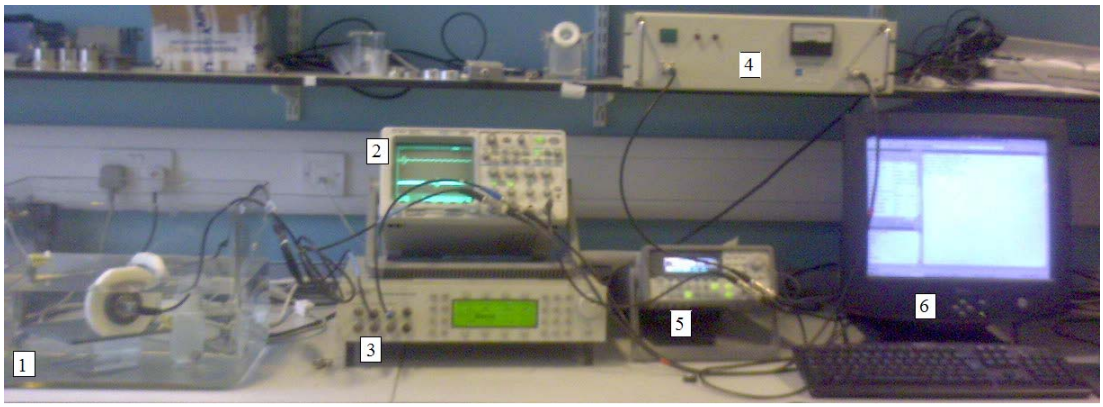


**Figure 4.7 – Photograph of the experimental set-up showing 1 - tank, 2 - oscilloscope, 3 - receiving pre-amplifier, 4 - transmitting power amplifier, 5 - function generator and 6 – personal computer.**

The Matlab® programmes used were provided in previous collaborative CPACT/CUE projects and are detailed in reference 3. Also, the characterisation of the transducers used in the active acoustic experiments was carried out by C. Wang, Centre for Ultrasonic Engineering, University of Strathclyde.[3] The Matlab® programmes were used to generate the linear chip and another to set-up the oscilloscope and capture the data. Signal processing Matlab® programmes were

then used to average the signal and cross-correlate the data to extract the active harmonic, Fourier transform the data and calculate the area under the spectra.

### 4.4.1 Investigation of Drive Voltage

Before experiments were carried out the drive voltage had to be investigated to determine the optimum conditions that produce a received signal with appropriate amplitude, this was done for both ultrasound contrast agents and bubbles. Without the use of an amplifier the maximum drive voltage that could be achieved was 10 V. Hence, the use of a power amplifier to produce drive voltages of 6.4, 12.0, 18.1, 24.0, 30.8 and 36.6 V. The transducers were selected for transmission at 2.25 MHz and reception at 5 MHz. The chirp used here ranged from 1.75 MHz to 2.75 MHz and had a duration of 5 μs. In all cases the ten repeat measurements of each experiment were acquired prior to the processing stage.

### 4.4.2 Ultrasound Contrast Agent Experiments

This experiment was intended to replicate the work carried out by Ferrera *et al.*[4] in order to validate the Matlab® software used to process the received signals. During the experiments carried out on the contrast agent the transducers were arranged to be transmitting at 2.25 MHz and receiving at 5 MHz (to detect for the second harmonic). The excitation chirp used here ranged from 1.75 MHz to 2.75 MHz and had a duration of 5 μs. The second harmonic frequency component was cross-correlated using a chirp signal ranging between 3.5 MHz and 5.5 MHz.

Cellulose tubing with a diameter of 6 mm was placed diagonally at an angle of 45° between the two transducers. Cellulose tubing was selected because it is acoustically transparent, as the acoustic impedance of cellulose is close to that of water, also that this tubing was that used by Ferrara. The contrast agent, SonoVue® (Bracco, UK) was delivered into the tubing from two syringes which were manually operated and the waste was collected in a waste bottle.

### 4.4.3 Active Acoustic Sizing of Bubbles

The cellulose tubing was replaced by a thin wire, which remained at an angle of 45° between the two transducers. The wire was coated with a thin layer of petroleum jelly. The drive voltage was investigated using the conditions described in section 4.4.1, to find the optimum conditions for signal capture. After analysis of the received frequency spectrum the set-up was then modified such that the both the transmitting and receiving transducers were at 0.5 MHz and the excitation chirp was changed to one which ranged from 250 kHz to 750 kHz and had a duration of 10 μs. Bubbles of estimated diameter of 1, 2 and 4 mm were produced from tubing with internal diameters of 1, 2 and 4 mm, respectively, and placed on the wire in the focus of the transducers and both Fourier analysis and cross-correlation techniques were used to investigate the relationship between the received acoustic signals and bubble diameter.

## 4.5 References


1. M. Tramontana, A. Gachagan, G. Hayward, A. Nordon and D. Littlejohn, 'Ultrasonic Monitoring of Heterogeneous Chemical Reactions', *IEEE International Ultrasonics Symposium*, 2006, 910
2. http://www.bksv.com/doc/bp0317.pdf Calibration Chart for Hydrophone Type 8103 [cited 20/07/08]
3. Chuangnan Wang, *Monitoring of Pharmaceutical Processes using Non-Linear Ultrasound*, Final Year Report, University of Strathclyde, Dept. of EEE, June 2008
4. D. N. Patel, S. H. Bloch, P. A. Dayton, K. W. Ferrara, Acoustic Signatures of Submicron Contrast Agents, *IEEE Transactions on Ultrasound, Ferroelectrics and Frequency Control*, 2004, **51 (3)**, 293 – 301

# Chapter 5
# Passive Acoustics Results

The inverse relationship between bubble size and resonance frequency was described in Chapter 3, Equation 3.8.[1] The experiments in this section use this relationship as a method for characterising bubbles of different diameters. The three bubble production methods investigated were bubbles produced from a syringe pump, a peristaltic pump and an air cylinder. Each spectrum shown in this chapter is an example of the typical spectrum that was obtained for the experiment.

The overall aim of the experiments carried out in this chapter was to evaluate each of three methods of bubble production in terms of bubble resonance frequency and area under the spectra to determine which method gave rise to the most analytically repeatable measurements. Throughout this chapter any reference to bubble bursting indicates that the bubble burst at the surface of the water.

## 5.1 Syringe Pump

Spectra of bubbles produced from the syringe pump were obtained with the hydrophone in two positions, at the centre of the beaker and at the side of the beaker. Tubing was attached to the inner surface of the beaker wall. There were no peaks present in either spectra obtained for bubbles produced which could be related to bubble generation. Any signals that were present were attributed to either background noise or noise associated with the operation of the syringe pump. A reason why the hydrophone did not pick any signals arising from bubble production was that the syringe pump had some drawback of water, therefore the pressure forcing the air out of the syringe was not large enough to push the drawn back water out and produce a bubble of a suitable size to be detected.

From these results it was concluded that the use of the syringe pump should be discontinued. The focus of the remaining experiments was placed on the peristaltic pump and air cylinder as methods of generating bubbles.

## 5.2 Peristaltic Pump

Bubbles were produced using a peristaltic pump connected to tubing, with the tubing outlet secured on the inner surface of the beaker wall with electrical tape. Fifty signals were taken and summed into 5 blocks of 10 signals, this gave 5 repeat measurements with each spectrum formed from the summation of 10 signals.

### 5.2.1 Using the Hydrophone as the Bubble Detection Device to Investigate the Effect of Hydrophone Position on Bubble Detection

Acoustic emission arising from the production of bubbles was detected using a hydrophone. To study the effect of hydrophone position on bubble detection the hydrophone was placed in two positions. Firstly, the hydrophone was placed in the centre of the beaker away from the bubble production site, the spectra obtained at this position can be seen in Figure 5.1(a). The hydrophone was then placed 1 cm from the inner wall of the beaker close to the bubble production site, the spectra obtained at this position can be seen in Figure 5.1(b). In both cases the hydrophone was in the same horizontal plane as the tubing outlet and a tubing of diameter 2.5 mm was used and the flow rate was 5.6 mL $min^{-1}$. Figure 5.1(a) and (b) show two traces which highlight the difference in spectral intensity obtained during these experiments.

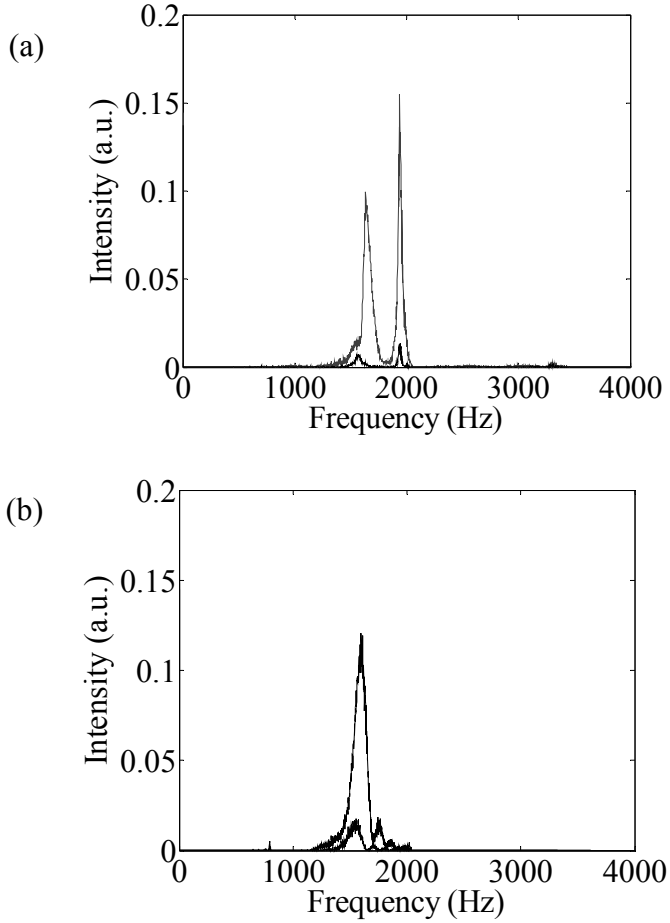


**Figure 5.1 – AE spectra of bubbles produced using tubing with a diameter of 2.5 mm and a flow rate of 5.6 mL min$^{-1}$, and detected using a hydrophone positioned (a) in the centre of the beaker and (b) 1 cm from the inner wall of the beaker, next to tubing outlet**

Figure 5.1 (a) shows the spectra obtained of bubbles produced detected by the hydrophone in the centre of the beaker. When the hydrophone was placed away from the bubble production site, i.e. in the centre of the beaker, it was detecting both bubbles being produced and bubbles being burst, as illustrated in Figure 5.1(a). The peaks present in Figure 5.1(a) were at frequencies of 1600 and 1938 Hz, which can be attributed to bubble production and bubble bursting at the surface of the water.

In Figure 5.1(b) the peak with lowest frequency was seen at 1600 Hz, which was the same as the peak of lowest frequency in Figure 5.1(a). When the hydrophone was placed close to the bubble production site it only detected bubbles being produced.

From this and Figures 5.1(a) and (b), it was possible to assign the peak at 1600 Hz to bubble production and the peak at 1938 Hz to bubble bursting.

At both hydrophone positions the intensities of the spectra obtained were variable, as can be seen by comparing the spectra in Figure 5.1(a) and those of Figure 5.1(b). A reason for this may have been that there was a change in bubble concentration in the beaker. The RSD of the peak area was 25.4 %, when the hydrophone was close to the bubble production site, compared with a RSD of the peak area of 55.4 % (n = 5) when the hydrophone was in the centre of the beaker. A decrease in RSD of the peak area would be expected, since the hydrophone was moved closer to the bubble production site it would be likely that only bubble production would be detected.

For bubbles to be detected when the hydrophone was positioned in the centre of the beaker, the minimum flow rate required was 5.6 mL $min^{-1}$. As the hydrophone had a linear sensitivity between 4 and 100 kHz, this explains why higher flow rates were needed to produce detectable bubbles when the hydrophone was further away from the bubble production site. It was also found that the hydrophone did not detect a signal on every occasion of a bubble being produced; this indicated that only bubbles which oscillated with a larger amplitude were being detected as larger amplitude oscillations give rise to bigger signals. This can be related to the theory of signal decay; which states that, as a signal travel through a medium, the pressure amplitude of spherical sounds waves decays as a function of 1/radius, if absorption is present.[3] Therefore, using the theory of signal decay, it was discovered that when the hydrophone was placed closer to the bubble production site, 1 cm from the tube outlet, it was possible to use lower flow rates; the minimum flow rate that could be used was 2.0 mL $min^{-1}$.

There was also the possibility of the bubble interacting with the glass wall of the beaker, since the tubing is attached to the beaker wall. To test this hypothesis the tubing was displaced 1 cm from the beaker wall, with the hydrophone next to the tubing outlet. This experiment was carried out for tubing diameter in the range from 1.1 to 2.5 mm. The flow rate was 2.7 mL $min^{-1}$. Figure 5.2 shows the spectra

obtained of bubbles produced from tubing of 1.1 mm diameter, displaced 1 cm from the beaker wall.

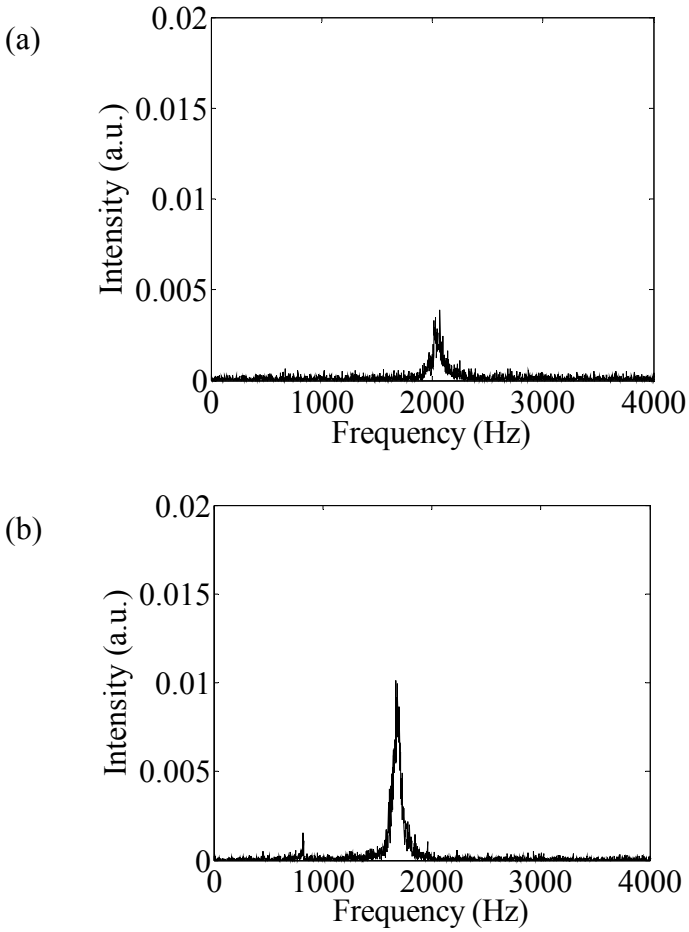


**Figure 5.2 - AE spectrum of bubbles produced using tubing with a diameter of 1.1 mm (a) displaced 1 cm from the beaker wall and (b) against the beaker wall, with a flow rate of 2.7 mL min$^{-1}$, and detected using a hydrophone positioned 1 cm from tubing outlet**

In the spectrum of bubbles produced from each tubing diameter only one peak was present and the intensity of the peak increased as tubing diameter increased. The frequency of acoustic emission was higher when the tubing was displaced from the beaker wall, this was observed for a number of different tubing diameters. For example, as shown in Figure 5.2, the frequency obtained when tubing of 1.1 mm diameter was displaced from the beaker wall was 2020 Hz compared to 1684 Hz when the tubing was against the beaker wall. This indicates that the signal may have

been affected by the close proximity to the beaker wall. Therefore, it can be concluded that, for bubbles to be detected and characterised using acoustic emission the hydrophone must be placed close to the bubble production site to improve signal detection of bubbles being produced.

### 5.2.2 Using the Hydrophone as the Bubble Detection Device to Investigate the Effect of Tubing Diameter and Flow Rate on Bubble Detection

Using a 2 factor, 3 level design of experiments approach, the effect of changing tubing diameter with flow rate was investigated. The three tubing diameters were 1.1, 1.9 and 2.5 mm and three flow rates were 2.7, 3.1 and 5.6 mL $min^{-1}$. The hydrophone was positioned 1 cm from the bubble production site, in the same horizontal plane as the tubing outlet. It was decided to keep the tubing attached to the inner wall of the beaker as this set-up was the most durable over time.

Figure 5.3 shows the effect of changing tubing diameter on the frequency of the acoustic emission spectra and Figure 5.4 shows the effect of changing flow rate on frequency of the acoustic emission spectra.

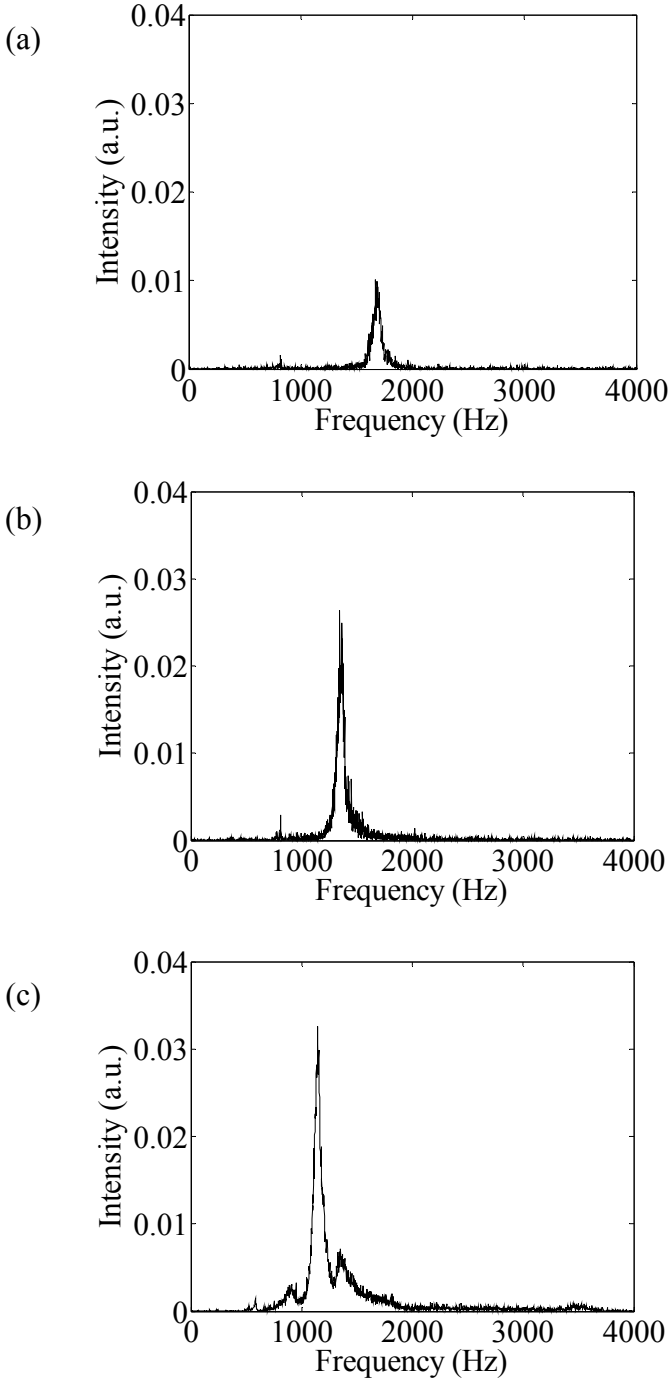


**Figure 5.3 – AE spectra of bubbles produced using tubing of diameter (a) 1.1 mm (b) 1.9 mm and (c) 2.5 mm with a flow rate of 2.7 mL $min^{-1}$, detected using a hydrophone positioned 1 cm from the inner wall of the beaker, next to tubing outlet**

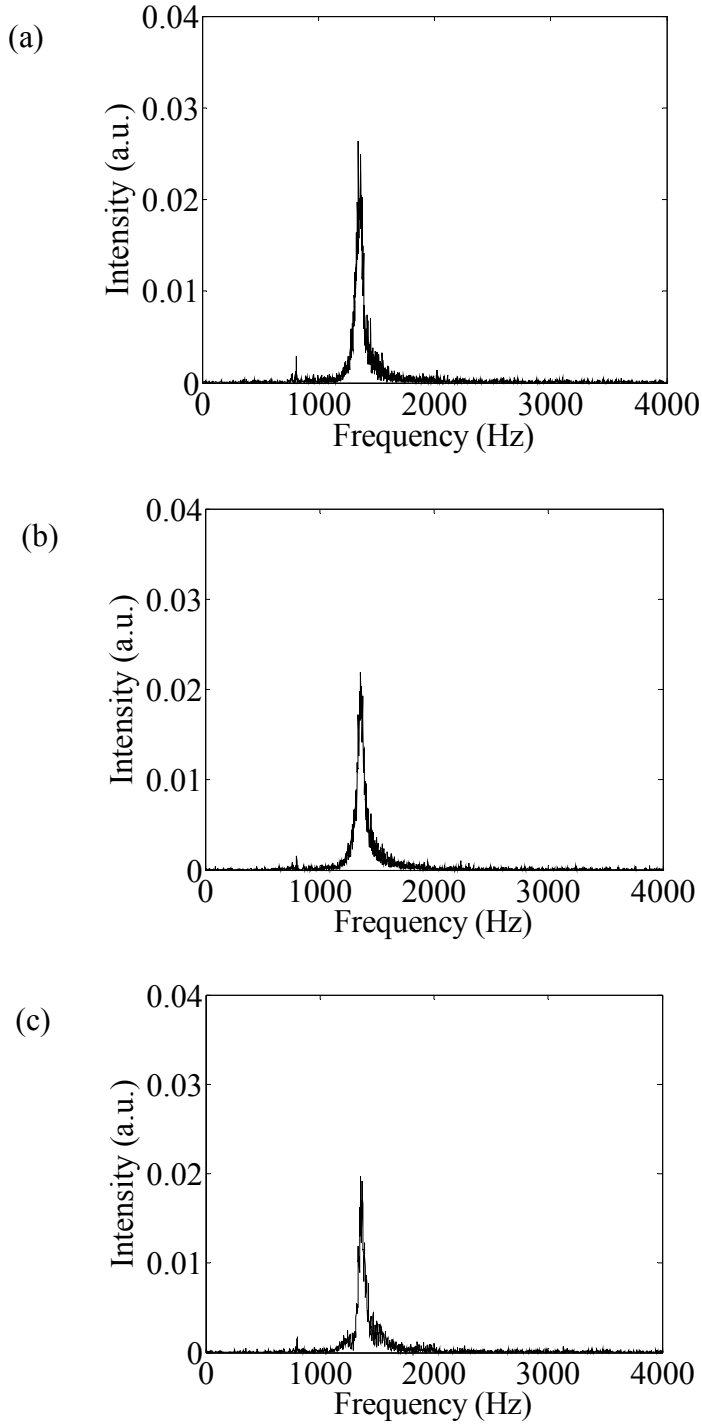


**Figure 5.4 – AE spectra of bubbles produced using tubing with a diameter of 1.9 mm at flow rates of (a) 2.7 mL $min^{-1}$ (b) 3.1 mL $min^{-1}$ and (c) 5.6 mL $min^{-1}$, detected using a hydrophone positioned 1 cm from the inner wall of the beaker, next to tubing outlet**

From Figure 5.3 it can be seen that as tubing diameter increased, the frequency of acoustic emission decreased. The spectra of bubbles produced using the 2.5 mm tubing diameter showed the presence of two shoulders on the main peak at frequencies of 912 and 1352 Hz. The peaks at these frequencies could be due to interferences from bubble coalescence at the water surface or the changing shape of the bubble as it was detached from the tubing outlet and travelled up the water column. The presence of two peaks only occurred for the largest bubble diameter investigated. A reason for this could be as larger bubbles have larger surface areas, there was more manoeuvrability for the bubble. Wu *et al.* reported that a bubble changes geometry (between spherical and ellipsoidal) from when it is released from the tubing orifice to when it bursts at the water surface.[4] This will cause a change in the bubble diameter and hence, give rise different resonance frequencies. Manasseh *et al.* reported, using photography to image bubbles, that bubbles change shape as they form and detach from a nozzle, they found up to a 10 % error in bubble size for nozzles between 0.3 and 0.5 mm.[5] From Figure 5.4 it can be seen that there was little variation of frequency with changing flow rate. The spectra obtained of bubbles produced from the 1.1 and 2.5 mm tubing diameters also showed little variation of frequency with changing flow rate. Boyd and Varley have shown that as flow rate was increased, from 2 to 4 L $min^{-1}$, there was a slight variation in bubble resonance frequency.[6] Table 5.1 shows the relationship between tubing diameter and flow rate to frequency.

**Table 5.1 – Variation of frequency as a function of tubing diameter (1.1, 1.9 and 2.5 mm) and flow rate (2.7, 3.1 and 5.6 mL $min^{-1}$), detected using a hydrophone (n = 5)**

| Tubing Diameter (mm) | Mean frequency ± Std. dev (Hz) | | |
|---|---|---|---|
| | 2.7 mL $min^{-1}$ | 3.1 mL $min^{-1}$ | 5.6 mL $min^{-1}$ |
| 1.1 | 1684 ± 5 | 1688 ± 5 | 1636 ± 7 |
| 1.9 | 1359 ± 2 | 1368 ± 4 | 1364 ± 5 |
| 2.5 | 1145 ± 2 | 1152 ± 3 | 1148 ± 11 |

A two-way Analysis of Variance (AOVA) was performed on the data in Table 5.1. The purpose of carrying out an ANOVA was to show if any variation between the resonance frequencies was due to changing tubing diameter, changing flow rate or due to random variation. The variation from the rows (tubing diameter) gave an *f* value of 735.8 and the variation from the columns (flow rate) gave and *f* value of 1.1. The $f_{crit}$ value at a 95 % confidence interval was approximately 7.0. Since the *f*-value for the tubing diameter is greater than the $f_{crit}$ value then the test fails. This is as expected because it is already known that tubing diameter (or bubble diameter) has an effect on the resonance frequency of a bubble.[1] The *f* value for the flow rate was less than the $f_{crit}$ value and therefore the *f*-test passes, indicating that the flow rate does not affect the resonance frequency of a bubble.

According to Minnaert[1] there should be an inverse relationship between bubble resonance frequency and bubble diameter. A simplistic analysis can be carried out of it is assumed that tubing diameter is equal to bubble diameter. From carrying out the experiments it was observed that the size of the bubble produced was not the same as the tubing diameter from which it was produced. To gain an understanding of the typical frequencies which should be obtained, the frequencies were calculated using the assumption that tubing diameter was the same as bubble diameter. Theoretical bubble resonance frequencies were calculated on the basis that bubble diameter was equal to tubing diameter. The theoretical bubble resonance frequencies for bubble produced from the tubing diameters investigated in Table 5.1, calculated using Equation 3.9, are 5455, 3157 and 2400 Hz for 1.1, 1.9 and 2.5 mm bubble diameters, respectively. From Table 5.1 and Figure 5.3(a) the inverse relationship between bubble resonance frequency and bubble diameter was observed; where bubble resonance frequency decreased as bubble diameter increased. A reason for the differences was that there may be a pressure factor as a bubble is forced round the tube under water. Indeed, in the equation used to calculate the theoretical bubble resonance frequency, there is a pressure term.[1] Also, it is possible that bubbles were not forming properly due to changes in geometry at the sparger source as discussed on page 95.

Further investigations were carried out to investigate the effect of tubing diameter on bubble resonance frequency. This was undertaken by extending the range of tubing diameters to include diameters of 0.38, 0.76 and 1.4 mm. These experiments were carried out at the lower flow rate of 2.7 mL $min^{-1}$ and the bubbles produced were detected using a hydrophone, placed 1 cm from the tubing outlet. There was no detectable AE from bubbles produced from the 0.38 mm tubing diameter. However, the AE spectrum obtained of bubbles produced from the 0.76 and 1.4 mm tubing contained a peak at 1796 and 1584 Hz, respectively. This suggested that the hydrophone could not detect frequencies above 1796 Hz in this position.

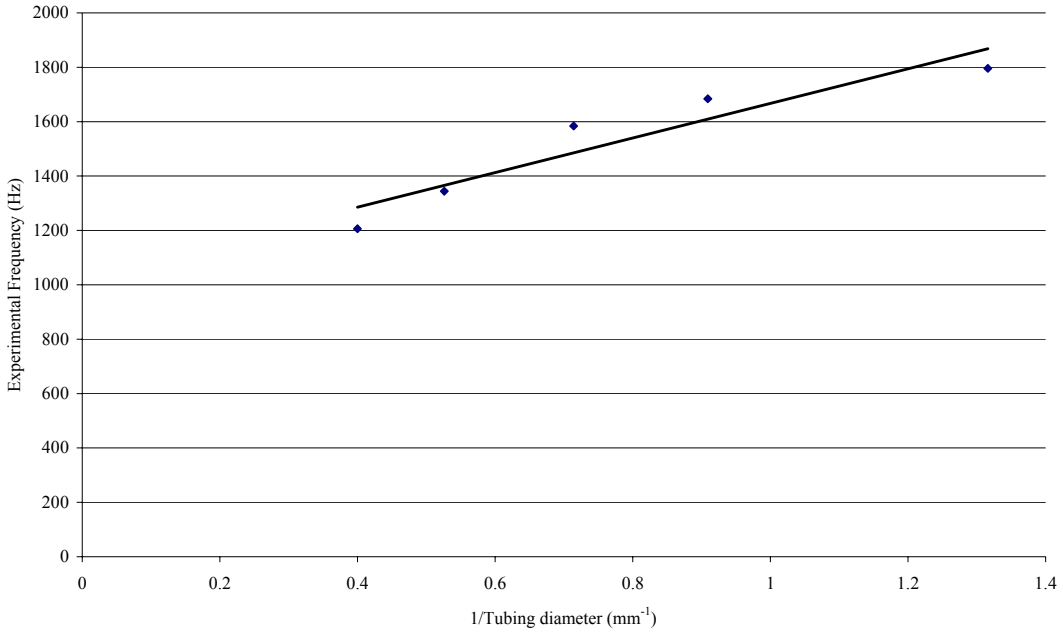


**Figure 5.5 – Experimental bubble resonance frequency versus the inverse of tubing diameter for tubing of diameters of 0.76, 1.1, 1.4, 1.9 and 2.5 mm at a flow rate of 2.7 mL $min^{-1}$, detected using the hydrophone**

Figure 5.5 shows the relationship between the experimental frequencies versus the inverse of the internal tubing diameter. The inverse of tubing diameter was taken because it was assumed that the bubble size was proportional to tubing diameter. From Figure 5.5 it can be seen that the relationship between the experimentally obtained frequency and bubble diameter was as would be expected using Minnaert's inverse relationship. The difference in the frequencies obtained was explained by the

arguments given on page 94 relating to changing geometries giving rise to changing bubble diameter, also, it was observed that bubbles produced were larger than the tubing diameter from which they originated. This was supported by the fact that the experimental frequencies obtained indicated that the bubbles were larger than the tubing from which they were produced. For example, using Minnaert's theory to predict the bubble sizes from the experimental frequencies of 1684 and 1145 Hz (corresponding to the tubing of diameters 1.1 and 2.5 mm) give the estimated bubble size to be 3.6 mm and 5.2 mm, which is over double the size of the tubing that was used to produce the bubbles. In addition to this, the equation on which Minnaert's theoretical frequency is based contains a pressure term. There was a pressure factor as the bubbles were generated in the tubing and pushed round the tubing underwater.

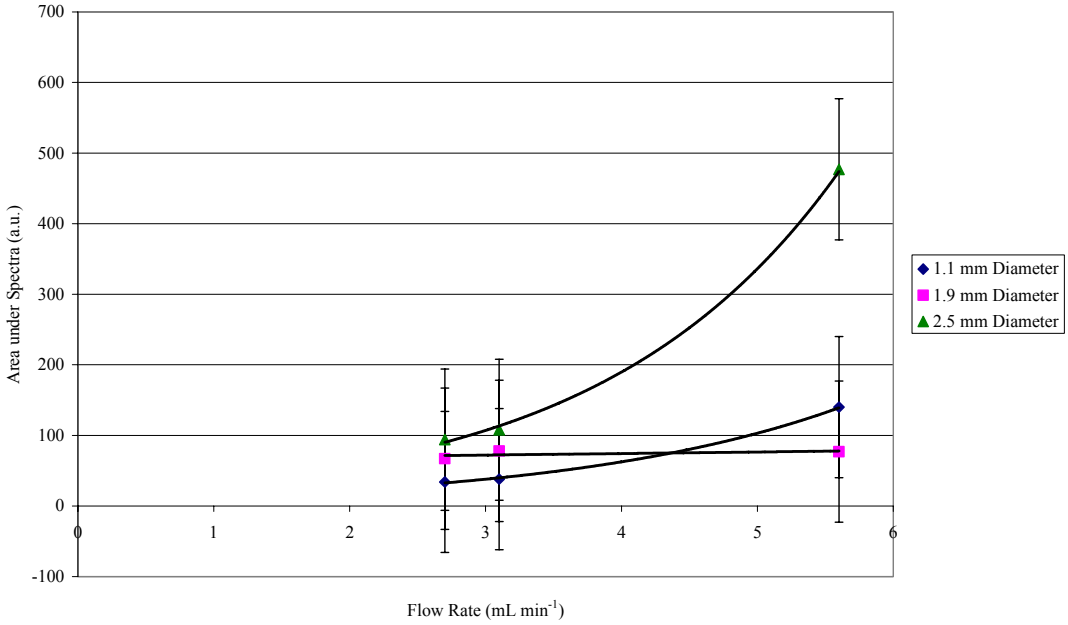


**Figure 5.6 – Relationship between area under spectra and flow rate for three tubing diameters (1.1, 1.9 and 2.5 mm) at three flow rates, (2.7, 3.1 and 5.6 mL $min^{-1}$), detected using a hydrophone**

Figure 5.6 shows a graph of the area under the spectra versus flow rate for the three tubing diameters of 1.1, 1.9 and 2.5 mm investigated. From this graph it can be seen that, for the largest tubing diameter investigated (2.5 mm), as flow rate increased the

area under the spectra increased from 7.6 ± 1.1 to 28.1 ± 5.7 a.u. The intensity of peaks and the area under the spectra can be related to bubble diameter in that larger bubbles will oscillate with a higher amplitude, giving rise to larger spectral intensity and a larger area under the spectra.

**Table 5.2 – Relationship between repeatability, tubing diameter (1.1, 1.9 and 2.5 mm) and flow Rate (2.7, 3.1 and 5.6 mL $min^{-1}$), detected using the hydrophone**

| Tubing diameter (mm) | % RSD of area under the spectra (a.u.) | | |
|---|---|---|---|
| | 2.7 mL $min^{-1}$ | 3.1 mL $min^{-1}$ | 5.6 mL $min^{-1}$ |
| 1.1 | 14.7 | 19.6 | 20.3 |
| 1.9 | 3.3 | 3.8 | 9.8 |
| 2.5 | 8.1 | 4.7 | 19.8 |

In general bubble production had highest repeatability at lower flow rates, as can be seen in Table 5.2. This would be expected because lower flow rates gave rise to a lower rate of bubble production and therefore created less turbulence in the vessel. Bubbles produced from the 1.9 mm diameter tubing gave the most repeatable results at the lower flow rate of 2.7 mL $min^{-1}$. The RSD of the peak area for the spectrum obtained of bubbles produced at a flow rate of 2.7 mL $min^{-1}$ using the 0.76 mm diameter tubing was 18 % and that for the 1.4 mm diameter tubing was 4.1 %. Problems encountered when carrying out tests using the peristaltic pump were the time taken to collect spectra and signal interference from bubbles coalescing; these signals were discarded.

### 5.2.3 Using the Transducer as the Bubble Detection Device

The hydrophone was replaced with a 3-1 connectivity transducer, which was placed on the outside of the beaker directly opposite the tubing orifice with the centre of the transducer in the same horizontal plane as the tubing outlet. When carrying out tests

using the 3-1 connectivity transducer a problem encountered was interference from background noise, mechanical interference from near-by construction work, vibrations on the work bench and other workers in the laboratory; these signals were discarded. This was due to two reasons, firstly the sensitivity of the transducer and secondly that because that transducer was attached to a glass wall, it was picking up the vibrations travelling through the glass. To investigate the effect of flow rate on tubing diameter, spectra of bubbles produced were obtained with tubing of diameters of 0.38, 0.76, 1.1, 1.4 and 2.5 mm, detected using the 3-1 connectivity transducer. The flow rate was 2.7 mL $min^{-1}$. The spectra can be seen in Figure 5.7(a) – (e).

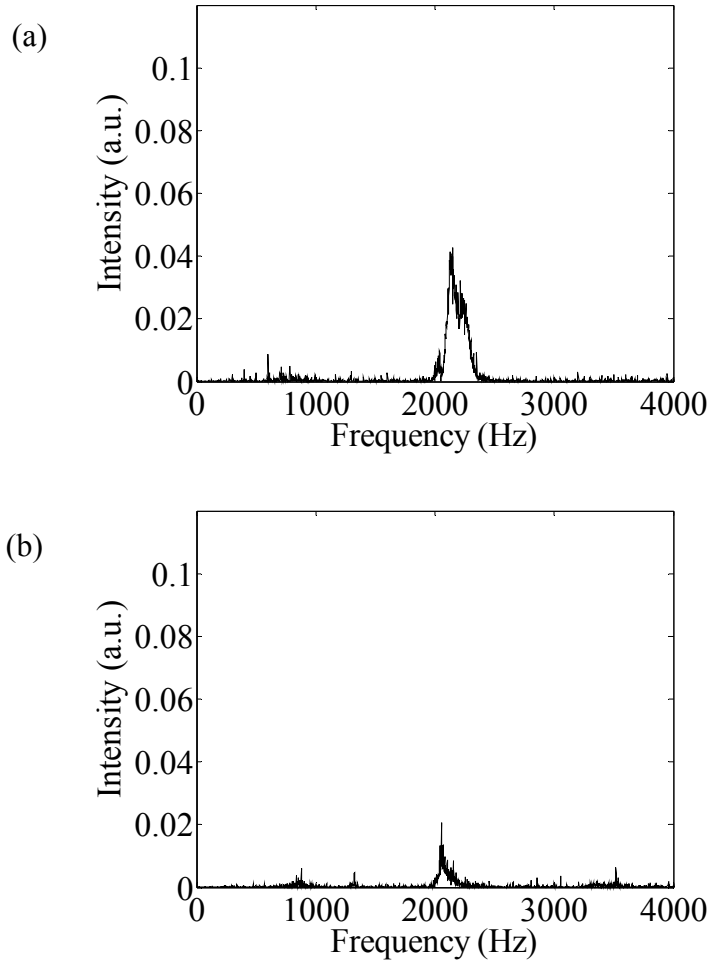

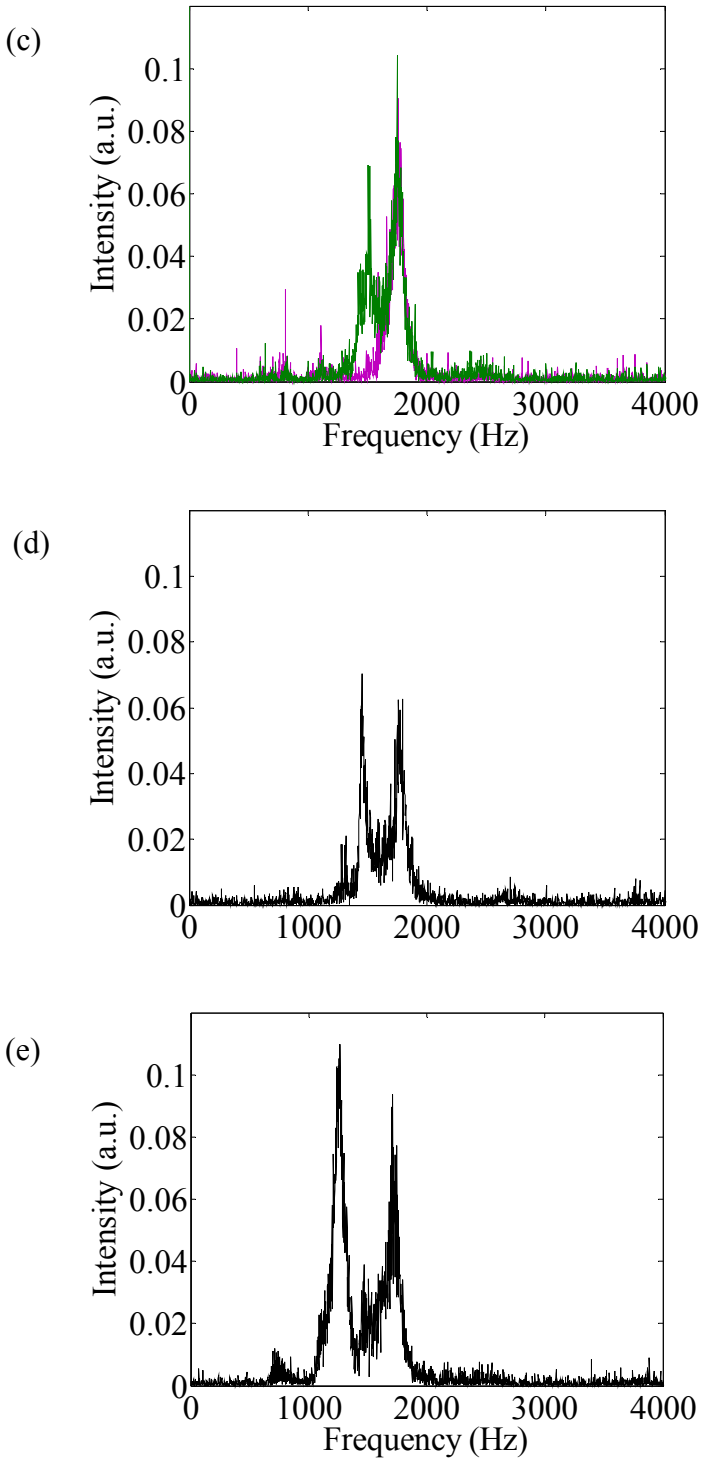


**Figure 5.7 – AE spectra of bubbles produced using tubing with diameter of (a) 0.38 mm (b) 0.76 mm (c) 1.1 mm (d) 1.4 mm (e) 2.5 mm and a flow rate of 2.7 mL min$^{-1}$, detected using the transducer positioned adjacent to tubing outlet**

For larger diameters of tubing, namely the 1.1, 1.4 and 2.5 mm, the spectra showed the presence of two peaks. Figure 5.7 (c) showed the presence to spectra with two peaks, this was obtained for bubbles produced from tubing of 1.1 mm diameter and shows the point where bubble bursting was being detected. It should be noted that the second peak was not always present. In all cases one peak was invariant with tubing diameter and was present at a frequency of 1752 Hz. The observation that two peaks were present has already been observed when using the hydrophone to detect bubbles being produced and bursting, see Figure 5.1(a). Therefore, it can be deduced that it was likely the transducer was detecting both the sound of the bubble being produced and the sound of the bubble busting at the surface of the water. These results are summarised in Table 5.3.

**Table 5.3 – Summary of data for Figure 5.7 (a) – (e), showing bubble formation frequencies and repeatability (repeatability studies based on statistical analysis of data for area under the peak of bubble formation).**

| Tubing diameter (mm) | Bubble formation frequency (Hz) | RSD of area under the bubble formation peak (%) |
|---|---|---|
| 0.38 | 2394 ± 16 | 14.6 |
| 0.76 | 2151 ± 30 | 10.6 |
| 1.1 | 1556 ± 58 | 27.0 |
| 1.4 | 1452 ± 4 | 10.3 |
| 2.5 | 1289 ± 8 | 13.0 |

By comparing the first two columns of Table 5.3 it can, again, be seen that the inverse relationship between tubing diameter and bubble resonance frequency was apparent. Figure 5.8 shows a graph of experimental bubble resonance frequencies versus the inverse of tubing diameter, obtained using the 3-1 connectivity transducer.

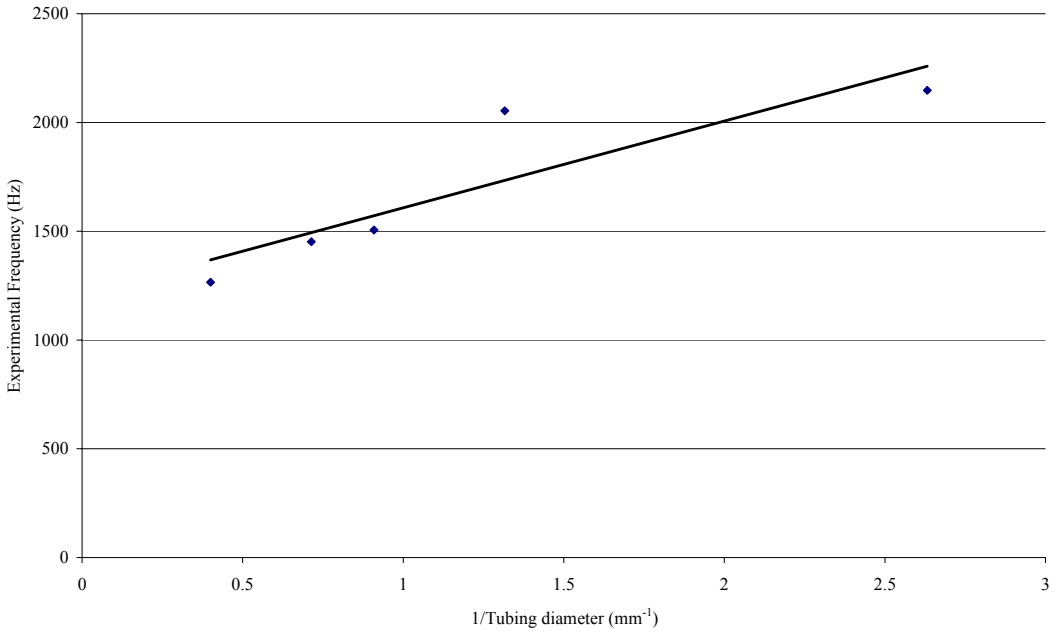


**Figure 5.8 – Experimental bubble resonance frequencies versus the inverse of tubing diameter for tubing of 0.38, 0.76, 1.1, 1.4 and 2.5 mm diameter, detected using the transducer**

Figure 5.8 shows the presence of an outlier, the data point at 2152 Hz. If this point is ignored a similar trend to Figure 5.5 can be seen; the relationship between the experimentally obtained frequency and bubble diameter was as would be expected using Minnaert's inverse relationship. This can be explained by the discussion given on page 94.

It should be noted that the frequencies of bubble formation and bubble bursting were slightly different when measuring using the transducer compared to the hydrophone. These differences may be due to the different response characteristics of the devices at the frequencies in question. Also, since the transducer was situated on the other side of the beaker from the tubing outlet, it was likely that there were filtering effects as the signal passed through the beaker wall. This would be explained by the theory of signal decay. Where a signal decreases as a function of 1/radius, this was discussed on page 90. This is further explained by the discussion on page 95.

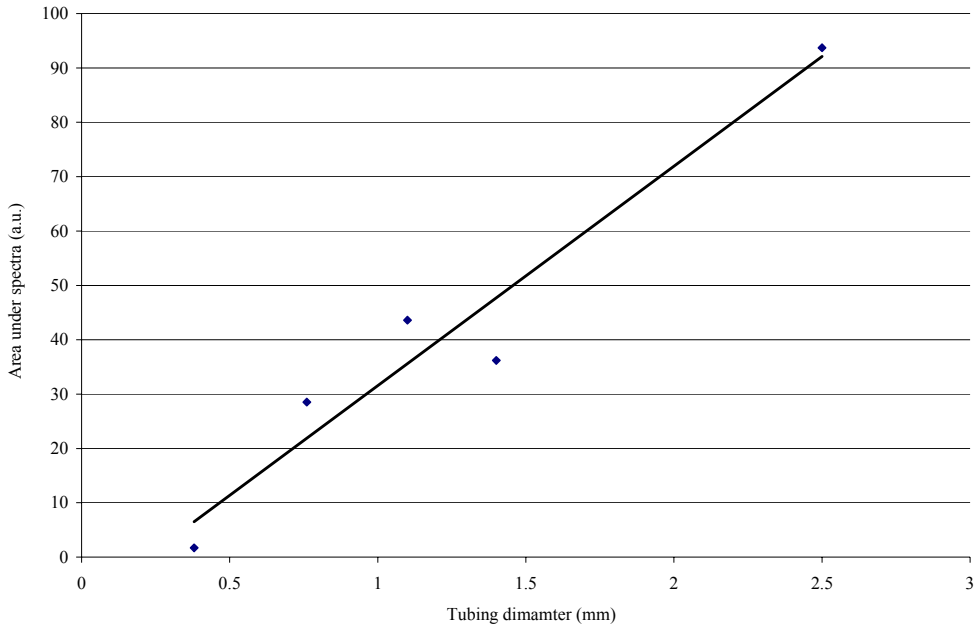


**Figure 5.9 – Graph of area under the spectra of bubble formation versus tubing diameter for 0.38, 0.76, 1.1, 1.4 and 2.5 mm tubing diameter**

Figure 5.9 shows that as tubing diameter increased the area under the spectra of bubble formation increased. When using the 3-1 connectivity transducer the most repeatable results were obtained for bubbles produced using the tubing diameters 0.76 and 1.4 mm. The most repeatable results obtained from detecting bubbles using a hydrophone were obtained using tubing of diameter 1.1 and 1.9 mm, when the tubing was moved out from the beaker wall. From this work it was concluded that using the hydrophone as the bubble detection device gave, generally, more repeatable results.

## 5.3 Air Cylinder

This section details the results obtained when using an air cylinder as the method of bubble production, as described in section 4.2.3. The set-up employed here was that of a 5 L beaker filled to 192 mm (4 L mark) from the base of the beaker with ordinary tap water. The sparger was located in the centre of the beaker, the sparger orifice was 9.7 cm vertically from the base of the beaker.

### 5.3.1 Investigation of Repeatability and Attachment of Bubble Detection Device

The aims of these experiments were to determine which bubble detection device gave the most repeatable measurements and to determine the variability of attachment of the bubble detection device. The sparger used had an internal diameter (ID) of 2 mm. The flow meter ranged from 0.6 – 5 L $min^{-1}$ and the pressure regulator ranged from 0 – 15 bar. During analysis of the results for measurement repeatability and attachment 90 repeat signals were taken and summed into 3 blocks of 30 spectra, which gave 3 repeat measurements.

#### 5.3.1.1 Using the Transducer as the Bubble Detection Device

Ninety repeat measurements were taken using a 3-1 connectivity transducer when the transducer was left in place for the duration of the 90 measurements. The transducer was held in place by a clamp stand. A further 90 measurements were taken using the transducer when it was taken off and re-attached after every 30 measurements. The transducer was attached to the outer wall of the beaker, in the same horizontal plane as the sparger. The flow rate was kept constant at 4 L $min^{-1}$. The spectrum of detecting AE from bubbles using a 3-1 connectivity transducer can be seen in Figure 5.10(a) and (b).

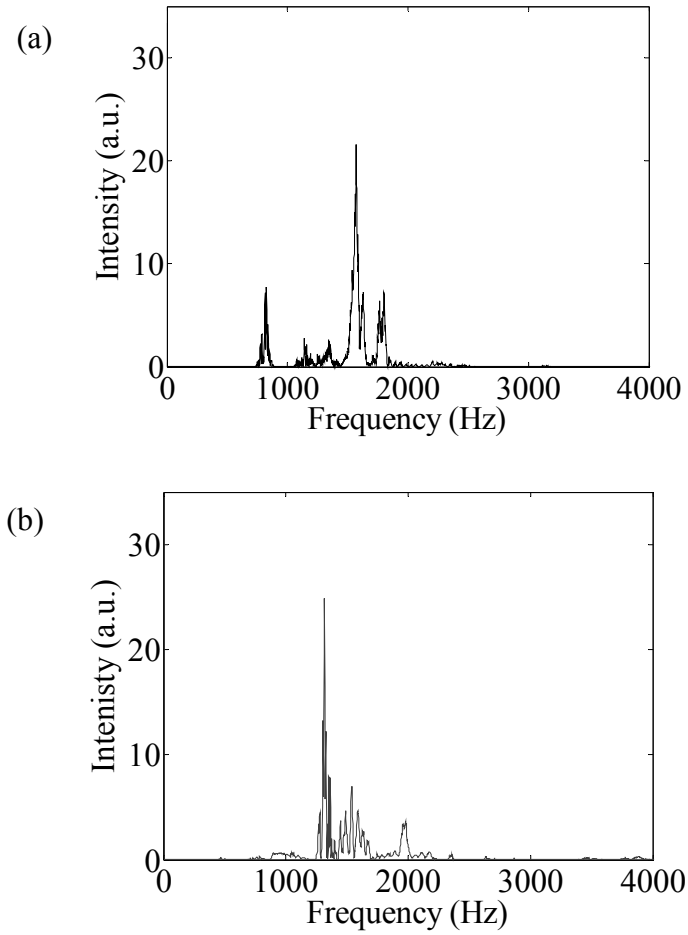


**Figure 5.10 – AE spectra of bubbles produced with sparger of ID 2 mm and flow rate of 4 L min$^{-1}$, detected using a transducer level with the sparger at 9.7 cm from the base of the beaker showing (a) the sum of 30 spectra with transducer attached for the duration of 90 measurements and (b) the sum of 30 spectra with the transducer taken off and re-attached after every 30 measurements**

From Figure 5.10 it can be seen there were multiple peaks present, this was because the high flow rate used generated bubbles of different sizes. It was also possible that some peaks were due to bubbles bursting at the surface of the water (as was seen in the peristaltic pump experiments) and bubble coalescence. Martín *et al.* have studied coalescence of bubbles and they concluded that when two bubbles meet the degree to which they coalesce depends on the flow rate and whether they behave as rigid or deformable objects and that this in turn was dependent on the physical properties of the liquid.[7]

The area under the spectra, when the transducer was left in place for the 30 measurements was 3980 ± 1077.3 a.u. (n = 3). When the transducer was taken off and re-attached after 30 measurements the area under the spectra increased to 4300.3 ± 1591.7 a.u. (n = 3). The RSD of the areas under the spectra were 27 and 37 %, respectively (n = 3). This showed that leaving the transducer attached for the duration of the measurements gave rise to more repeatable results. This was as expected because the transducer was a large device; consequently it was difficult to re-attach the transducer with the same surface area and pressure contact with the beaker wall. This would be unacceptable in an industrial setting because in order to obtain comparable results the transducer would have to recording acoustic emission from the same point in the process.

#### 5.3.1.2 Using the Hydrophone as the Bubble Detection Device

Ninety repeat measurements were taken using a hydrophone as the bubble detecting device. The hydrophone was placed in the centre of the beaker 9.7 cm from the base of the beaker and in the same horizontal plane as the sparger. The hydrophone was left immersed for the duration of the 90 measurements, the spectra were summed into 3 blocks of 30 to give 3 repeat measurements. A further 90 measurements were taken with the hydrophone taken out and re-immersed after every 30 measurements, again the spectra were summed into 3 blocks of 30 to give 3 repeat measurements. These spectra are shown in Figure 5.11(a) and (b), respectively.

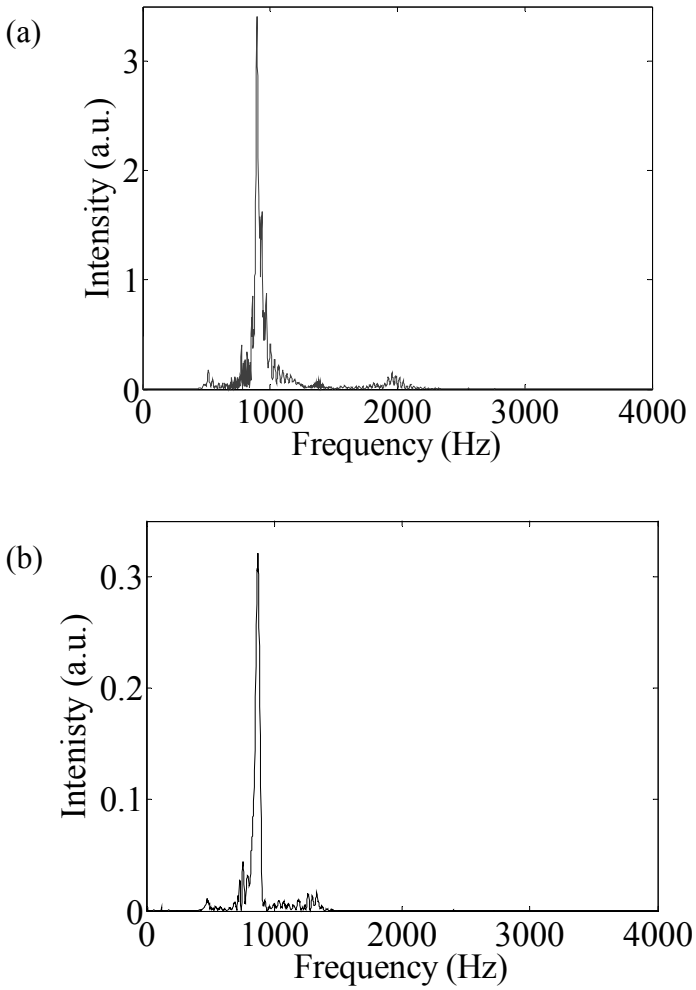


**Figure 5.11 – AE spectra of bubbles produced with sparger of ID 2 mm and flow rate of 4 L min$^{-1}$, detected using a hydrophone level with the sparger at 9.7 cm from the base of the beaker showing (a) the sum of 30 spectra with hydrophone immersed for the duration of the 90 measurements and (b) the sum of 30 spectra with the hydrophone taken out and re-immersed after every 30 measurements**

Figure 5.11(a) showed the presence of a peak at 896 Hz and Figure 5.11(b) showed the presence of a peak at 872 Hz. It was seen from comparing Figures 5.10 and 5.11 that the spectra for the hydrophone did not vary as much as that for the externally attached transducer, with the exception of the intensity. The area under the spectra when the hydrophone was left in place for the 90 measurements was 636.1 ± 88.2 a.u. (n = 3) and when they hydrophone was taken off and re-immersed after every 30 measurements the area under the spectra was 172.7 ± 38.2 a.u. (n = 3). These areas

under the spectra gave an RSD of the area of 13.9 and 22 %, respectively. The areas are different because, like the transducer, it was difficult to re-immerse the hydrophone to exactly the same position, because the hydrophone was held in place, at the top of the beaker, by a clamp stand. Although this is not an ideal experimental arrangement it proved adequate to gather the data presented. A more suitable approach would involve taking detailed measurements of the hydrophones position to improve accuracy.

From carrying out these experiments it was decided not to use the transducer, due to it variability in acoustic emission frequencies, and focus on the hydrophone. One advantage the air cylinder had over the peristaltic pump was that longer lengths of tubing could be used. This was due to restraints in the equipment that was available.

### 5.3.2 Investigation of Effect of Flow Rate and Sparger Diameter

In this section fifty repeat signals were taken and summed into 5 blocks of 10 signals, which gave 5 repeat measurements. Unfortunately, the flow rate was difficult to regulate. The aim of these experiments was to determine if changing flow rate affects bubble resonance frequency or repeatability. To study the effect of flow rate an experimental design was set up. The experimental design comprised of three flow rates: 50, 100 and 150 mL $min^{-1}$ and three sparger diameters: 1, 1.5 and 2 mm. The air cylinder was again used to produce bubbles. The hydrophone was used as the bubble detection device and placed 1 cm from the sparger orifice. Note that these flow rates are larger than those investigated in the peristaltic pump experimental design (section 5.2.2.).

Figure 5.12 shows the effect of changing sparger diameter on the acoustic emission spectra and Figure 5.13 shows the effect of changing flow rate on the acoustic emission spectra. Since the hydrophone was placed close to the sparger orifice, it was likely that the most intense signal would arise form bubble production. The additional peaks can be attributed to production of smaller bubbles and/or bursting of bubbles.

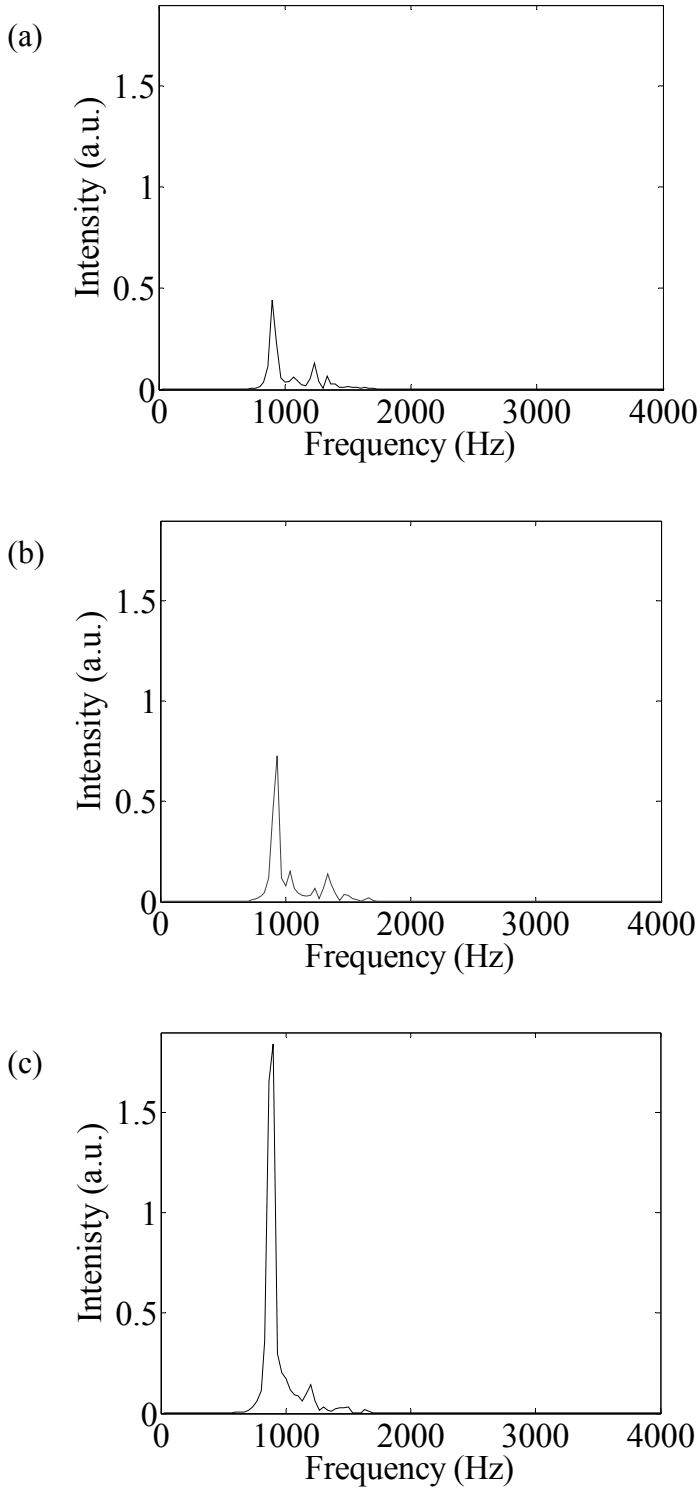


**Figure 5.12 – AE spectra of bubbles produced using sparger diameters (a) 1 mm (b) 1.5 mm and (c) 2 mm with a flow rate of 50 mL min$^{-1}$, detected using a hydrophone positioned 1 cm from the sparger orifice**

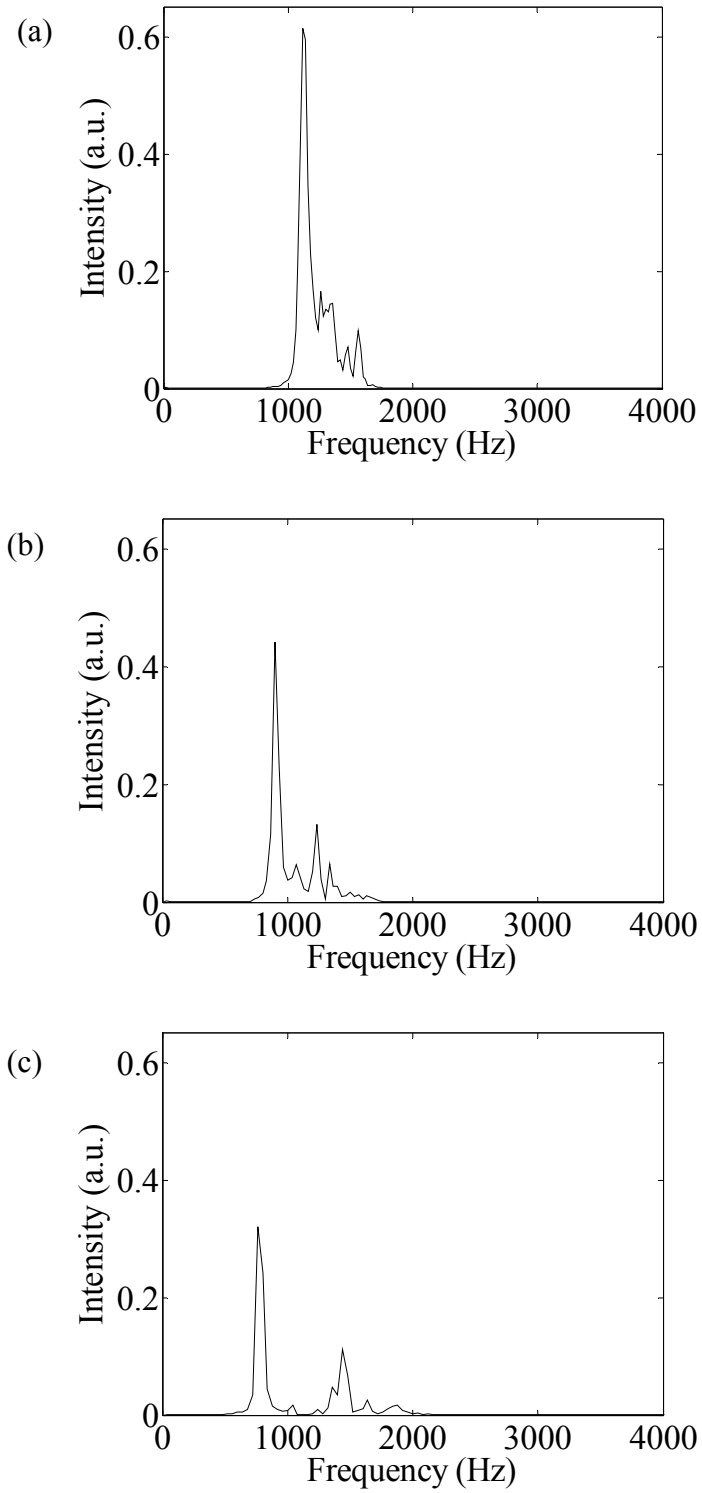


**Figure 5.13 – AE spectra of bubbles produced using sparger diameter of 1 mm with flow rates of (a) 50 mL min$^{-1}$ (b) 100 mL min$^{-1}$ and (c) 150 mL min$^{-1}$, detected using a hydrophone positioned 1 cm from the sparger orifice**

From Figure 5.12 it can be seen that as sparger diameter increased the intensity of the peaks increased, this was expected as larger bubbles will oscillate with a higher amplitude giving rise to increased intensity. The peak attributed to bubble formation was 900, 933 and 900 Hz for the 1, 1.5 mm and 2 mm diameter, respectively. The results obtained here do not support Minnaert's inverse theory. An explanation for this was that since there were a train of bubbles being produced, the bubbles may have been of slightly different sizes.

Figure 5.13 shows that as flow rate is increased the frequency of the largest peak decreased, assuming the largest peak was due to bubble production. This has been seen by Boyd and Varley when they used high flow rates of 2 – 4 L $min^{-1}$.[4] The experiments carried out using the air cylinder to show the effect of flow rate and sparger diameter gave different results to those carried out using the peristaltic pump; the effect of flow rate on frequency, using the air cylinder, is more apparent. This was possibly because at higher flow rates, flow rate has a larger effect on the acoustic emission frequency than the sparger diameter. Figure 5.13 shows the presence of bubble formation peaks at 1120, 900 and 760 Hz for the flow rates of 50, 100 and 150 mL $min^{-1}$, respectively. In both Figures 5.12 and 5.13 the frequencies which were common to all spectra arose because there was a trail of bubbles being produced and also due to bubble bursting. It was observed that flow rate was the dominating factor on acoustic emission frequency.

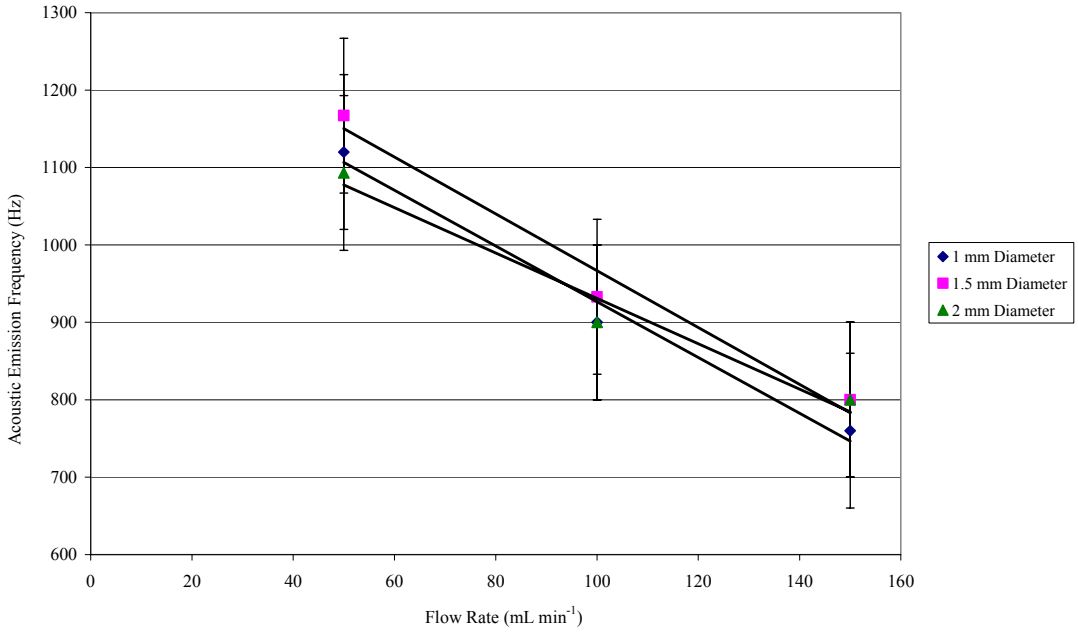


**Figure 5.14 – Relationship between experimental frequency versus flow rate for three sparger diameters (1, 1.5 and 2 mm) at three flow rates (50, 100 and 150 mL $min^{-1}$)**

As flow rate increased, for a particular sparger diameter, the acoustic emission frequency decreased, this can be seen in Figure 5.14. This was possibly due to bubble coalescence. The diameter of bubbles which have coalesced will be larger, therefore, decreasing bubble resonance frequency. Another explanation was that higher flow rates produced larger bubbles since the air was being ejected from the sparger with a larger force.

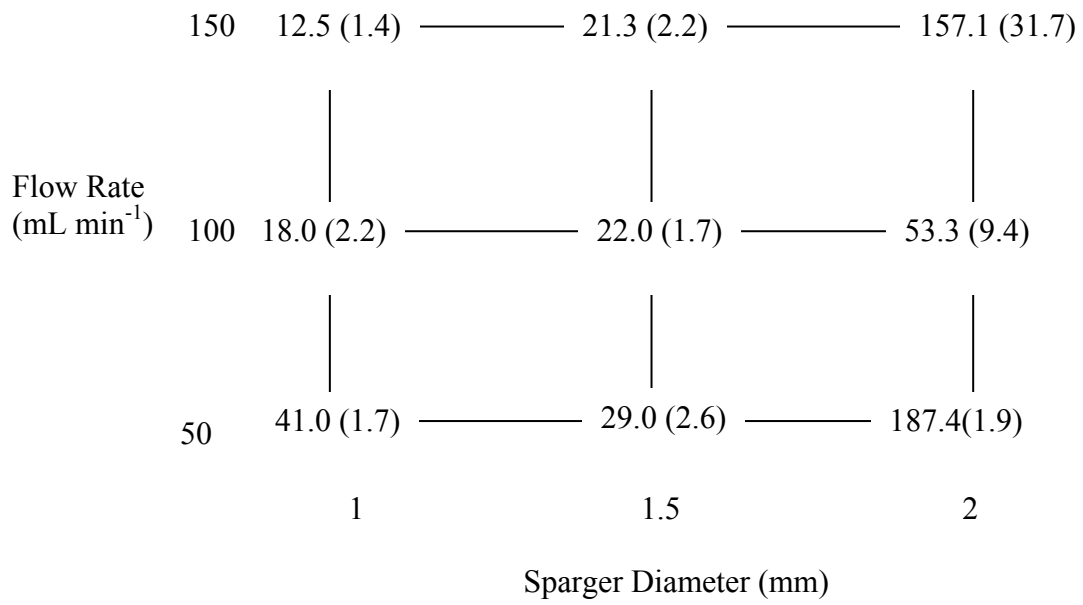


**Figure 5.15 – Mean area ± standard deviation for three flow rates of 50, 100 and 150 mL min$^{-1}$ and three sparger diameters of 1, 1.5 and 2 mm. The mean area is given as the first number and the standard deviation in parenthesis.**

As the flow rate was kept constant and the sparger diameter was increased from 1 mm to 2 mm the area under the spectra increased. Figure 5.15 shows the relationship between the mean area ± standard deviation and sparger diameter for each of the three flow rates investigated.

The most repeatable measurements were obtained at the lowest flow rates. The RSD of the area under the spectra were 4.1, 9.0 and 1.9 % for the 1, 1.5 and 2 mm sparger diameter at a flow rate of 50 mL min$^{-1}$. This was expected because lower flow rates will produce fewer bubbles per unit time and therefore the environment in the beaker will not be as chaotic as higher flow rates. It was observed that as flow rate increased repeatability decreased, for example, the RSD of the area under the spectra for sparger of 2 mm diameter was 1.9, 17.6 and 20.2 % for flow rates of 50, 100 and 150 mL min$^{-1}$, respectively.

### 5.3.3 Investigation of the Effect of Viscosity

The aim of these experiments was to determine if changing the viscosity affects the repeatability of results and/or changes the acoustic emission frequency. It was considered that changing the viscosity of the solution would affect the bubble resonance frequency,[8] as described in chapter 3, section 3.2.1; if the viscosity is increased then overdamping will occur where there would be restriction on a bubbles oscillations, giving a bubble less movement and consequently, the hydrophone would detect less variation in frequency and intensity. If viscosity is decreased underdamping will occur and the effect would be the opposite of that for overdamping.

Two litres of water were added to one beaker and 2 L of glycerol were added to another beaker. A third beaker was placed on a magnetic stirrer plate and portions of water and glycerol were added together over a period of time. The water-glycerol mixture was stirred for 30 minutes to ensure complete mixing of the phases.

Fifty repeat measurements were carried out with the hydrophone placed 1 cm from the sparger orifice. The experimental design was a two factor three level design with the three flow rates (50, 100, 150 mL $min^{-1}$) and three sparger diameters (1, 1.5 and 2 mm). Again the resolution of the spectra in this section was changed in the same way as for the flow rate experiments (chapter 4, section 4.3); because a train of bubbles were detected and the signals divided into single bubble sections.

Figure 5.16 shows the variation from sparger diameter on the acoustic emission spectra and Figure 5.17 shows the variation from flow rate on the acoustic emission spectra.

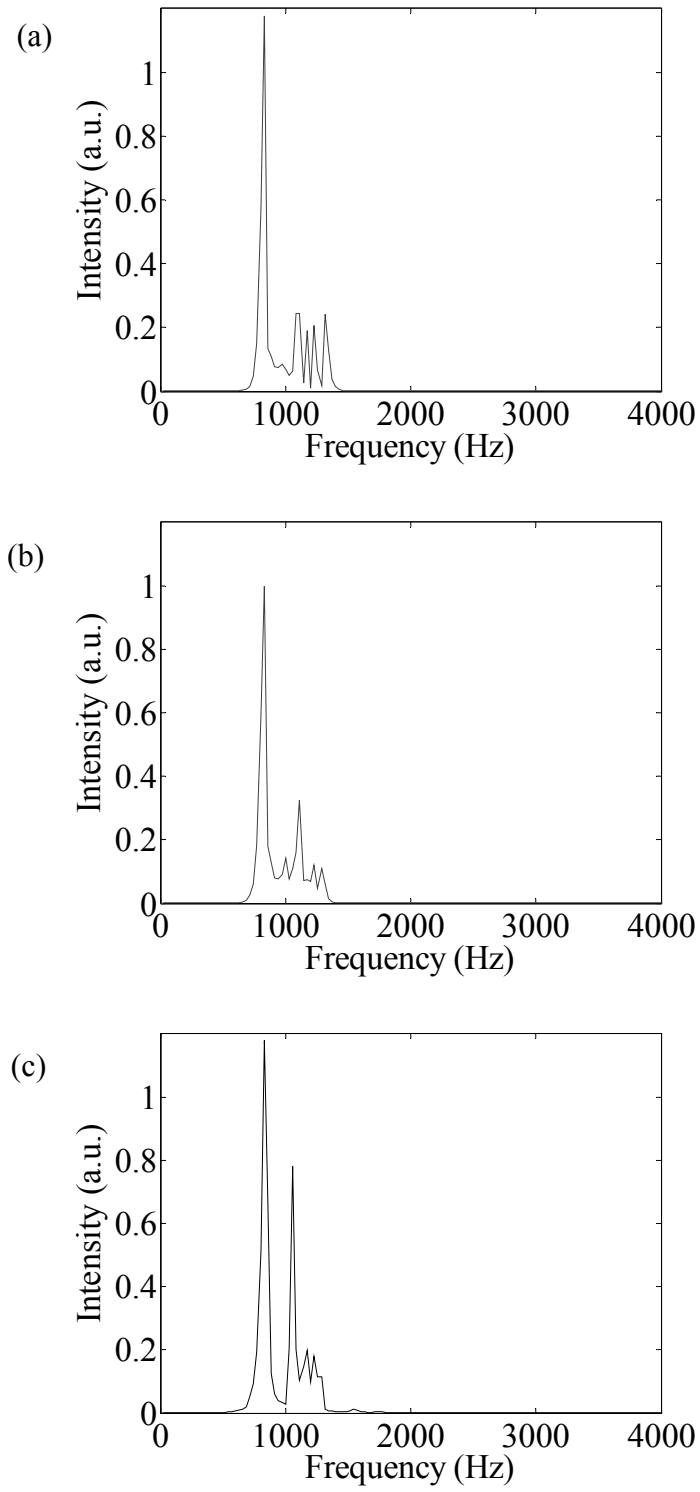


**Figure 5.16 – AE spectrum of bubble produced using an air cylinder in a viscous medium of 50:50 mixture of glycerol and water with a flow rate of 100 mL $min^{-1}$ and a sparger of diameter (a) 1 mm (b) 1.5 mm and (c) 2 mm, detected using a hydrophone**

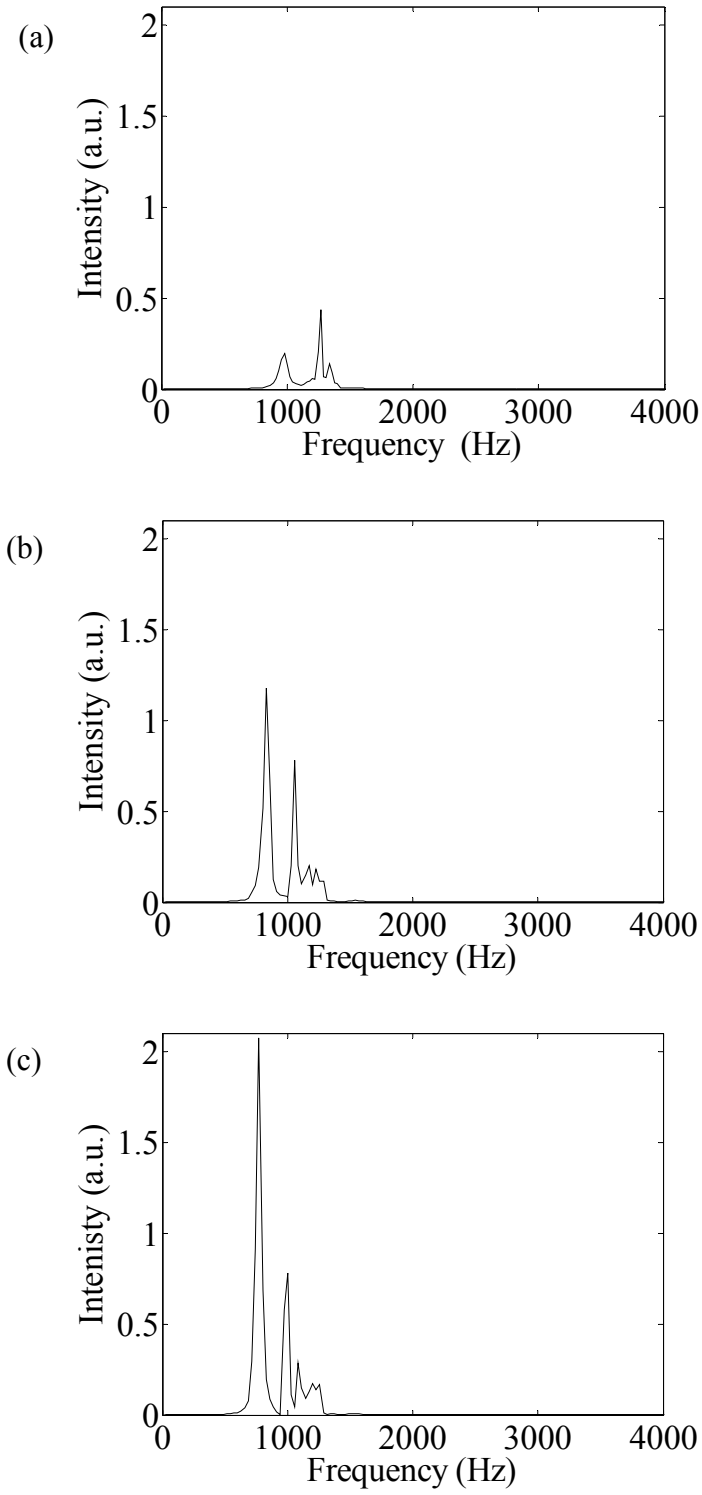


**Figure 5.17 – AE spectrum of bubble produced using an air cylinder in a viscous medium of 50:50 mixture of glycerol and water with a sparger diameter of 2 mm at flow rates of (a) 50 mL $min^{-1}$ (b) 100 mL $min^{-1}$ and (c) 150 mL $min^{-1}$, detected using a hydrophone**

From Figure 5.16 it can be seen that there was little variation in the intensity of the peaks when sparger diameter was increased at a single flow rate. The same was true for the other flow rates of 100 and 150 mL $min^{-1}$ investigated. The spectra in Figure 5.17 all have the same bubble production frequency of 827 Hz, which corresponded to the most intense peak.

Figure 5.17 illustrates that as flow rate was increased the intensity of the peaks increased. Whereas in section 5.3.2, Figure 5.13, it was found that as flow rate increased the acoustic emission frequency decreased, this showed that changing the viscosity of the medium through which the bubble travelled had a different effect on the acoustic emission spectra. In Figure 5.17 the bubble production peak was seen at 1057, 827 and 771 Hz. The observations from these experiments were the same as those found in section 5.3.2, where high flow rates have an effect on acoustic emission frequency in water, that being that increasing the flow rate, decreased the acoustic emission frequency.

The main difference in the experiments in this subsection was that there was less variation in both frequency and intensity. This supports the discussion on page 114 which suggested that increasing the viscosity of the solution does change the frequency at which the bubble resonates and reduces the variation in the measurements. This was due to an increase in surface tension around a bubble. This would occur because increasing surface tension would restrict the oscillation and movement of a bubble. Therefore a dampening effect was present.

Figure 5.18 shows the relationship between the mean area ± standard deviation and sparger diameter for each of the three flow rates investigated.

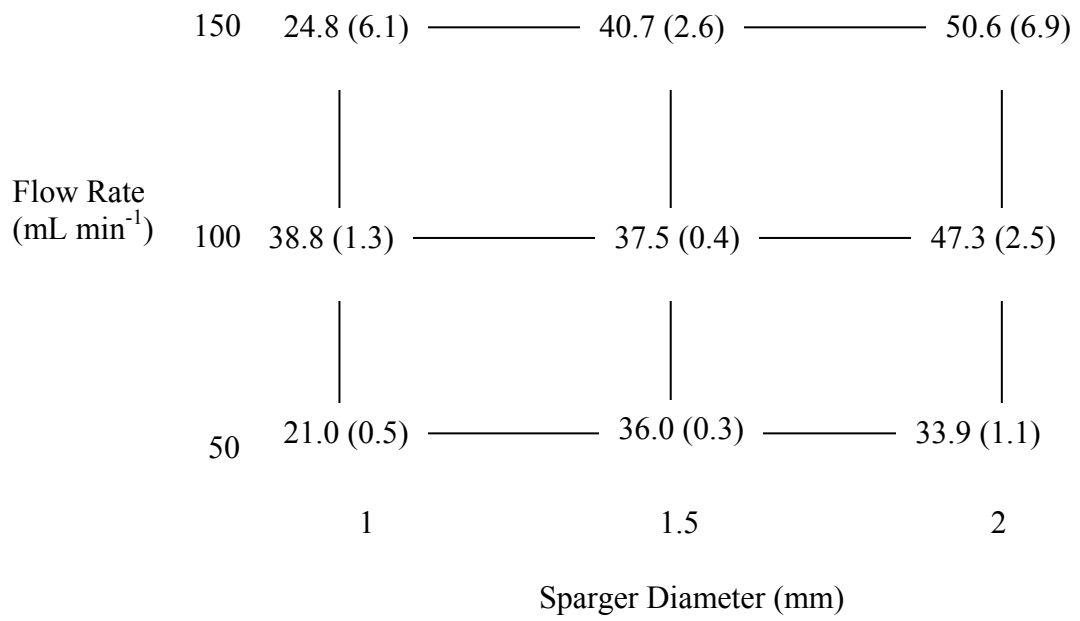


**Figure 5.18 – Mean area ± standard deviation for three flow rates of 50, 100 and 150 mL min$^{-1}$ and three sparger diameters of 1, 1.5 and 2 mm. The mean area is given as the first number and the standard deviation in parenthesis**

Generally, the area under the spectra increased and the intensity of the peaks increased as flow rate increased. When the viscosity was increased to a 50 : 50 mixture of glycerol and water an immediate observation from the data analysis was that the repeatability of the area analysis was improved primarily at low flow rates, where the RSD of the area under the spectra were 2.1, 0.9 and 3.1 % for the 1, 1.5 and 2.5 mm diameter spargers, respectively. The 1.5 mm sparger gave the most repeatable results at all three flow rates. This was because increasing the viscosity restricted a bubbles movement, consequently, there was less variation from geometry changes and, hence, radius changes as a bubble was released from the sparger to the surface of the water.

## 5.4 Conclusions of the Chapter

To conclude, it was observed that bubbles produced from a peristaltic pump or an air cylinder can be characterised in terms of acoustic emission frequency and by the inverse relationship between tubing diameter and acoustic emission frequency. It

was also shown that for a bubble to be detected by the hydrophone (or transducer), the bubble needed to be large enough so that the amplitude of the oscillations of the bubble was large and could be detected and also, that the device must be close to the source of bubble production for bubbles produced from small tubing diameters to be detected. The main advantage of using the peristaltic pump to produce bubbles was that as the flow rates were low it was easy to control the rate of bubble release to give rise to the detection of individual bubbles, a disadvantage was the time taken to collect spectra. The experiments using the peristaltic pump and the air cylinder showed that the hydrophone gave rise to more repeatable results than the transducer and that the spectra obtained for bubble detected using the hydrophone were not as variable as those of the transducer.

In both the peristaltic pump experiments and the air cylinder experiments it was observed that the hydrophone detected the sound of bubbles forming when it was placed close to the bubble production site. However, when the hydrophone and transducer were placed further away from the bubble production site it was likely that they was detecting a mixture of signals from bubbles forming, bubbles bursting and bubble coalescence.

Furthermore, it was shown that increasing the flow rate decreased the acoustic emission frequency, when the experiments were carried out in water. It was also shown that increasing the viscosity of the medium through which a bubble passes, and oscillates in, does have an effect on the intensity of the acoustic emission spectra of a bubble. This being that increasing viscosity restricts the movement in which a bubble can oscillate and hence, gave rise to more repeatable results.

In this work bubbles of several diameters were investigated. To follow on from this an active acoustic study of bubbles of estimated diameters of 1, 2 and 4 mm was carried out to investigate frequency and repeatability. These results are given in the next chapter.

## 5.5 References


1. M. Minnaert, On Musical Air Bubbles and the Sounds of Running Water, *Philosophy Magazine*, 1933, **16**, 235 – 248
2. http://www.bksv.com/doc/bp0317.pdf Calibration Chart for Hydrophone Type 8103 [cited 20/07/08]
3. http://www.isvr.soton.ac.uk/SPCG/Tutorial/Tutorial/Tutorial_files/Web-basics-pointsources.htm [cited 30/07/08]
4. M. Wu, M. Gharib, Experimental Studies on the Shape and Path of Small Air Bubbles Rising in Clean Water, *Physics of Fluids*, 2002, **14 (7)**, L49 – L52
5. R. Manasseh, R. F. LaFontaine, J. Davey, Y. –G, Zhu, Passive Acoustic Bubble Sizing in Sparged Systems, *Experiments in Fluids*, 2001, **30**, 672 – 682
6. J. W. R. Boyd, J. Varley, Acoustic Emission Measurements of Low Velocity Plunging Jets to Monitor Bubble Size, *Chemical Engineering Journal*, 2002, **88**, 111 – 118
7. M. Martín, J. M. García, F. J. Montes, M. A. Galán, On the Effect of the Orifice Configuration on the Coalescence of Growing Bubbles, *Chemical Engineering and Processing*, 2008, **47**, 1799 – 1809
8. T. G. Leighton, *The Acoustic Bubble*, 1st ed., London, Academic Press, 1997

# Chapter 6
# Active Acoustics Results

This chapter discusses the results obtained from the active acoustic experiments detailed in Chapter 4, sections 4.4 – 4.7. Recreating the experiment of Ferrara *et al.*[1] using ultrasound contrast agents, the software used in this work was validated. Subsequently, the experimental set-up described in section 4.4 was used to study the active acoustic sizing of bubbles.

## 6.1 Establishment of Experimental Arrangements for the Active Acoustic Experiments

Ultrasound contrast agent experiments and bubble experiments can analyse both sub and super harmonics of the fundamental operating frequency. To replicate the Ferrara experimental arrangement, see Figures 4.6 and 4.7, the transmitting transducer operating frequency was at 2.25 MHz and receiving device operating frequency was at 5 MHz. This set-up was designed to detect any second harmonic generation from the system. The excitation signal was a linear chirp which ranged from 1.75 MHz to 2.75 MHz, the chirp peaked at 2.25 MHz and had a duration of 5 μs. The time trace and Fourier transform of the chirp signal can be seen in Figure 6.1(a) and (b), respectively.

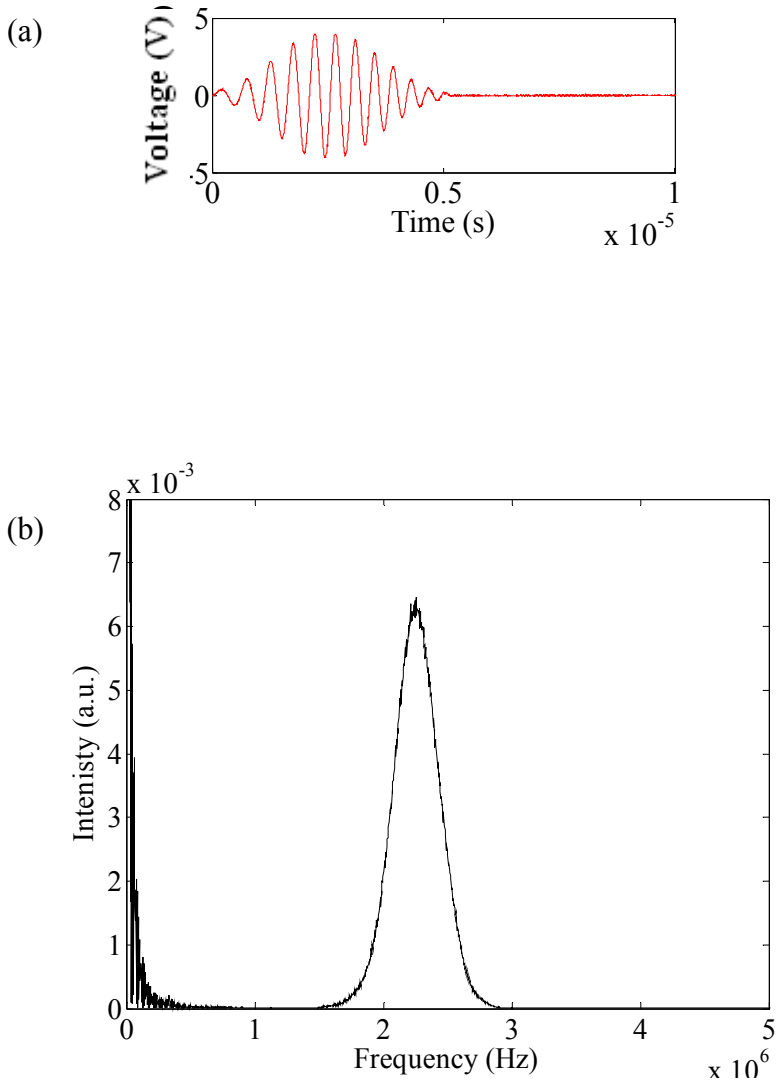


**Figure 6.1 – (a) Time spectrum versus (b) FFT spectrum of 2.25 MHz chirp of duration of 5 µs, used when transmitting at 2.25 MHz and receiving at 5 MHz**

The experiment here differed from that carried out by Ferrara *et al.*, due to equipment restrictions, as follows; the tubing Ferrara used had a diameter of 200 µm,[1] where as the tubing used in these experiments had a diameter of 6 mm. The contrast agent used by Ferrara was a nitrogen filled microbubble with a bilayered shell made from a biodegradable polymer and a human serum albumin coating whereas the contrast agent used here was filled with sulfur hexafluoride. Also, the tank used by Ferrara was made from polycarbide and the tank used in these experiments was made from glass. Finally, in Ferrara's experiments acoustically absorbent material was placed in the tank to minimise reflections. The fact that in

this experimental set-up no acoustically absorbent material was in the tank meant that it was possible to pick up reflections from other objects in the tank e.g. the waste bottle. Nevertheless, the experimental arrangement was considered appropriate for the generation of harmonic components from the contrast agent. The contrast agent solution was made by dissolving 500 mg of the powder in 5 mL of distilled water. When the contrast agent was injected into the cellulose tubing the tubing was clamped so that the contrast agent was held at the focus of the transducers.

### 6.1.1 Validation of Excitation Signal and Post Processing Software

Ten repeat measurements were taken with drive voltages of 6.4, 12.0, 18.1, 24.0, 30.8 and 36.6 V. This was done both for water alone and contrast agent solution present in the tubing. An example of the time trace obtained from the oscilloscope can be seen in Figure 6.2.

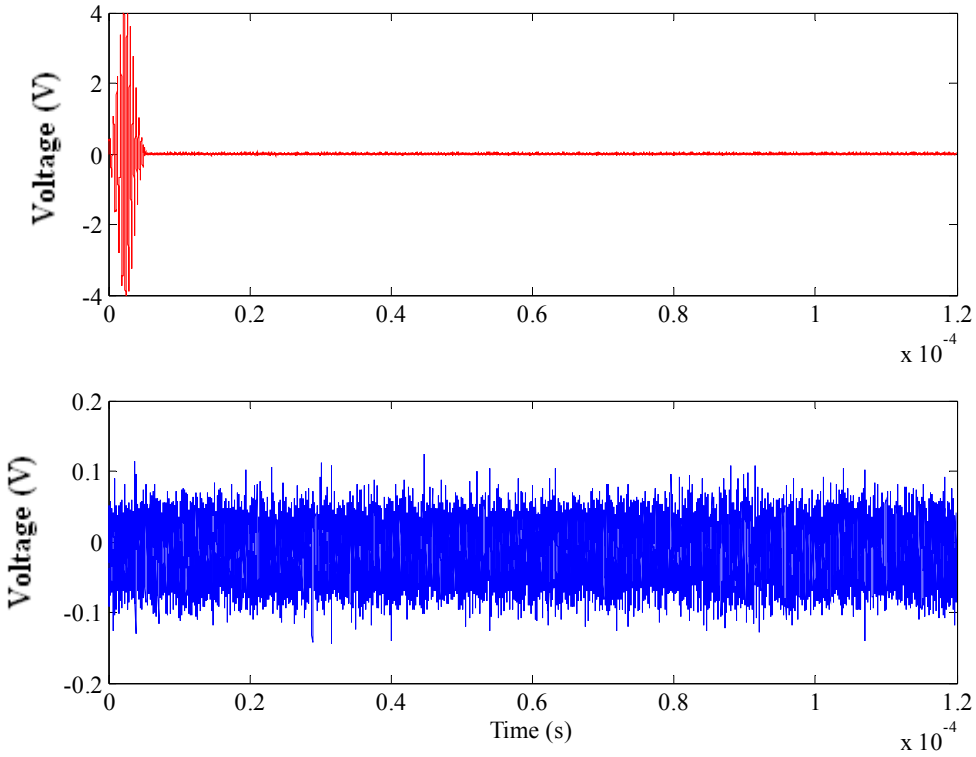


**Figure 6.2 – Time trace obtained from the oscilloscope. Upper spectrum is the time trace of the 2.25 MHz chip and the lower spectrum is the time trace of the received signal over a capture time window of 120 µs**

The upper trace in Figure 6.2 shows the excitation (chirp) signal. The lower trace shows the signal received by the 5 MHz transducer. Any direct reflections from the focal region between these two devices would occur at around 90 μs and from Figure 6.2 it is evident that there was either no reflected signal or that the received signal has a low signal to noise ratio. Hence, there was a requirement for signal processing techniques to improve the system signal to noise ratio. This can be achieved by using cross-correlation[1], which is a signal processing technique that can extract signals with a desired frequency characteristic if they are embedded in background noise.

The time trace for the received signal was then Fourier transformed, with Figures 6.3(a) and (b) illustrating the frequency spectrum for water and contrast agent, respectively. Following this the received signal was cross correlated for the fundamental and second harmonic frequency components, with Figure 6.4 (a) and (b) illustrating the frequency spectrum for water and contrast agent, respectively.

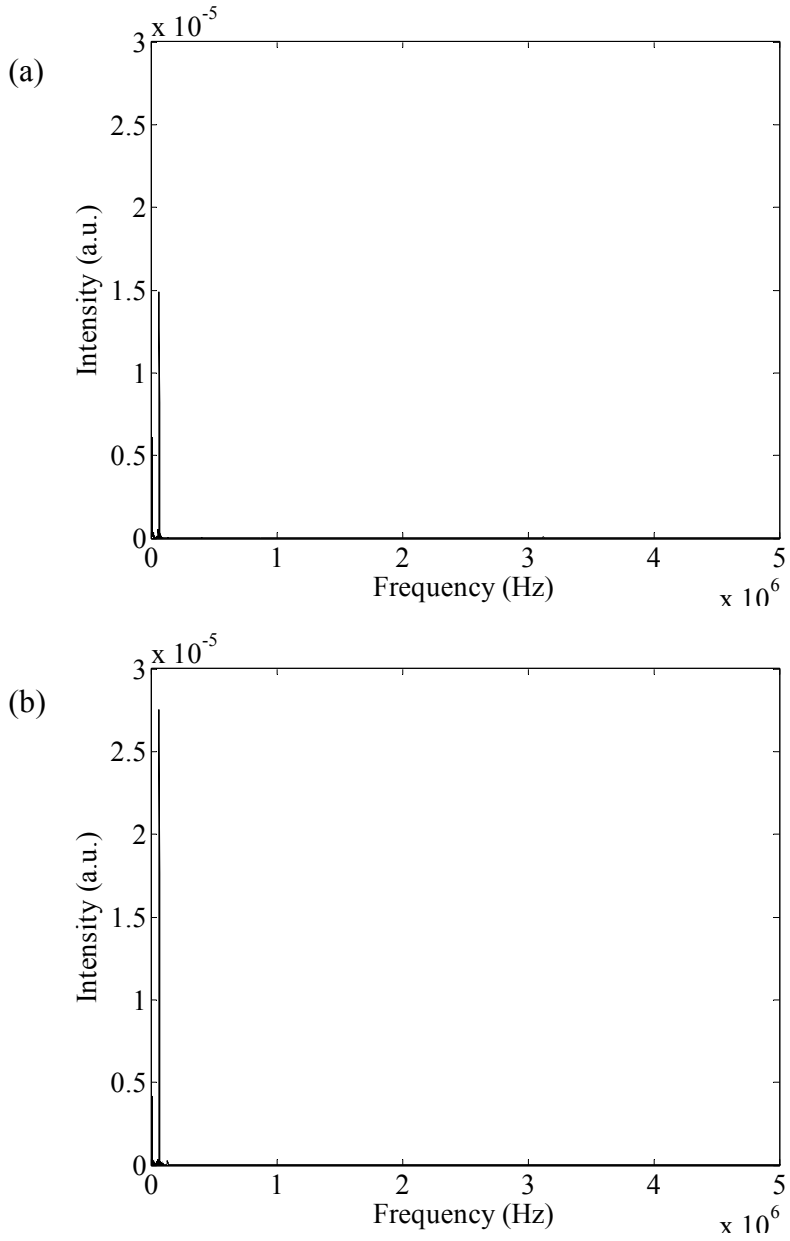


**Figure 6.3 – Fourier transformed spectrum of (a) water and (b) contrast agent obtained from transmitting at 2.25 MHz and receiving at 5 MHz with a drive voltage of 30.8 V**

From Figure 6.3 it can be seen that the Fourier transform spectra for water and the contrast agent had the same two peaks present at 12 and 66 kHz, this was true for each voltage tested. Also it can be seen that there are no spectral features above 100 kHz in the Fourier transformed spectra. One difference between Figure 6.3(a) and Figure 6.3(b) was that the intensity of the peaks in the spectra obtained for the contrast agent solution were always greater than those of the spectra obtained for

water, again this was true at every voltage tested. A reason for this was that there was more scattering of ultrasound as it passed through the water.

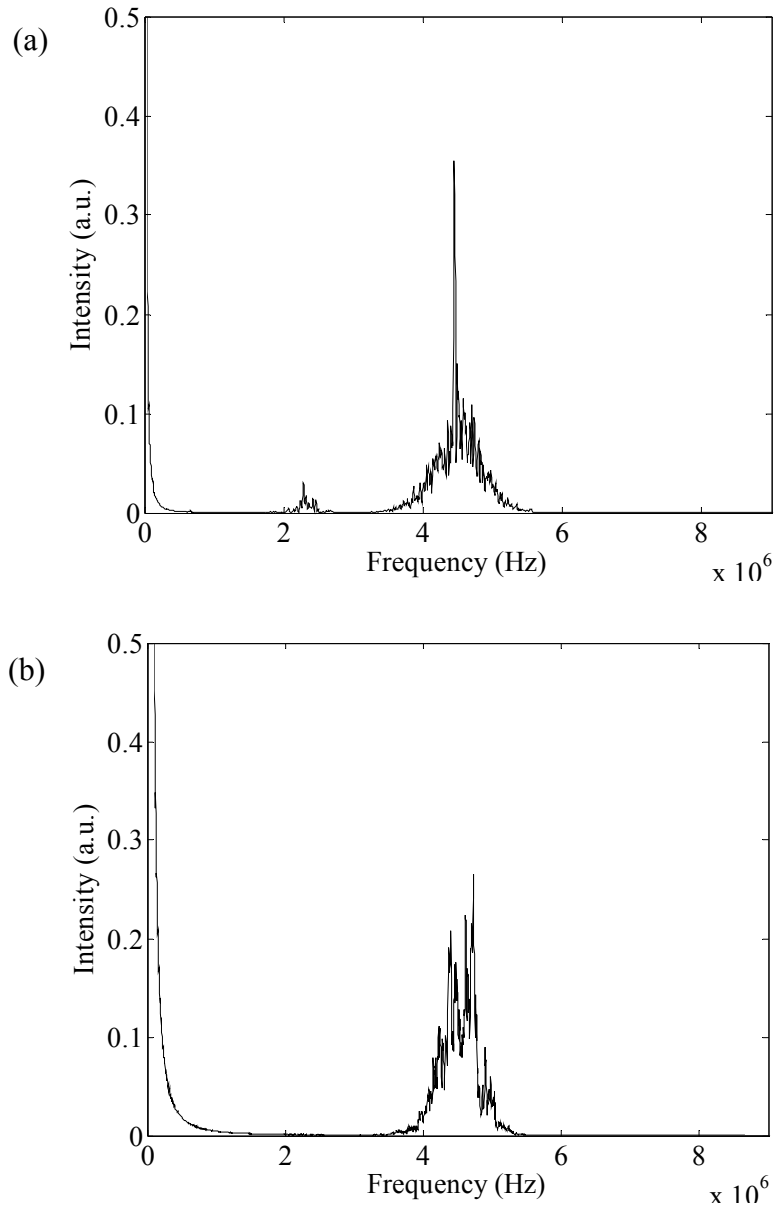


**Figure 6.4 – Cross-correlated spectrum of (a) water and (b) contrast agent obtained from transmitting at 2.25 MHz and receiving at 5 MHz with a drive voltage of 30.8 V**

However, cross-correlating the data showed that the second harmonic (twice the harmonic frequency, 2 x 2.25 MHz) was present in the spectra obtained for water and contrast agent, Figures 6.4(a) and 6.4(b). In Figure 6.4 (a) and (b) the cross-

correlation procedure was carried out between frequencies of 3.5 and 5.5 MHz, which includes the second harmonic. For both water and contrast agent the intensity of the peaks increased as voltage was increased. In Figure 6.4(a) the fundamental frequency can be observed at approximately 2.25 MHz. This was important because it confirmed that the experimental set-up could detect both the fundamental and harmonic frequencies.

### 6.1.2 Investigation of Drive Voltage

The aim of these experiments was to determine at which drive voltage the second harmonic signal was best excited. Again ten repeat measurements were taken with drive voltages of 6.4, 12.0, 18.1, 24.0, 30.8 and 36.6 V when water was in the tube. This was repeated for contrast agent, which was trapped in the cellulose tube. Figure 6.5 shows the relationship between the area under the cross-correlated spectrum, between 3.5 and 5.5 MHz (second harmonic), and drive voltage, for both water and contrast agent solution. The area corresponding to the cross-correlated spectral area between 3.5 and 5.5 MHz can be seen in Figure 6.4(a) and (b).

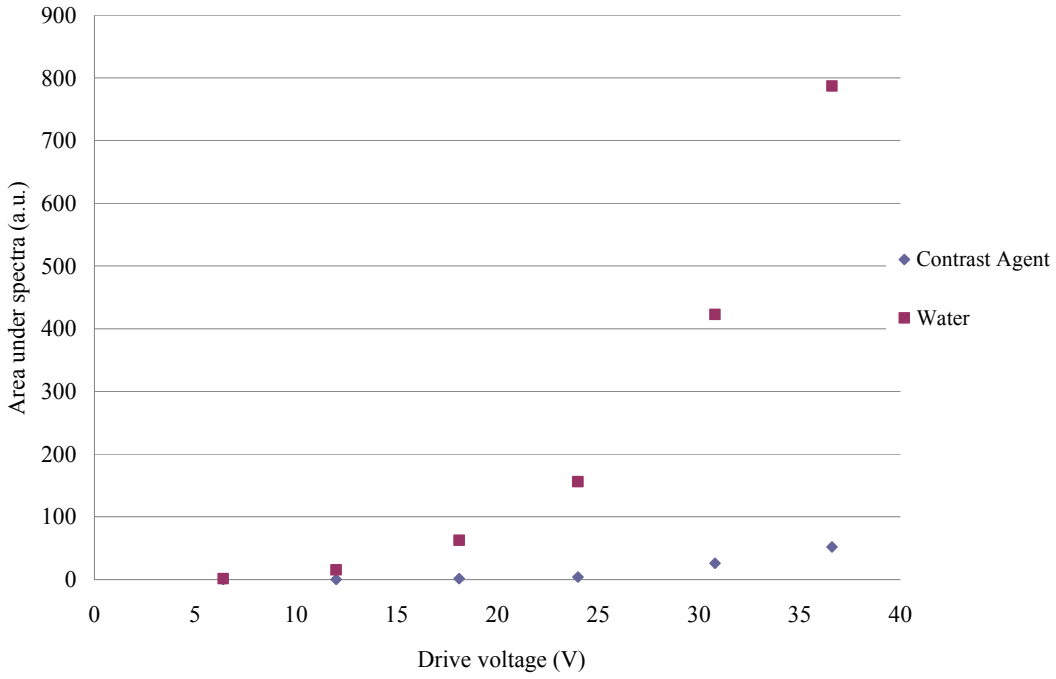


**Figure 6.5 – Relationship between area under spectra and voltage obtained from analysing the second harmonic at 4.5 MHz.**

From Figure 6.5 above it can clearly be seen that the area under the spectra increased as drive voltage was increased, possibly due to some non-linear effects. This was especially true for the experiments carried out with water in the tube. It also shows that there was a second harmonic component in the received signal at every drive voltage. However, the higher drive voltage produced higher harmonic signals.

The results from sections 6.1.1 and 6.2.2 illustrate that the second harmonic information can be extracted from low signal to noise ratio signals and hence, this post-signal processing approach can be used in the investigation into active acoustic sizing of bubbles. This work has replicated that of Ferrara's, in that, detection arose from harmonic components.[2]

## 6.2 Active Acoustic Sizing of Bubbles

The experiments carried out in this section aim to size bubbles using active acoustics and to establish any relationships between bubbles of difference sizes using the post-signal processing techniques that were validated in section 6.1.

### 6.2.1 Investigation of Bubble Sizes using MHz Frequencies

The excitation signal was again the same linear chirp that was used in section 6.1, see Figure 6.1. The experimental set-up was the same as that for section 6.1.1 with the following modifications; the tubing was replaced by a wire which was coated in petroleum jelly and a bubble of estimated diameter of 4 mm, produced from tubing of diameter 4 mm, was placed on the wire. The same experimental set-up was chosen because it is consistent with the ultrasound contrast agent work, for which the software was validated. Again 10 repeat measurements were taken at each excitation voltage. Figure 6.6(a) shows the Fourier transform spectrum of the wire alone over the full frequency range with no bubble present, at 30.8 V. It can be seen that there were no frequencies of interest in the megahertz range. Figure 6.6(b) shows an expanded spectrum of Figure 6.6(a) between 0 – 200 kHz. It can be seen there are two main peaks present at 12 kHz and 66 kHz. These frequencies were also

observed in spectra obtained from the contrast agent solution experiments, it was possible these were due to system artefacts.

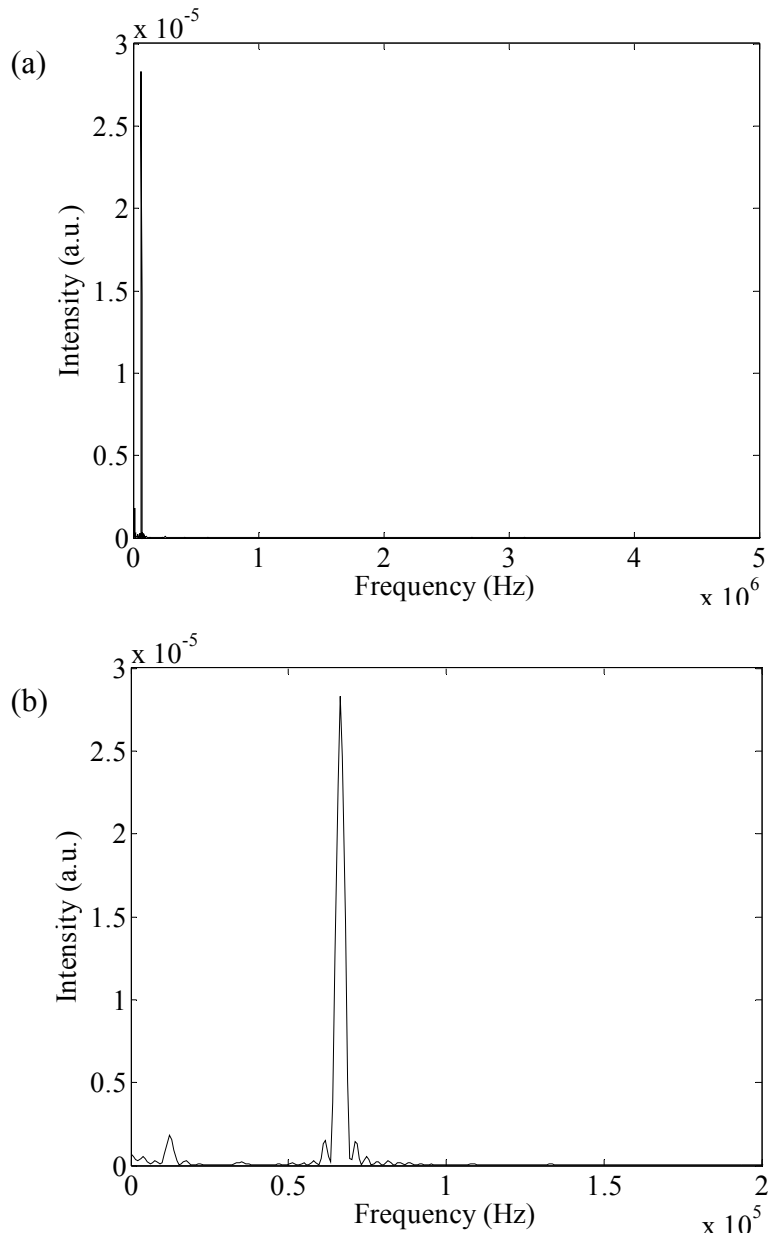


**Figure 6.6 – FFT spectra of wire (a) covering full megahertz range and (b) expanded to cover the range of 1 – 200 kHz, obtained from transmitting at 2.25 MHz and receiving at 5 MHz with a drive voltage of 30.8 V**

Once a bubble of 4 mm diameter was placed on the wire, the spectra obtained were altered by the removal of the peak at 66 kHz and the presence of other spectral

features between 0 and 100 kHz. The Fourier transformed spectrum from experiments carried out at 30.8 V can be seen in Figure 6.7.

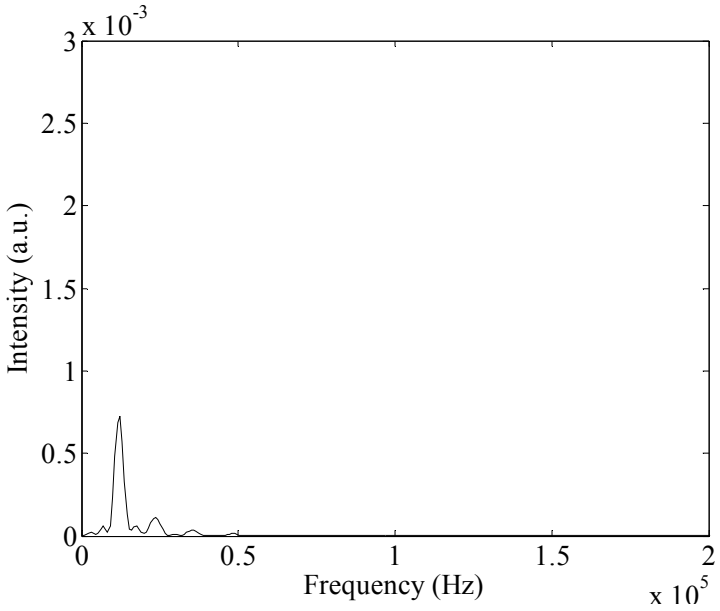


**Figure 6.7 – FFT spectrum of bubble with diameter 4 mm obtained from transmitting at 2.25 MHz and receiving at 5 MHz with a drive voltage of 30.8 V**

There are no signals present above 100 kHz therefore from here on analysis was concentrated in the 0 – 100 kHz region. Most changes in the FFT spectra between the wire and the bubble were above approximately 20 kHz. Therefore, the ratio of the area under the spectrum between 20 – 100 kHz and the total area between 0 – 100 kHz was plotted to see if the was any relationship(s) evident. This type of data analysis was successfully carried out by Nordon *et al*. to extract information regarding particle size in a heterogeneous reaction.[3] Figure 6.8 shows the relationship between area and voltage for the wire in isolation and for a bubble attached to the wire.

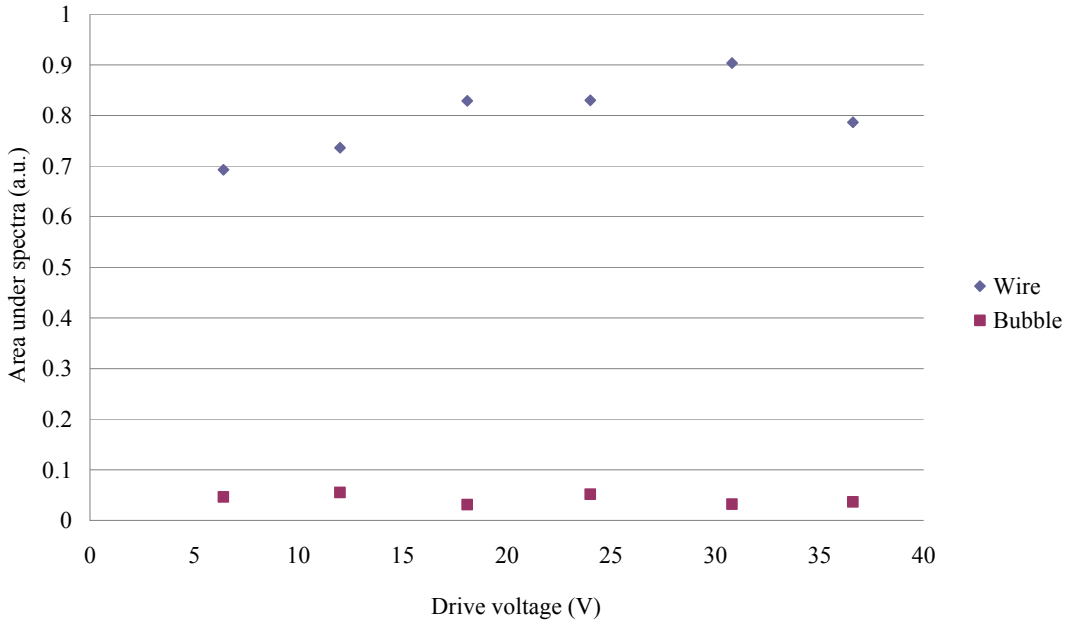


**Figure 6.8 – Ratio of the area under the spectrum between 20 – 100 kHz and the total area as a function of drive voltage for both the wire and a 4 mm bubble obtained when transmitting at 2.25 MHz and receiving at 5 MHz**

From Figure 6.8 it can be seen that there is no obvious relationship between the ratio of area under spectra between 20 – 100 kHz and total area under the spectra versus voltage for either the wire or the bubble and that the ratio of the areas for the wire are higher than that of the bubble. It was therefore concluded that drive voltage did not have a significant influence on the received signal.

The conclusion from these set of experiments was that the experimental set-up must be changed since the frequencies detected are less than 100 kHz. The experimental set-up was changed to accommodate this requirement. Unfortunately, the lowest available ultrasonic transducers for use on this project operated at 500 kHz. It was decided to use this pair of 500 kHz devices as they will offer a better potential for an acceptable system signal-to-noise ratio in the 0 – 100 kHz range than the original high frequency pair. In addition, it was decided to use the Fourier transformed data on the received signals as the cross-correlated spectra offered no additional improvement at these lower frequencies.

### 6.2.2 Investigation of Bubble Sizes using kHz Frequencies

The configuration was altered with both the transmitting and receiving transducers having an operating frequency of 500 kHz. Since it was shown above there was no relationship between voltage and the ratio of areas under the spectra it was decided to carry out these experiments with a drive voltage of 6.4 V. Also the chirp was altered to range from 250 kHz to 750 kHz and had a duration of 10 μs. All areas under the spectra in this section were calculated between 0 – 100 kHz. Fifty repeat measurements were taken and summed into 5 blocks of 10 spectra, to give 5 repeat measurements. This was chosen because it was consistent with the passive acoustic work. The Fourier transform spectrum obtained of the wire can be seen in Figure 6.9.

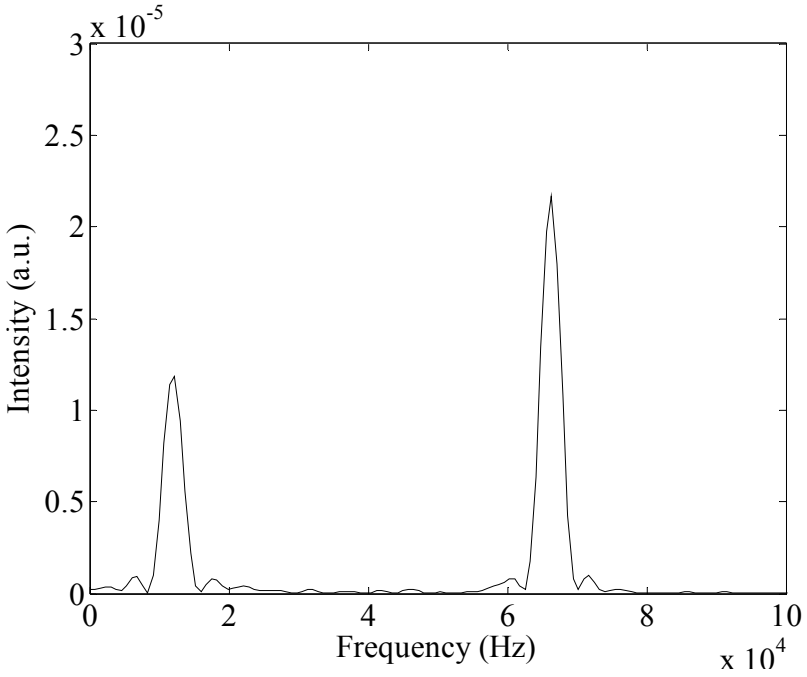


**Figure 6.9 – FFT spectrum of wire obtained from both transmitting and receiving at 500 kHz with a drive voltage of 6.4 V**

The average area under the spectra was 1.7 x $10^{-3}$ a.u. Again, the two peaks present were at 12 kHz and 66 kHz. The intensity of both peaks remained the same for each of the 5 average spectra.

The sizes of bubble which were investigated were estimated to be 1, 2 and 4 mm. The bubbles were produced from tubing of diameter of 1, 2 and 4 mm. There was a restriction on the size of bubble which could be held on the wire; it was found that bubbles with a diameter greater than 4 mm would not stay in place on the wire. This is most likely due to the increased buoyancy force.

Figure 6.10(a), (b) and (c) show the Fourier transform spectrum of bubbles of diameter 1, 2 and 4 mm, respectively. An extension of this work would be use optical methods to visualise the bubbles produced. This is discussed in more detail in Chapter 7.

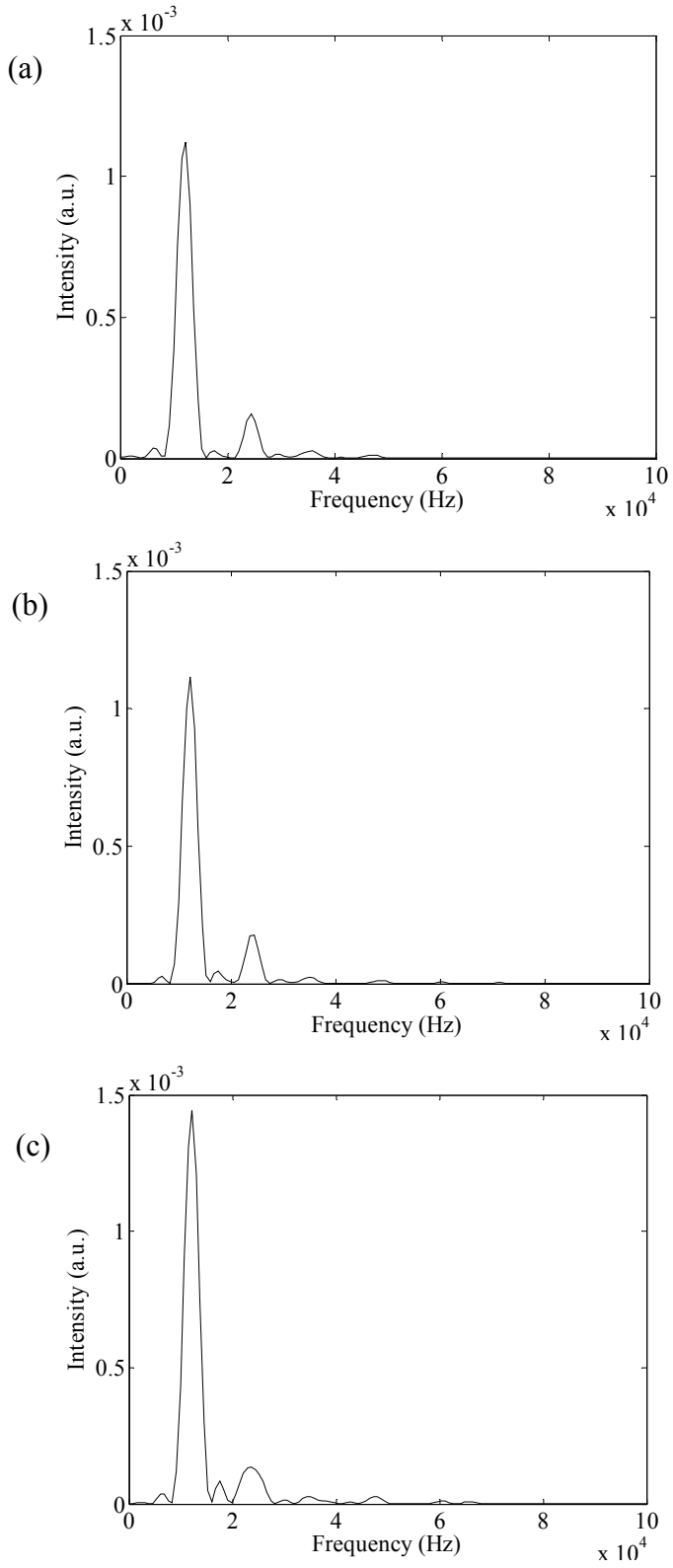


**Figure 6.10 - FFT spectrum of bubble of (a) 1 mm, (b) 2 mm and (c) 4 mm diameter obtained from both transmitting and receiving at 500 kHz, with a drive voltage of 6.4 V**

Comparing Figures 6.10 (a) – (c) showed that as bubble diameter was increased, higher frequency components (above 12 kHz) were generated by the system i.e. the spectrum obtained for the 2 mm bubble showed the presence of a peak at 62 kHz and that of the 4 mm bubble showed the presence of peaks at 60 kHz and 66 kHz. Also, it can be seen that the intensity of the 12 kHz peak increased as bubble diameter increased. The peaks which are common to all bubble diameters, i.e. 6, 12, 17, 24, 36 and 47 kHz, were attributed to the wire/jelly combination

**Table 6.1 – Area under spectra for three bubble diameters analysed between 0 – 100 kHz and 20 – 100 kHz**

| Bubble diameter (mm) | Area under spectra (a.u.) | |
|---|---|---|
| | 0 – 100 kHz | 20 – 100 kHz |
| 1 | $5.2 \times 10^{-3}$ | $1.2 \times 10^{-4}$ |
| 2 | $5.9 \times 10^{-3}$ | $1.8 \times 10^{-4}$ |
| 4 | $8.4 \times 10^{-3}$ | $3.1 \times 10^{-4}$ |

Table 6.1 shows the average area under the spectra for the three bubble diameters analysed between 0 – 100 kHz and 20 – 100 kHz. By looking at both columns of Table 6.1 it can be seen that as bubble diameter increased the area under the spectrum increased in both the 0 – 100 kHz range and the 20 – 100 kHz range. Figure 6.11 shows a graph of the area under the spectrum between 20 – 100 kHz versus bubble diameter.

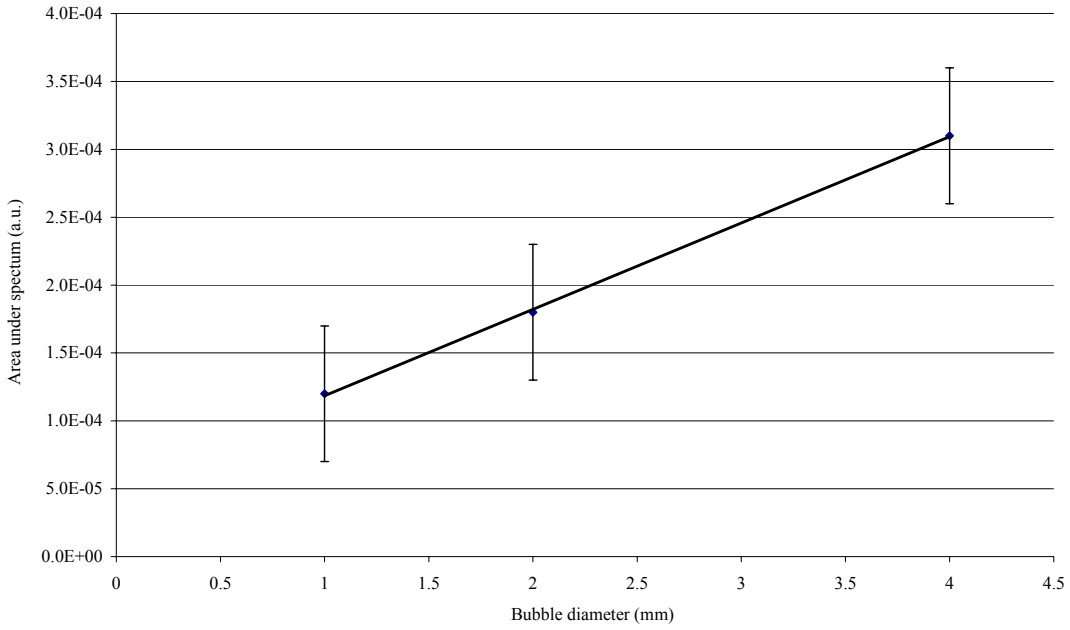


**Figure 6.11 – Graph of area under spectrum between 20 – 100 kHz as a function of bubble diameter**

From Figure 6.11 it there was a linear relationship between the area under the spectrum between 20 – 100 kHz and bubble diameter. Although the data set was small, this result offers potential for the sizing of bubbles in a bioprocess.

An ANOVA was carried out on the average area under the spectra obtained for each bubble diameter after summing the data in to 5 blocks of 10 spectra. The results are presented in Table 6.2. The $f_{crit}$ value was calculated at a 95 % confidence limit.

**Table 6.2 – Results of ANOVA tests carried out on the area under the spectra of bubble 1, 2 and 4 mm diameter**

| Bubble diameter (mm) | F-value | $F_{crit}$ | Result of ANOVA |
|---|---|---|---|
| 1 | 17.9 | 5.3 | FAIL |
| 2 | 17.9 | 5.3 | FAIL |
| 4 | 17.9 | 5.3 | FAIL |

For all bubble diameters investigated the *f*-value was greater than the $f_{crit}$ value indicating that the test fails and that any variation is due to changing bubble diameter.

The RSD of the area under the spectra were 31.4 %, 6.8 %, and 10.7 % for the 1, 2 and 4 mm diameter bubbles respectively.

The work carried out in this section is similar to that of Didenkulov *et al.*,[4] where two focused transducers with resonance frequencies of 2.25 MHz where used to acoustically size bubbles. The group concluded that bubbles with resonance frequencies between 70 kHz and 200 kHz could be used to size bubbles.

## 6.3 Conclusion of Chapter

This chapter provided a validation of the software used for signal capture and data processing. The experimental arrangement was used to study bubble characteristics using active acoustics in the frequency range 20 – 100 kHz. A linear relationship between bubble diameter and the received spectral characteristics was demonstrated. This result provides confidence in the applicability of active acoustic techniques for bubble characterisation in bioprocesses.

## 6.4 References


1. Chuangnan Wang, Monitoring of Pharmaceutical Processes using Non-Linear Ultrasound, Final Year Report, University of Strathclyde, Dept. EEE, June 2008
2. D. N. Patel, S. H. Bloch, P. A. Dayton, K. W. Ferrara, Acoustic Signatures of Submicron Contrast Agents, *IEEE Transactions on Ultrasound, Ferroelectrics and Frequency Control*, 2004, **51 (3)**, 293 – 301
3. A. Nordon, Y. Carella, A. Gachagan, D. Littlejohn, G. Hayward, Factors Affecting Broadband Acoustic Emission Measurements of a Heterogeneous Reaction, *The Analyst*, 2006, **131**, 323 – 330
4. I. N. Didenkulov, S. W. Yoon, A. M. Sutin and E. J. Kim, Nonlinear Doppler Effect and its use for Bubble Flow Velocity Measurements, *Journal of the Acoustic Society of America*, 1999, **106**, 2431 – 2435

# Chapter 7
# Project Conclusions and Future Work

## 7.1 Project Conclusions

From the literature review it can clearly be seen that there are a lack of applications in which fermentation reactions and bioprocesses are monitored on-line; where most bioprocess monitoring was carried out off-line or at-line. A disadvantage with on-line analysis was the additional cost of adding infrastructure to the process, for example sampling loops. However, from the literature it was apparent that some bioprocess monitoring has been carried out in-line, this was less expensive than on-line analysis because of the design of in-line systems i.e. that an additional sampling loop is not required. Chromatographic techniques, such as gas chromatography, tend to be used as an off-line reference method. As fermentation reactions are complex there is a need to establish robust techniques of multivariate data analysis to process the data and obtain meaningful results.

Two acoustic techniques were used in this research; these were passive acoustics and active acoustics. Passive acoustics (or acoustic emission) is a 'listening' technique, where the process generates acoustic waves itself. Active acoustics occurs when a wave is transmitted through the process and the effect the process has on the wave is monitored.[1]

An experimental programme was devised to investigate the application of passive acoustic techniques for the characterisation of bubbles invasively and non-invasively. Bubbles were produced by three methods; a syringe pump, a peristaltic pump and an air cylinder. The diameter of the bubbles investigated was determined by the diameter of the tubing from which the bubbles were produced. An inverse relationship between tubing size and frequency was observed. It was found that the process of bubble production could also be monitored when the flow rate and/or viscosity were altered, where increasing the flow rate decreased the acoustic emission frequency and that increasing viscosity restricts the movement in which a

bubble can oscillate. Increasing the viscosity to a 50 : 50 mixture of glycerol and water gave rise to more repeatable results.

Following from this a test cell was developed for active acoustic measurements of bubbles contrast agent. The ultrasound contrast agent work resulted in the successful validation of the signal capture and data processing software used It was shown that active acoustic techniques can be used to study bubbles; in particular, the spectral characteristic was utilised to demonstrate that the area under the spectra between the 20 – 100 kHz range varies linearly with bubble size. Bubbles of estimated diameters of 1, 2 and 4 mm were investigated.

Overall, both passive and active acoustic experiments have demonstrated that acoustics can yield physical information i.e. bubble size. The conclusions found in this project offer great potential for this work to be further researched and applied to the monitoring of bioprocesses because this work has demonstrated that information on the physical state of the system can be obtained from using an acoustic technique.

## 7.2 Future Work

In a future study of passive acoustics a more detailed analysis of a bubbles' behaviour, including a study of the size and shape changes which occur as it is ejected from the sparger and travels up the water column, should be carried out. The use of video imaging could be employed in a study of this type. Where video imaging could take still photographs of a bubble travelling up a water column and these pictures could be analysed for changes in size and shape. A technical requirement is that it should be a high speed video camera operating in full frame mode. This technique was used by Vazquez *et al.* to study bubbles. In this case they used a Motion Systems 8000S (MASD-Red Lake Inc.) which operated at 4000 frames per in the full frame mode with a resolution of 100 x 98 pixels. The images taken by the cameras should be directly digitised.

The effect of flow rate and sparger diameter should also be investigated further to test the effects of larger sparger diameters and higher flow rates. This would be useful because in a typical 10 L fermenter the sparger diameter is 4 mm and the flow rate is 8 L $min^{-1}$.

The experiments carried out to show the effect of viscosity on frequency should be repeated with a more viscous solution to determine if this does indeed make measurements more repeatable. Since increasing viscosity increases surface tension, it would be thought that the ability of a bubble to change shape from when it is eluded at the sparger to the top of the vessel will be further restricted, this could be studied using photographic equipment. Also experiments should be carried out in NaC*l* solutions. This has been shown to reduce the coalescence of bubble in liquids.[2,3]

Since all work carried out in this project was invasive, future work, using active acoustics, will be conducted both invasively and non-invasively using focused transducers at frequencies of below 200 kHz to detect harmonic and/or subharmonic frequencies. There will need to be experiments carried out to investigate whether the vessel has any influence, for example are bubble oscillations affected by the size of the vessel or the thickness of the vessels glass wall (that the oscillations have to pass through to be detected non-invasively by a transducer). It may be necessary to design transducers which are specific for the kHz frequencies found in this project. An investigation of bubbles of different sizes to those investigated in this project is necessary to test the hypothesis that the area under the spectra increases linearly with bubble size.

Also, further work should be carried out using a mini-fermenter to apply the results and principles of this thesis to the on-line monitoring of a fermentation reaction. This should be carried out jointly with the application of an optical technique to provide complementary chemical information alongside the physical information obtained from an acoustic technique. This would involve the use of multivariate methods of data analysis.

The data processing techniques which were used in this project were time consuming, there is a need to develop an automated system which can process the data and generate results i.e. the development of an automated data processor which can deliver real-time measurements.

## 7.3 References


1. J. W. R. Boyd and J. Varley, The use of Passive Measurement of Acoustic Emissions from Chemical Engineering Processes, *Chemical Engineering Science,* 2001, **56**, 1749 – 1767
2. J. W. R. Boyd, J. Varley, Acoustic Emission Measurements of Low Velocity Plunging Jets to Monitor Bubble Size, *Chemical Engineering Journal*, 2004, **97**, 11 – 25
3. D. Ruen-ngam, P. Wongsuchoto, A. Limpanuphap, T. Charinpanitkul and P. Pavasaat, Influence of Salinity on Bubble Size Distribution and Gas-Liquid Mass Transfer in Airlift Contactors, *Chemical Engineering Journal*, 2008, **141**, 222 – 232